A Pilot Study on Discriminative Power of Features of Superficial Venous Pattern in the Hand

Alice Bellini

Advisor: Prof. Alfredo Ruggeri

Co-Advisor: Prof. Emanuele Trucco

Academic Year 2009/2010

Contents

Contents iv

List of Figures vii

Ringraziamenti xii

Acknowledgement xiii

Sommario xiv

Summary xvi

1 Introduction 1

1.1 Aim and Brief Description of the Methods……1
1.2 Outline of the Thesis……7

2 Related Works 8

2.1 Biometric……8
2.1.1 Characteristics and Typologies of Biometric Features……8
2.1.2 Vascular Pattern as a Biometric Recognition System……16
2.1.3 Acquisition of the Images for Biometric Purposes……25
2.1.4 Enhancement Algorithms for Infrared Images……26

2.2 Vessel Tracking Techniques……29
2.2.1 Matched Filters……30

2.3 Image Registration and Pattern Matching……36
2.3.1 Image Registration Techniques……36
2.3.1.1 Registration for Hand Vein Pattern Systems……39
2.3.1.2 PSO: Particle Swarm Optimization Technique……40
2.3.2 Pattern Matching for Biometric Purposes……42

2.4 Features Selection and Shape Indicators……46

3 Acquisition and Enhancement of Infrared Images 50

3.1 Infrared Images: Contrast Problems and Application of Enhancement Algorithms……54
3.1.1 Enhancement Algorithms……57
3.1.1.1 First Design: Manta-Ray Function……57
3.1.1.2 Second Design: the Polynomial Function……64
3.1.1.3 CLAHE: Contrast Limited Adaptive Histogram Equalization……68

4 Detection of the Venous Pattern 73

4.1 Vessel Tracking Technique.....74
4.1.1 Problems in the Extraction of the Vessel Network.....77

5 Skeletonization and Features Detection 82

5.1 Skeletonization of the Binary Mask.....82

5.2 Evaluation of the Width of the Veins.....83

5.3 Pattern Matching and Particle Swarm Optimization.....85
5.3.1 Registration of the Images.....85
5.3.2 Particle Swarm Optimization.....89
5.3.2.1 PSO Design.....90
5.3.2.2 Evaluation of the Values of the PSO Parameters.....93

5.4 Creation of the Graph and Characteristics of the Vessel Tree.....97
5.4.1 Reconstruction of the Shapes by Attributed Skeletal Graph.....98

6 Experimental Results 104

6.1 Database of Images.....104

6.2 Acquisition of the Images.....109
6.2.1 Introduction to Infrared Photography.....109
6.2.1.1 Human tissue as an Optical Medium.....111
6.2.1.2 Fuji IS-1 Camera.....111
6.2.1.3 Lens Filtration.....111
6.2.1.4 Infrared Light Source.....112
6.2.1.5 Infrared Light Source Mount.....112
6.2.1.6 Material Used.....112

6.3 Features Detection.....117
6.3.1 Width of the Veins.....117
6.3.1.1 Discussion.....121
6.3.2 Branching Angles.....121
6.3.2.1 Discussion.....124
6.3.3 Vessels Length.....124
6.3.3.1 Discussion.....127
6.3.4 Sum of Squares Distances (SSD) within the Features Detected.....128
6.3.4.1 SSD for the Branching Angles and the Vessels Lengths.....128
6.3.4.2 Discussion.....131
6.3.5 Joint Histogram of the Features.....131
6.3.5.1 Discussion.....134

6.4 Pattern Matching ……135
6.4.1 Results of the PSO……135
6.4.2 Discussion……137

7 Conclusions **139**

7.1 Analysis of the Limits……141
7.2 Possible Improvements and Future Works……142

Appendix **144**

Bibliography **162**

List of Figures

1.1 Comparison between visible and infrared image 2
1.2 Histogram of the original infrared image 2
1.3 A tracking operation during the vessel detection 3
1.4 Profile of a general vein 3
1.5 Binary mask representing the venous pattern 4
1.6 Vascular network with junctions (blue) and vessels (red) 5
1.7 Examples of different images from the database 5
1.8 Binary mask to be registered on the left; overlap of two binary masks, the reference (green) and the registered (red) after PSO on the right 6
2.1 Block diagrams of the algorithm of Im et Al, 2001 [20] 17
2.2 Processing flow diagram of the proposed algorithm [21] 18
2.3 Block diagram of hand verification systems 19
2.4 CCD camera 20
2.5 Digital processing algorithm to extract the vascular network as binary mask[11] 21
2.6 Proposed steps of the algorithm of [23] 22
2.7 FIR images in a normal environment [6] 24
2.8 NIR images of the palm and wrist of a hand [6] 24
2.9 Special sensitivity characteristic of CCD sensor [11] 25
2.10 Fingerprint before and after histogram equalization [23] 27
2.11 Fingerprint before and after CLAHE [23] 28
2.12 Estimate vessel segment and the actual one located by the matched filter[36] 30
2.13 Result of the vessel tracking with the centerlines detected, the vessels profiles and memberships analysed [35] 32
2.14 Tracking results, in black the seed points [32] 33
2.15 Cross sectional brightness profile of a vein. a) cross sectional profile, b) position of the section [33] 35
2.16 Dark line detection [33] 35
2.17 SEs for the end points: the fundamental A (in bold) and its rotations $\theta_1(A)$; $\theta_2(A)$; ... ; $\theta_7(A)$ in order. [51] 48

2.18 SEs for the junction points: B (in bold) and its rotations $\theta_1(B)$; $\theta_2(B)$; ... ; $\theta_7(B)$ in order. [51] 48
2.19 A wrench binary shape and its morphological skeleton before pruning [51] 49
2.20 The skeleton after pruning short external branches and after eliminating short internal branches [51] 49
3.1 Tracing of the veins with Photoshop 51
3.2 Example of infrared back hand image 52
3.3 Example of arm image 52
3.4 Example of feet image 53
3.5 Example of legs, the infrared image is not clear enough 53
3.6 Visible image (left) and infrared image (right) of a back hand 54
3.7 Profile of a vein, with good contrast 55
3.8 A low contrast back hand image with a circle indicating the vein of interest 55
3.9 Profile of a vein from a low contrast image 55
3.10 Infrared image of a dorsum of the hand 57
3.11 Infrared image of a dorsum of the hand 57
3.12 Plot of the first function for the enhancement 58
3.13 A 3x3 neighbourhood of a point (x,y) in an image [31] 59
3.14 MANTA function with different values of k 61
3.15 Modified images after three iterations of the algorithm 62
3.16 Modified images after three iterations of the algorithm 63
3.17 Original image (left corner), modified image after one iteration (right corner) and after two iterations (last image) with k = 0.6 66
3.18 Comparison of profiles of a vessel in the original and processed image 67
3.19 Original image (left corner) and modified image after one (right corner) and two iterations (last image) with k = 0.6 67
3.20 Comparison of profiles of a vessel in the original and processed image 68
3.21 Example of histogram of the original image 69
3.22 Histogram and equalized histogram of a fingerprint image [26] 69
3.23 CLAHE and CLAHE with clip limit of a fingerprint image [26] 70
3.24 Image after CLAHE operation 71
3.25 Processed image and relative histogram after enhancement operations 72
3.26 Comparison between original, processed image and relative histogram 72

4.1 a, b Cross sectional profile of a vein in a finger: a) cross sectional profile, b) position of the cross section [33] 74
4.2 Dark line detection [33] 75
4.3 Tracking line during the operation 76
4.4 Complete tracking operation in a selected back hand image 77
4.5 Retinal image usually used with the Vessel Segmentation software 78
4.6 Example of a back hand image 78
4.7 Back hand image and its structures, veins and tendons 79
4.8 Back hand image with tendons visualized as vessels, dark lines: the selected part in the image shows a tendon 80
4.9 Hand closed in a fist 80
4.10 Back hand with hairs in the dorsum 81
4.11 Binary mask resulting from the detection of the vessel network through the vessel tracking algorithm 81
5.1 Skeleton obtained with thin operation (left) and skel operation (right) 83
5.2 Evaluation of the width with the Euclidean distance; in yellow the skeleton, A and B are two points on the borders of the vein 84
5.3 Widths of the vessel network 84
5.4 Example of an image of the database 86
5.5 Example of an image of the database 86
5.6 Binary masks of two different images 87
5.7 Result of XOR operation; after that the white pixels are counted 91
5.8 Various results of the PSO: in green the reference mask, in red the registered image, in yellow the overlapped points between the two masks 95
5.9 Before and after the registration, the white mask is the original one and the red mask is the registered 96
5.10 Another example of the result obtained after the registration 97
5.11 Original binary image (left) and small spots removed from it (right) 101
5.12 Binary mask (red) and the operation of closing (green) 101
5.13 Skeleton (left) and final vessels graph with relative junctions displayed (right) 102
6.1 Examples of infrared images collected 104/5
6.2 Infrared images of legs showing difficulties to find the venous pattern 105

6.3 Visible (left) and infrared image (right) of two back hands 106
6.4 Examples of lack of contrast in two infrared images 107
6.5 Original image (up), cropped and enhanced image (down) 108
6.6 CCD camera 109
6.7 Infrared light source 112
6.8 Studio: camera with tripod, black velvet sheet 114
6.9 Black velvet sheet and positions 114
6.10 Distance from: Camera – scale centre – black feet = 54cm; Camera – screen = 210 cm; Camera – Red feet = 182.9 cm; Between Blue feet = 63.5 cm; Between Yellow feet = 63.5 cm 115
6.11 View of the studio 115
6.12 View of the studio 116
6.13 Camera and infrared light source 116
6.14 Image of a vein with a blue line that indicates its width 117
6.15 Range of the widths in a back hand image 118
6.16 Histograms of the widths for the left hands 119
6.17 Histograms of the widths for the right hands 120
6.18 Branching angle selected with a blue square 121
6.19 Histograms of the branching angles for the left hands 122/3
6.20 Histograms of the branching angles for the right hands 123/4
6.21 Histograms of the lengths for the left hands 125/6
6.22 Histograms of the lengths for the right hands 126/7
6.23 Histogram of the SSD for the branching angles, left hands 129
6.24 Histogram of the SSD for the branching angles, right hands 129
6.25 Histogram of the SSD for the vessels length, left hands 130
6.26 Histogram of the SSD for the vessels length, right hands 130
6.27 Joint histogram for left hands 133
6.28 Joint histogram for right hands 133
6.29 Examples of results of the pattern matching with PSO 136

Ringraziamenti

La tesi è stata svolta per portare a termine il corso di Laurea Specialistica in Bioingegneria all' Università di Padova (Italia).
Il progetto di 30 ECTS è stato realizzato da Ottobre 2009 a Giugno 2010 nel dipartimento di School of Computing, University of Dundee (UK) sotto la supervisione del Professore Emanuele Trucco (School of Computing) e del Professore Alfredo Ruggeri (Professore associato di Ingegneria Biomedica, Università di Padova).
Il lavoro è una collaborazione tra School of Computing e Centre for Human Anatomy and Identification, Università di Dundee.
In questo paragrafo, vorrei ringraziare tutte le persone coinvolte nel progetto, che ne hanno reso possibile la realizzazione e che mi hanno accompagnata in questa fantastica esperienza a Dundee.
Come sempre, prima di tutto, grazie alla mia famiglia, le persone più importanti, mi hanno sempre sostenuta in tutto e per tutto, letteralmente da una vita, e senza di loro non saprei cosa fare. (Barba e Miky siete presenti anche voi)
I miei supervisori, Prof. Alfredo Ruggeri e Prof. Emanuele Trucco. Vorrei ringraziare il Prof. Trucco per la fantastica accoglienza, i suggerimenti, gli immancabili meeting settimanali e l'aiuto costante. Mi ha guidato attraverso la realizzazione del progetto con i suoi consigli per risolvere problemi sorti durante i mesi.
L'intero staff di School of Computing per il loro caldo benvenuto e trattamento.
Il grande Vision Group con tutti i suoi componenti, specialmente Adria Perez Rovira, Vijay John, Wei (Jerry) Jia, Špela Ivekovič, pronti ad ascoltare ogni mia inaspettata domanda, facendomi sentire parte della squadra.
Dall'altra parte ringrazio Helen Meadows, ed i suoi supervisori Prof. Sue Black and Dr. Roger Soames, per l'aiuto, gli incontri, le piacevoli chiacchierate, le innumerevoli email.
Tutte le persone conosciute a Dundee e per la Scozia: è stata la più bella esperienza avuta fin'ora, non sarebbe stata la stessa senza di voi, mi avete sopportata, sostenuta e accompagnata in ogni momento. Mi mancherete tanto, spero di rivedervi presto.
Ringraziamenti speciale alla 'Mediterranean Parea', non vi dimenticherò ragazze!
Grazie ancora di tutto!

Acknowledgement

This thesis has been carried out to complete the Master Science Degree in Bioengineering at the University of Padova (Italy).

The project of 30 ECTS has been realized from October 2009 to June 2010 in the Department of School of Computing, University of Dundee (UK), under the supervision of Prof. Emanuele Trucco (Professor of Computational Vision, SoC) and Prof. Alfredo Ruggeri (Associate Professor of Biomedical Engineering).

This is a collaboration between the School of Computing and the Centre for Human Anatomy and Identification, University of Dundee.

In this paragraph, I wouldd like to mention all the people that made this project possible and the experience in Dundee, great.

First of all, my family that made everything possible, and supports me in the best way ever in each moment of my life, I cannot live without them. (Barba and Miky, you are in this group)

The supervisors, Prof. Alfredo Ruggeri and Prof. Emanuele Trucco. I would like to thank Prof Trucco for the suggestions and the unfailing weekly meetings and for his constant aid. He drove me through the project, addressing me in the right way to solve the problems arisen during the months.

The entire staff of School of Computing for the warm welcome and treatment during the year.

The great Vision Group, especially Adria Perez Rovira, Vijay John, Wei (Jerry) Jia, Špela Ivekovič, ready to help with illuminating ideas at each questions, making me feel part of the team.

On the other part, many thanks to Helen Meadows, and her supervisors Prof Sue Black and Dr Roger Soames, for the help, the meetings, the pleasant time spent together. I'll miss our chats and the countless emails.

The people known in Dundee and around Scotland: this was the greatest experience of my life, it would not has been the same without you; you supported me, bore me in each moment and laughed with me. I'll miss you, hope to see you as soon as possible.

Especially the 'Mediterranean Parea', I will not forget you girls!

Thank you again!

Sommario

Qualsiasi caratteristica umana fisica e comportamentale può essere utilizzata come una caratteristica biometrica se soddisfa proprietà di unicità, universalità e stabilità.
La formazione della rete vascolare è influenzata da fattori genetici ed ambientali. L'influenza di singoli eventi fa sì che il modello sia unico per ogni individuo, quindi può essere eventualmente utilizzato per l'identificazione personale.
L'unica caratteristica della rete dei vasi sanguigni che può cambiare durante la vita è la dimensione ed il grado di tortuosità del singolo vaso, in quanto l'intera rete non varia se non attraverso intervento chirurgico. Non solo gemelli identici hanno diversa rete vascolare, ma anche nel singolo non c'è simmetria bilaterale. Da questa proprietà deriva l'elevata considerazione da parte delle industrie di sicurezza.
L'obiettivo del progetto è di sviluppare un metodo automatico per identificare e rappresentare la rete vascolare superficiale presente nel dorso della mano ed investigare sul suo potere discriminativo come caratteristica biometrica.
Il motivo per il quale il progetto è stato introdotto è per migliorare il modo di identificazione della rete sanguigna, da manuale, attraverso l'uso di Photoshop, ad automatico.
In questa tesi, un prototipo di sistema che estrae l'albero superficiale delle vene da immagini infrarosse del dorso della mano sarà descritto.
Algoritmi per il miglioramento del contrasto delle immagini infrarosse saranno applicati. Per tracciare le vene, una tecnica di *tracking* verrà utilizzata per ottenere una maschera binaria della rete vascolare.
Successivamente, un metodo per stimare il calibro e la lunghezza dei vasi sanguigni, la posizione e gli angoli delle giunzioni sarà trattato.
Il potere discriminativo delle precedenti caratteristiche verrà studiato in modo indipendente o considerando due caratteristiche contemporaneamente in un unico vettore. Una tecnica di *pattern matching* di due modelli vascolari sarà presentata per verificarne l'unicità; modificando il metodo di estrazione dei vasi per ottenere un miglior risultato, potrebbe far sì che il confronto tra i modelli sia più significativo.
Osservando i risultati statistici, gli istogrammi riguardanti gli angoli di giunzione nella singola mano sembrano essere altamente discriminanti, se consideriamo questa caratteristica singolarmente. Studi futuri potrebbero essere indirizzati verso lo studio di questi angoli.

L’analisi di più caratteristiche prese simultaneamente potrebbe essere migliorato per ottenere conclusioni sull’unicità della rete vascolare nel dorso della mano, considerando un numero elevato di immagini e più caratteristiche.

Summary

Any human physiological and behavioral characteristics can be utilizied as a biometric feature as long as it is universal, distinct and permanent.

The vascular pattern is influenced by both genetic and environmental factors. The influence of individual factors results in a pattern that is unique to the individual and can therefore be utilizied for personal identification.

The only characteristics of a venous profile that may change during life are size and degree of tortuosity (varicosity) of the single vessel, as the entire pattern does not vary without surgery intervention.

Not only identical twins have different venous patterns but there is no bilateral symmetry within the individual. For this reason the value of this anatomical feature is highly regarded in the security industry.

The goal of the project is to develop an automatic way to identify, represent the superficial vasculature of the back hand and investigate its discriminative power as biometric feature. The pilot study was introduced to obtain a full vasculature map automatically, instead of a manual way, using the Photoshop tools.

In this thesis a prototype of a system that extracts the superficial venous pattern of infrared images of back hands will be described.

Enhancement algorithms are used to solve the lack of contrast of the infrared images. To trace the veins, a vessel tracking technique is applied, obtaining binary masks of the superficial venous tree.

Successively, a method to estimate the blood vessels calibre, length, the location and angles of vessel junctions, will be presented. The discriminative power of these features will be studied, independently and simultaneously, considering two features vector.

Pattern matching of two vasculature maps will be performed, to investigate the uniqueness of the vessel network. Improving the vessels extraction technique will be useful for interesting comparisons between the maps.

Observing the statistical results, angle histograms within the hand seem to be highly discriminative, taken independently, in that case future works could be addressed on the study of junction angles.

Multiple features vectors analysis could be improved with more images and features.

Chapter 1

Introduction

1.1 Aim and Brief Description of the Methods

The project aims to detect and characterize the superficial vasculature of back hands, to investigate the uniqueness of various quantifiable feature across a population of individuals and the potential of vein mapping as a reliable and statistically robust method of comparison in forensic investigations.

This pilot study is a collaboration done at the University of Dundee, between the School of Computing and the Centre for Human Anatomy and Identification.
The beginning is a dataset of infrared images, representing various parts of the body, e.g. feet, upper and lower limbs, back hands.
First point is to analyze the images, specifically the contrast, brightness, general conditions for the successive steps.
The images require enhancement steps, gained with different algorithms, because the lack of contrast is evident and it is not possible to apply directly a detection algorithm.

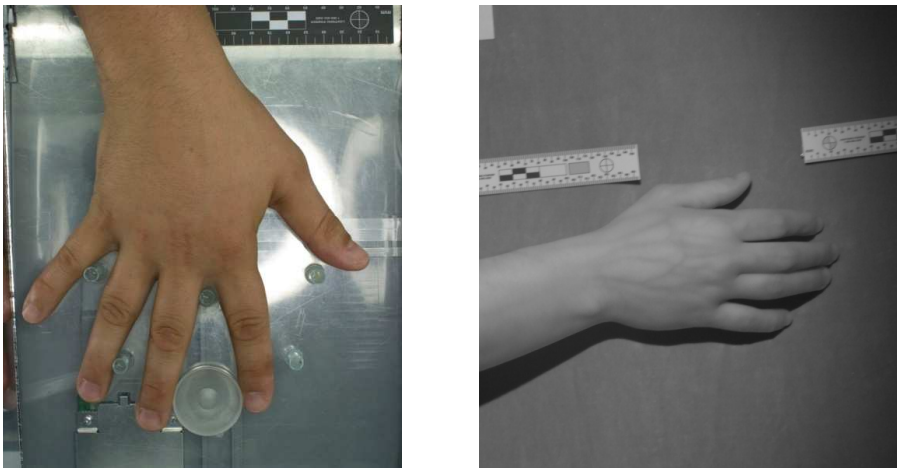

Figure 1.1: Comparisons between visible and infrared image.

As Figure 1.1 shows, the difference between the two type of images, the visible and the infrared one, is minimum.

The second step is to decide what type of detection algorithm could work with this type of particular images.

I have tried different functions, considering also the histogram of the images, where the range of possible values is not used, there is a lack of contrast, Figure 1.2.

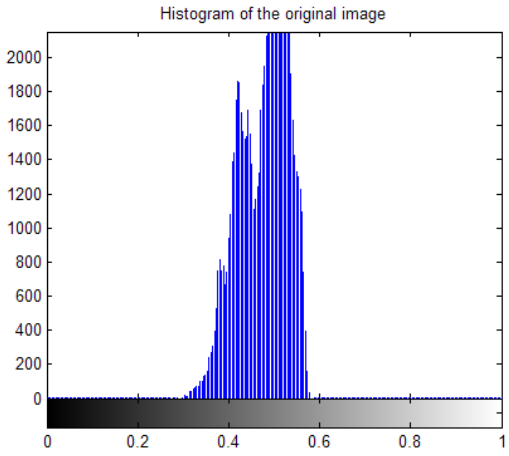

Figure 1.2: Histogram of the original infrared image.

A Contrast Limited Adaptive Histogram Equalization (CLAHE) is applied combined with another function, that works in this way: it improves the contrast of the elements of the

image, i.e. veins and background. The veins have to appears as dark lines in a light background, so the contrast is enhanced.

Third step is the application of a software of vessel segmentation based on vessel tracking technique, to detect the venous network.

Vessel tracking techniques start from a point on a vessel and move along it as far as possible by analyzing consecutive local areas (Figure 1.3), e.g. scan across the vessel, evaluating its profile and checking the depth of it, because a vein appears as a valley, Figure 1.4.

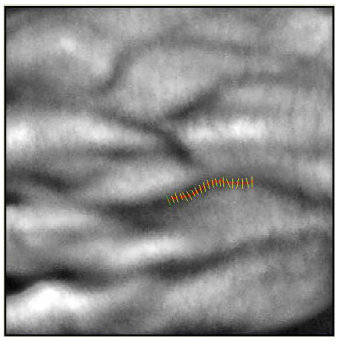

Figure 1.3: A tracking operation during the vessel detection.

The depth of a valley varies with the shading of the image, however the valley remains detectable.

In other words, the profile could provide a robust method to detect the vessels network, this is the reason of the research of a good algorithm to enhance the veins' contrast.

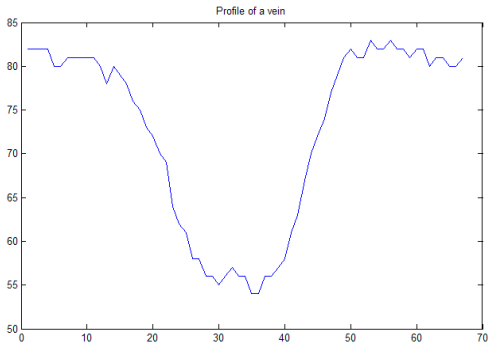

Figure 1.4: Vessel's profile of a general vein.

The starting point is user-provided; when a dark line is not detectable the tracking operation stops and another tracker starts in a different position.

After this step, a binary mask of the vessels network is obtained, ready to be skeletonized and analysed to find possible features, Figure 1.5.

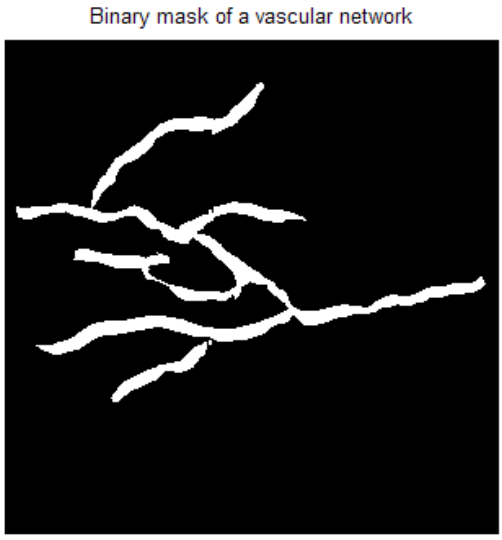

Figure 1.5: Binary mask representing the venous pattern.

I tried to find some quantifiable characteristics to describe uniquely the vein pattern of the back hand, for successive statistical purposes.

Examples of possible features are the branching angles of a junction, the vessel length between junction-junction and junction-end points, the width of the veins.

Figure 1.6 highlights junctions and vessels of a vascular network, a good representation of pattern's shape is via extracting its skeleton.

The skeleton is the thin version of the shape of vein pattern that is equidistant to its boundaries, emphasizes geometrical and topological properties, like connectivity topology length, direction and width.

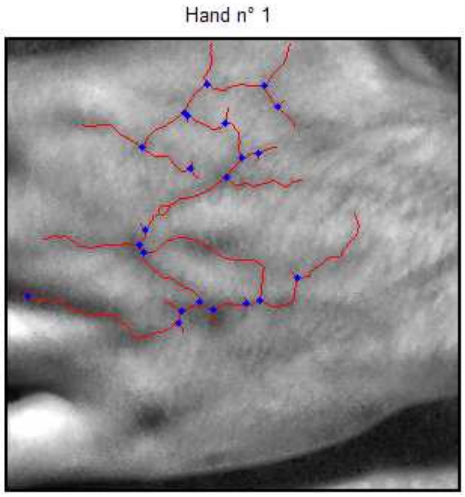

Figure 1.6: Vascular network with junctions(blue) and vessels(red).

The pattern matching is another way to notice differences in the venous pattern of different back hand images.
The images are distincts from each other, as Figure 1.7 displays.

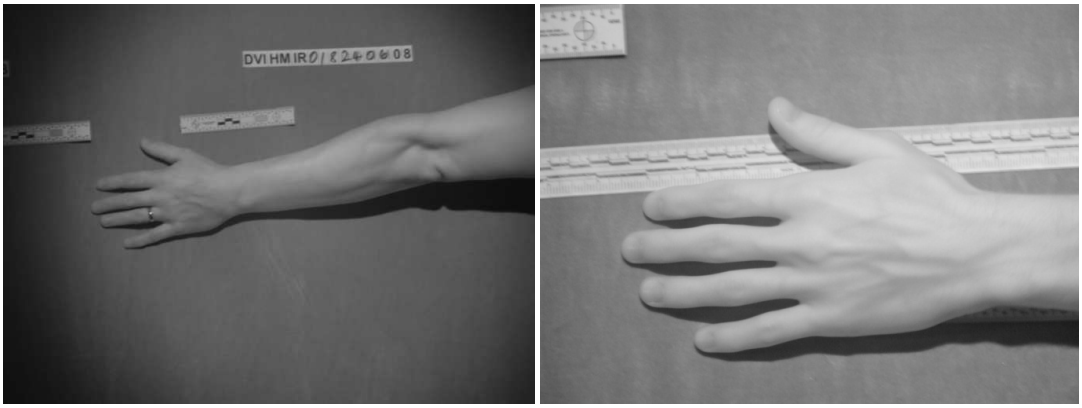

Figure 1.7: examples of different images from the database.

The registration is a fundamental task in pattern recognition, used to match two or more pictures taken, e.g. at different times, sensors, points of view.
In case of transformations of images with more degrees of freedom, as translations, rotations and scale operations, an optimizer algorithm is needed to find the best values to align the images.

A translation on x and y, a rotation and a scale operation is required for the infrared images of the database to register an image with a reference one, and an efficient research has to assure good solutions for their values.

Local optimization techniques such as the gradient descent method are frequently used, but they need good initial values to avoid the local minimum.

For the lack of this information, I used the Particle Swarm Optimization technique, PSO, that is a computation technique, similar to genetic algorithms, developed by Eberhart and Kennedy [50] in the 1995, inspired by social behaviour of bird flocking or fish schooling.

Figure 1.8 shows a result of the pattern matching of two binary masks, the green image is the reference and the red one is the image to be registered.

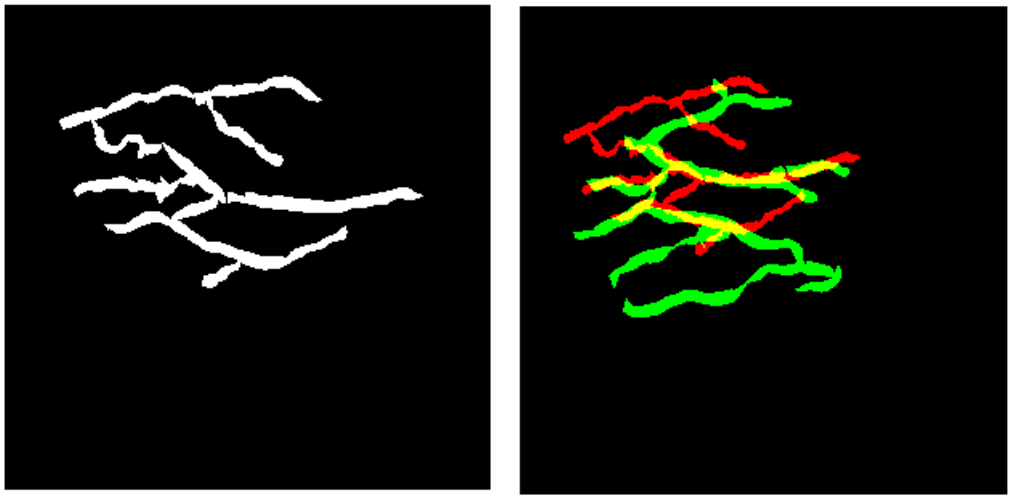

Figure 1.8: Binary mask to be registered on the left; overlap of two binary masks, the reference (green) and the registered (red) after PSO on the right.

Summarizing the main points of this project are: type of acquisition, starting from the IR images; image enhancement, vein pattern segmentation, pattern matching, PSO, features descriptors.

1.2 Outline of the Thesis

The structure of the thesis follows the previous brief description of the steps used for this preliminary initial pilot study.

The remainder of this document is organized as follows: Chapter 2 is a review of all the previous papers linked to the project, it is divided into the main subjects, such as Biometric, Vessel Tracking techniques and Pattern Matching.

From Chapter 3 to 5, the steps of the project are defined: Chapter 3 deals with the enhancement of the infrared images of the back hand, Chapter 4 talks about the extraction of the venous pattern of the dorsum and Chapter 5, skeletonization of the binary mask of the superficial venous pattern and relative features detection and pattern matching, with Particle Swarm Optimization technique.

Chapter 6 explores the experimental results, starting from a general view of the way to acquire the infrared images to the analysis of the discriminative power of the features detected and the uniqueness of the venous pattern.

The conclusions are developed in Chapter 7.

Chapter 2

Related works

2.1 Biometric

2.1.1 Characteristics and Typologies of Biometric Features

The main purpose of this pilot study is to investigate the uniqueness of various quantifiable features of the vessels network of the back hand images, across a population of individuals.

The aim of this analysis is to use the characteristic of uniqueness as a biometric for human forensic identification.

In simplistic terms [1] [2], any human physiological and/or behavioral characteristics can be used as a biometric characteristic as long as it satisfies the following requirements:

- Universality: each person should have the characteristic;
- Distinctiveness: any two person should be sufficiently different in terms of the characteristic;
- Permanence: the characteristic should be sufficiently invariant, with respect to the matching criterion, over a period of time;
- Collectability: the characteristic can be measured quantitatively.

However, in practical biometric system, i.e. a system that employs biometrics for personal recognition, there are other issues that should be considered:

- Performance: achievable recognition accuracy and speed, resources required to achieve the desired recognition accuracy and speed, as well as the operational and environmental factors that affect accuracy and speed;
- Acceptability: which indicates the extent to which people are willing to accept the use of a particular biometric identifier in their daily lives.
- Circumvention: which reflects how easily the system can be fooled using fraudulent methods.

The biometric characteristics or features range from physical traits line fingerprints, faces, retina, to personal behaviors.

The commonly used ones are:

1. *DNA*: Deoxyribonucleic fluid is the one-dimensional ultimate unique code for

one's individuality, except for the fact that identical twins have identical DNA patterns. It is currently used mostly in the contest of forensic applications for person recognition. Three issues limit the use of this biometric for other applications: contamination and sensitivity, it is easy to steal a piece of a DNA from an unsuspecting subject that can subsequently abused about it. Automatic real-time recognition issues: the technology requires cumbersome chemical methods, it is not a geared for online non invasive recognition, and privacy, there is a concern that the unintended abuse of genetic code information that may result in discrimination.

2. *EAR:* it has been suggested that the shape of the ear and the structure of the

cartilaginous tissue of the pinna are distinctive. The ear recognition approaches are based on matching the distance of salient points on the pinna from a landmark location on the ear. These features are not expected to be very distinctive in establishing identity of an individual.

3. *FACE:* face recognition is a non intrusive method, and facial images are probably the most common biometric characteristic used by humans to make a personal recognition. The most popular approaches to face recognition are based on either the location and shape of facial attributes, such as the eyes, eyebrows, nose, lips and chin, and their spatial relationships or the overall analysis of the face image.

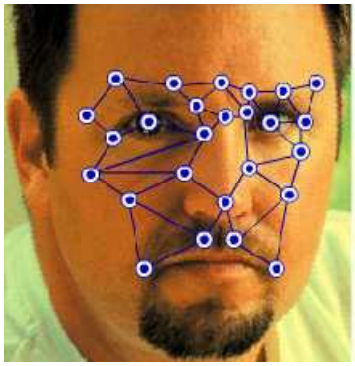

There are a lot of restrictions on how facial images are obtained, sometimes requiring a fixed and simple background or special illumination; plus the face recognition systems have difficulty in recognizing a face from images captured from two drastically different views and under different illumination conditions. The most common input sensors are 2D video or digital cameras, although 3D systems are becoming more commonplace.

4. *FACIAL, HAND, HAND VEINS THERMOGRAM:* the pattern of heat radiated by human body is a characteristic of an individual and can be captured by an infrared camera in an unobtrusive way much like a regular (visible spectrum) photograph. A thermogram-based system does not require contact and it's non invasive, but image acquisition is challenging in uncontrolled environments, where heat emanating surfaces are present in the vicinity of the body. A related technology using near infrared imaging is used to scan the back of a clenched fist to determine hand vein structure. Veins have also been recognized as a unique characteristic because are developed before birth and remain highly stable throughout life, even differing between twins.

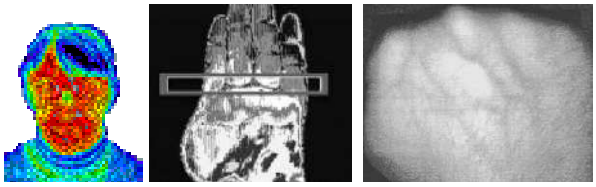

5. *FINGERPRINT:* human have used fingerprints for personal identification for many centuries and matching accuracy using those has been shown to be very high.

A fingerprint is the pattern of ridges and valleys on the surface of a fingerprint, the formation of which is determined during the first seven months of fetal development. Fingerprints of identical twins are different and so are the prints of each finger of the same person. Fingerprints of a small fraction of the population may be unsuitable for automatic identification because of genetic factors, aging, environmental or occupational reasons(e.g. manual workers may have a large number of cuts and bruises on their fingerprints that keep changing).

6. *GAIT:* it is the peculiar way one walks and is a complex spatiotemporal biometric. It is not suppose to be very distinctive, but it is sufficiently discriminatory to allow verification in some low-security applications. It may not remain invariant, especially over a long period of time, due to fluctuation in body weight, major injuries.

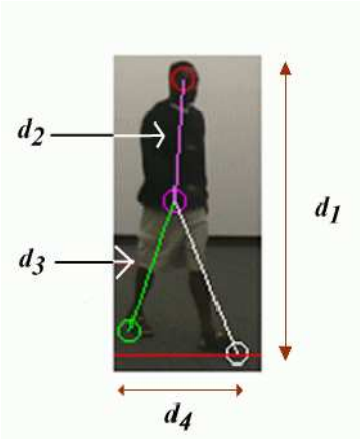

7. *HAND AND FINGER GEOMETRY:* based on a number of measurements taken from the human hand, including its shape, size of palm, lengths and widths of the fingers. Environmental factors do not appear to have any negative effects on the verification accuracy. Geometry of the hand is not known to be very distinctive and hand geometry based recognition systems cannot be scaled up for systems requiring identification of an individual from a large population. Further hand geometry information may not be invariant.

8. *IRIS:* visual texture of the iris is formed during fetal development and stabilizes during the first two years of life. The complex iris texture carries very distinctive information useful for personal recognition. Like the fingerprints, irises of identical twins are different. It is extremely difficult to surgically tamper texture of the iris.

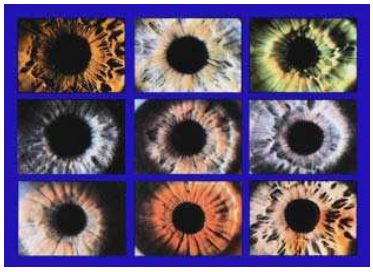

9. *KEYSTROKE:* it is hypothesized that each person types on a keyboard in a different way; it is not expected to be unique but it offers sufficient discriminatory information to permit identity verification. It is a behavioral biometric.

10. *ODOR:* each object exudes an odor that is characteristic of its chemical composition; a component of the odor emitted by a human body is distinctive to a particular individual.

11. *PALMPRINT:* contains pattern of ridges and valleys much like the fingerprints, but even more for its size. Human palms also contain additional distinctive features as principal line and wrinkles.

12. *RETINAL SCAN:* the retinal vasculature is rich in structure and is supposed to be a characteristic of each individual and each eye. It is not easy to change or replicate; the image acquisition requires a person to peep into an eye piece and focus on a specific spot in visual field so that a predetermined part of the retinal vasculature could be imaged. It involves cooperation of the subject, entails contact with eyepiece, requires a conscious effort from the user.

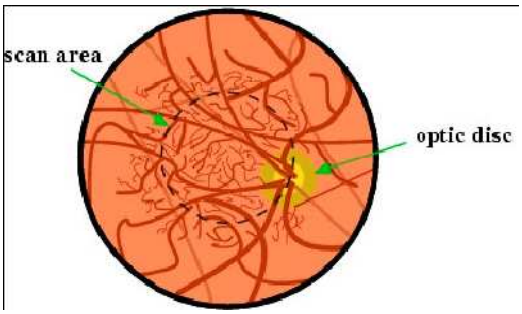

13. *SIGNATURE:* it is a behavioral biometric that change over a period of time and are influenced by physical and emotional conditions of the signatories. Professional forgers may be able to reproduce signatures that fool the system.

14. *VOICE:* it is a combination of physiological and behavioral biometrics. Features of an individual's voice are based on the shape and size of the appendages (e.g. vocal tracts, mouth, nasal cavities, lips) that are used to synthesis of the sound.

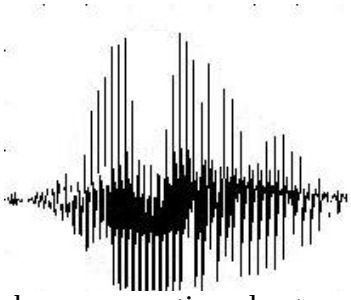

The behavioral part of the speech of a person changes over time due to age, medical conditions, emotional state, etc...

Voice is also not very distinctive and may not be appropriate for large-scale identification. A disadvantage of voice- based recognition is that speech features are sensitive to a number of factors such as background noise.

The Table 2.1 is a comparison of various biometric technologies based on the perception of the authors. High, Medium, and Low are denoted by H, M, and L, respectively.

Biometric identifier	Universality	Distinctiveness	Permanence	Collectability	Performance	Acceptability	Circumvention
DNA	H	H	H	L	H	L	L
Ear	M	M	H	M	M	H	M
Face	H	L	M	H	L	H	H
Facial thermogram	H	H	L	H	M	H	L
Fingerprint	M	H	H	M	H	M	M
Gait	M	L	L	H	L	H	M
Hand geometry	M	M	M	H	M	M	M
Hand vein	M	M	M	M	M	M	L
Iris	H	H	H	M	H	L	L
Keystroke	L	L	L	M	L	M	M
Odor	H	H	H	L	L	M	L
Palmprint	M	H	H	M	H	M	M
Retina	H	H	M	L	H	L	L
Signature	L	L	L	H	L	H	H
Voice	M	L	L	M	L	H	H

Table 2.1 : A comparison of the previous biometric technologies, with level high, low or medium[1].

In another paper [2], I found a recent summary of the range of biometrics and the classification is based accordingly to whether they are physiologically or behaviorally based and whether they are common (i.e. currently in use across a range of environments) still in limited use or under development, or still in research realm (i.e. have not yet been applied in any environment outside of research).

Biometrics	Physiological	Behavioural	Common	Limited	Research
Fingerprint	✓		✓		
Facial	✓		✓		
Hand Geometry	✓		✓		
Iris	✓		✓		
Speaker		✓	✓		
Signature		✓	✓		
DNA	✓			✓	
Ear	✓			✓	
Odour	✓				✓
Retina	✓			✓	
Veins	✓			✓	
Dynamic grip*	✓	✓		✓	
Skin	✓			✓	
Gait		✓		✓	
Lips*	✓	✓			✓
Work pattern		✓		✓	
Fingernail bed	✓			✓	
Thermogram	✓			✓	
Physiometrics	✓				✓
Footprint*		✓		✓	
Tongue	✓				✓

**Lip, dynamic grip and footprint biometrics are so diverse that they fit into both the physiological and behavioural categories*

Table 2.1: Classification of biometrics (adapted from Bolle et al, 2004) [2]

Other biometric features treated in this paper, added to the previous one, are:

15. *FINGERNAIL BED:* ridge and valleys are captured, like in the fingerprints and iris patterns, and are thought to be unique to each individual.

16. *SKIN:* reflectance spectrum of skin and its ability to provide information about the highly-person-dependent distribution of certain light sensitive chemicals, has lead to an increasing amount of research into skin biometrics.

17. *PHYSIOMETRICS:* biological indicators, as brainwaves. The research assumes that brainwaves, like iris and fingerprint patterns, are unique. The figure on the left shows brainwaves depicted in an electroencephalogram trace.

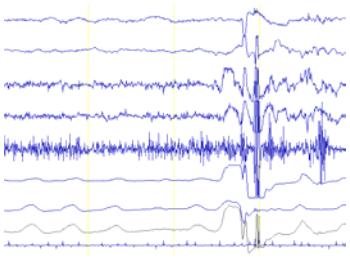

18. *LIPS:* it involves the capture of video footage of a subject's lip motion during a speech.

Type of biometric	What it does	Benefits	Disadvantages
Fingerprint	Measures characteristics associated with the friction ridge patterns on fingertips	• One of the oldest and most widely used biometrics • Relatively high accuracy • Generally fast and easy • Many vendors and forms available	• Dedicated device required • Small percentage of population have unusable prints • Occasional lingering criminal connotation
Face	Measures characteristics of facial features	• Standard still photos or video capture can be used • Passive ("no-touch") capture • Compatible with existing photo databases, such as those used for badging	• Sensitive to lighting conditions • Sometimes affected by eye glasses, facial hair, or expression • Privacy objections to covert use, such as surveillance applications
Iris	Measures the unique features of the random texture patterns of an iris	• Highly accurate; low false-match rate • Passive collection using infrared illumination • Users can wear glasses or goggles • Safe for eyes	• Dedicated device required* • Users sensitive about subjecting their eyes to scanning process • Usability affected by cataracts • Frequently confused with retinal scanning
Voice	Compares live speech with a previously created speech model	• Socially acceptable and nonintrusive • Standard components and audio channels can be used • Language independent • Interoperable with passphrases or challenge/response mechanisms	• Background noise can interfere with capture • Illness and stress can impede effectiveness • Relatively long enrollment times • Large data record generated
Hand geometry	Measures the dimensions of a hand, including the shape and length of fingers	• Deployed extensively for physical-access control and time and attendance • Fast and easy • Noninstrusive • Suitable for outdoor installation	• Devices are bulky—not generally suitable for desktop use • Those with arthritis may find it difficult to use • Somewhat less accurate than other biometrics, but suitable for one-to-one verification

**Dual-purpose iris/video cameras are now available.*

Table 2.2: Benefits and disadvantages of fingerprint, face, iris, speaker/voice and hand biometrics (reproduced from www.dell.com) [2]

Once dealt with general topic of biometric features comparisons, usability, systems, to make an idea of the request of the pilot study, I started to search for papers on hand vein pattern biometrics, and all the related works.

Even if the studies on this topic started in early time, there are not a lot of specific works about it.

2.1.2 Vascular Pattern as a Biometric Recognition System

As I said before, superficial pattern recognition is currently employed as a biometric authenticator in a number of high security areas to heighten the degree of sensitivity surrounding confirmation of personal identity (nuclear installations and banks).
Vascular pattern is influenced by both generic and environmental factors. Genetic factors determine 'where' the veins should form in the developing fetus [19] whereas the specific pattern adopted by the superficial venous network is influenced by individualistic events including position of the fetus in the womb at key ontogenetic periods, composition and density of the surrounding amniotic fluid and oxygen tension in the blood.
As such, the influences of the these individual events result in a pattern that is unique to the individual and can therefore be utilized for personal identification [12].
It is reported that the only characteristics of the venous profile that may change during life are size and degree of tortuosity(varicosity) of individual vessels, as the fundamental pattern and connectivity per se do not vary without outside intervention(sclerotherapy). Not only identical twins have different venous patterns but there is no bilateral symmetry within the individual and for this reason the potential value for this anatomical feature is highly regarded in the security industry.
Vascular pattern remains robust even in the case of such activities as brick laying, gardening, scars, cuts and moisture [9].

The first paper on vascular patterns as a biometric recognition system was published in 2001 [22], because there were disadvantages to solve with the other types of biometric systems commercially available.
In case of fingerprints, direct contact of fingers with the fingerprint-image-extracting sensor causes degradation in performance especially in factory construction sites where good quality fingerprints are hard to obtain due to oil from the fingers, moisture, dirt...

In the case of iris/retina scanner, users must place the eye close to the scanner, causing an uncomfortable feeling or privacy-infringing feeling.

About the hand-shape recognizers, problems may arise with users who suffers from arthritis or rheumatism.

The Im at Al [22] system acquires a vein pattern image, without direct contact with the hand or with the vein-pattern-extracting sensor, there exists no contamination.

Both user comfort and performance are improved and stable operation is also expected. The proposed pre-processing algorithm and processor architecture for vein pattern extraction follows these diagrams in Figure 2.1:

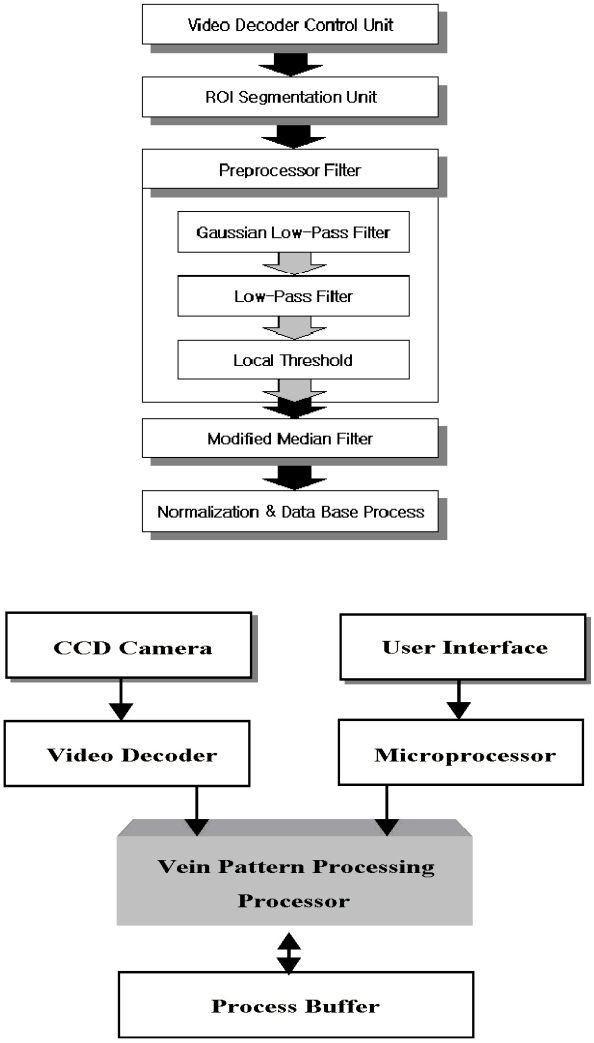

Figure 2.1: Block diagrams of the algorithm of Im et Al,2001 [22]

It takes 5 steps:

1. Extracts a region where hand vein patterns are concentrated and defines this region as the ROI;
2. Processes the proposed pre-processing algorithm step by step on the grabbed ROI image with only the vein pattern emphasized;
3. Applies a local threshold process and separates the vein pattern from the background, which results in the first vein pattern image;
4. Applies a modified median filter so the noise caused by hair, curvatures and thickness of fatty substances under the skin is removed;
5. Stores the final vein pattern image after the normalization and the database process are finished.

Two years later, a second paper was published by the same authors [23].
The algorithm was improved, adding the directional information of vascular patterns.
It applies two filters to the image: row vascular pattern extraction filter (RVPEF) for effective extraction of the abscissa vascular patterns and column vascular pattern extraction filter (CVPEF) for effective extraction of ordinate vascular patterns.
They used the combined output of both filters to obtain the final hand vascular patterns, in this way it prevents loss of vascular pattern connectivity.

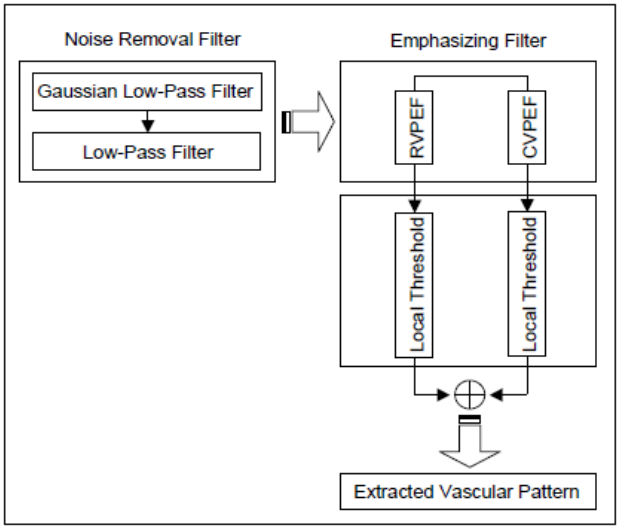

Figure 2.2: Processing flow diagram of the proposed algorithm [23].

After the DBVPE filter, a median filter is applied to remove noise caused by hair, skin curvatures and fatty substances under the skin.

I tried to find other papers about the hand vascular pattern technology, but the papers are not a lot, and not at all specific.

In general, the operations involved in a typical vascular biometric identification are more or less the same:

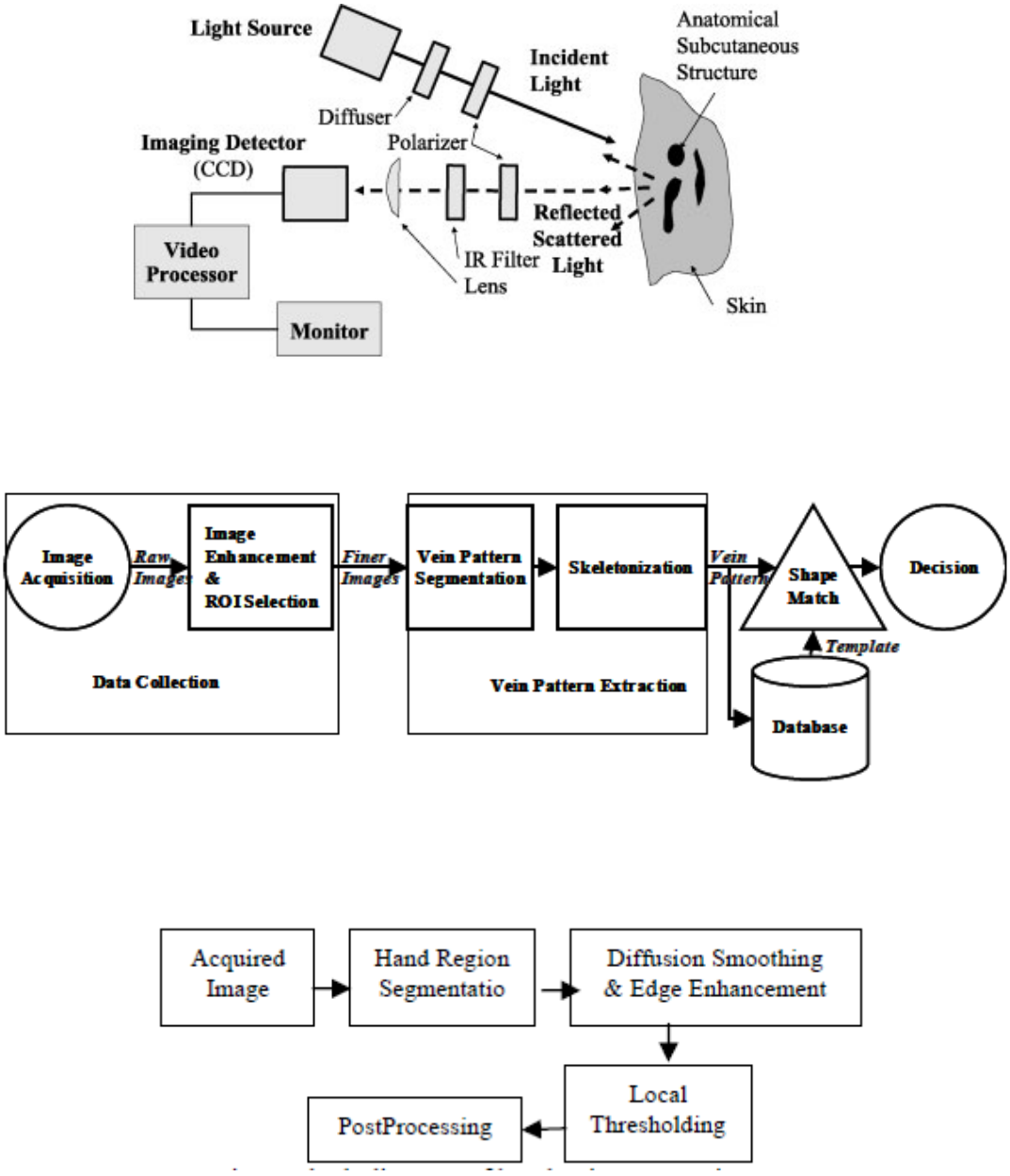

Figure 2.3: Block diagram of hand verification systems.

A general hand vascular pattern technology is explained in [13].

Since the hand vascular network lies under the skin, it cannot be seen by human eye. Therefore we cannot use visible light, which occupies a very narrow band 400-700 nm wavelength, for photographing.

Hand vascular patterns can only be captured under near-IR light (800-1000 nm wavelength) which can penetrate into the tissues. Blood vessels absorb more IR radiation than the surrounding tissue [14] which causes the blood vessels to appear as black patterns in the resulting image captured by a charge-couple device (CCD) camera.

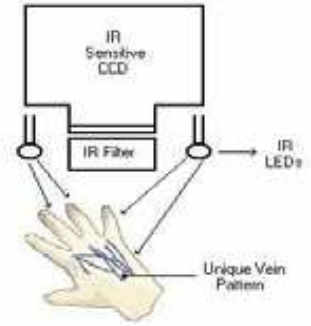

Figure 2.4: CCD camera [8]

The scanner uses a LED array to emit the light and illuminate the hand. A CCD camera sensitive to near-infrared light is used to photograph the image. A near-infrared filter is attached in front of the CCD camera to block all undesired visible light emitted by external sources. The image of blood vessels can be acquired by either reflection or transmission.

1. *Transmission*: hand is illuminates by a LED array and the CCD camera captures the light that passes through the hand.

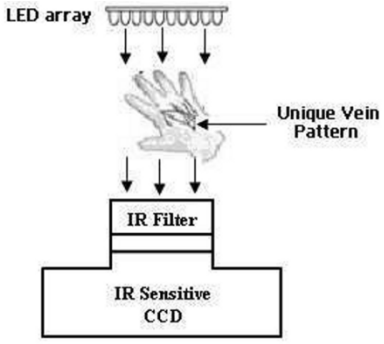

2. *Reflection*: the hand here is illuminated by a LED array and the CCD camera captures the light that is reflected from the hand. This method is referred since the transmission one is sensitive to changes in the hand's light transmittance, which is easily affected by temperature or weather. If the hand's light transmittance is relatively high, the blood vessels are not very clear, in contrast, the light

transmittance does not significantly affect the level or contrast of the reflected light.

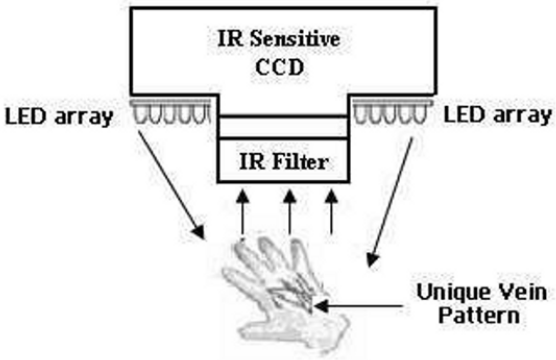

The vascular patterns are then extracted by various digital signal processing algorithms, because there is noise, irregular effects such as shadow of the hand and hairs on the skin surface. A typical feature extraction algorithm consists of various image processing steps to remove noise and irregular effects, enhance the clarity of vascular patterns, separate vascular patterns from the background. The final vascular patterns obtained are represents as binary images, display of the method in Figure 2.5.

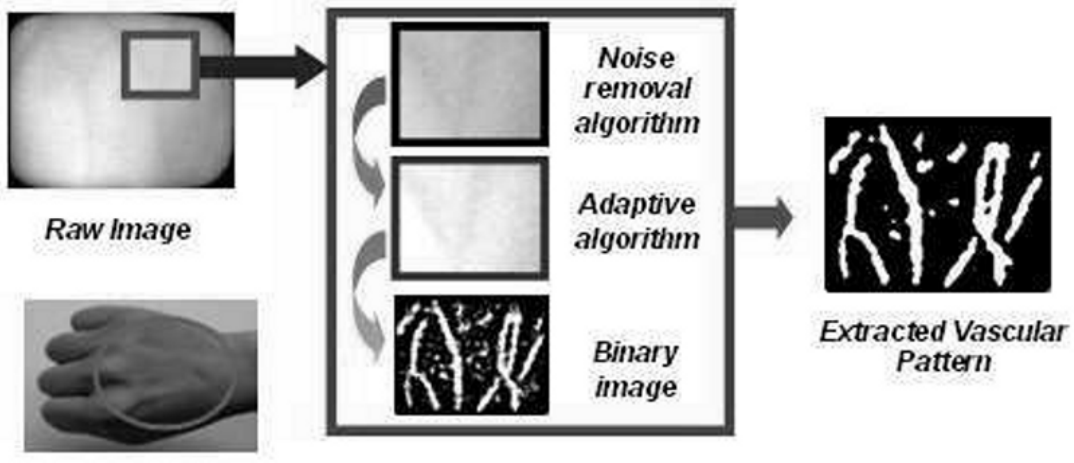

Figure 2.5: Digital processing algorithm to extract the vascular network as binary mask. [13]

The extracted vascular pattern is then compared against pre-registered patters in database to authenticate the individual. A matching score is used to can be authenticated or typical methods are structural matching and template matching.

One is based on comparing locations of feature points such as line endings and bifurcations extracted from to patterns being compared to obtain matching score.

The second one is widely used; it is based on the comparison of pixel values of two vascular pattern images.

Summarizing the main steps are image acquisition, feature extraction and pattern matching.

Another algorithm is proposed by Crisan et Al [25], Figure 2.6 shows it.

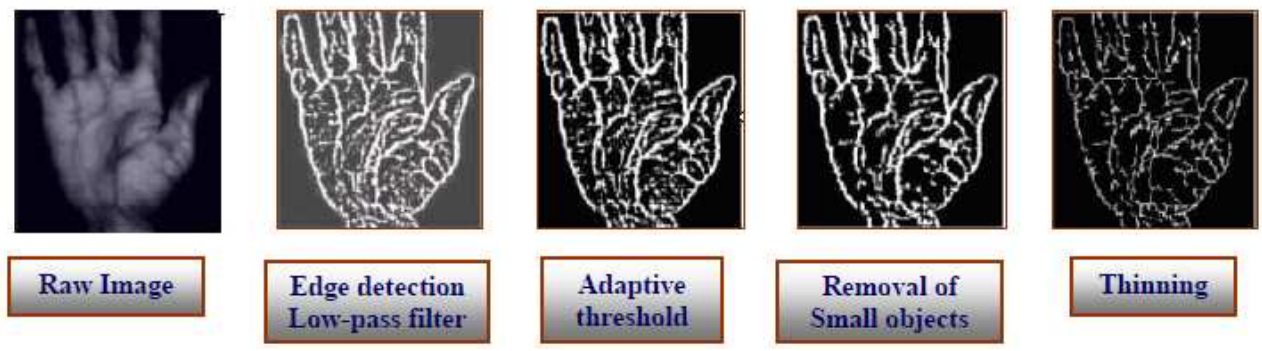

Figure 2.6: Proposed steps of the algorithm of [25]

Consecutive contrast operations in conjunction with a low pass Gaussian filter are used to enhance the image of the vein model, then a threshold is applied thus creating a binary image outlining the vein pattern.

The threshold cannot be applied statistically, since the images will differ due to the depth of the vein pattern for different subjects. The best approach is an adaptive threshold calculated in different part of the image.

After, a thinning algorithm is applied and all-lines are converted into a 1-pixel-width lines in order to compensate for the effects of aging, temporally vessel constriction or dilation, and other factors that can modify the width of the veins.

It is also necessary if the measurement data has been collected at various time stamps.

Wang and Leedham [14] use the same model of the hand vein pattern verification system(Figure 2.3) : image acquisition; image enhancement using a 5x5 median filter to remove speckling noise, 2D Gaussian low pass filter to suppress the effect of high frequency noise.

A normalization is applied to permit a specified mean and variance value for the images.

Let I(x, y) denote the intensity value at position (x, y), the mean and variance are μ and σ^2, respectively, then for an image sized NxM, I'(x, y) normalized image is obtained using pixel-wise operations where μ_d and σ_d^2 are the desired values for mean and variance:

$$I'(x,y) = \begin{cases} \mu_d + \sqrt{\dfrac{\sigma_d^2 (I(x,y) - \mu)^2}{\sigma^2}} & I(x,y) > \mu \\ \mu_d - \sqrt{\dfrac{\sigma_d^2 (I(x,y) - \mu)^2}{\sigma^2}} & otherwise \end{cases}$$

Next steps are vein pattern segmentation, utilising a local adaptive thresholding algorithm, and skeletonization.

Vein pattern matching is the last operation which consists of calculating the line segment Hausdorff distance(LHD) between a pair of vein patterns, to compare similarity of shapes. Basically it is a distance measure between two point sets.

Principally Wang and Leedham investigated infrared imaging technologies for acquiring hand vein networks for biometric purposes, concluding that the NIR imaging is the best choice for vein pattern biometrics.

FIR, far-infrared, and NIR, near-infrared, imaging are studied; the two infrared bands acquire the images using different physical phenomena and therefore exhibit differences in image quality and features, Figure 2.7 and 2.8.

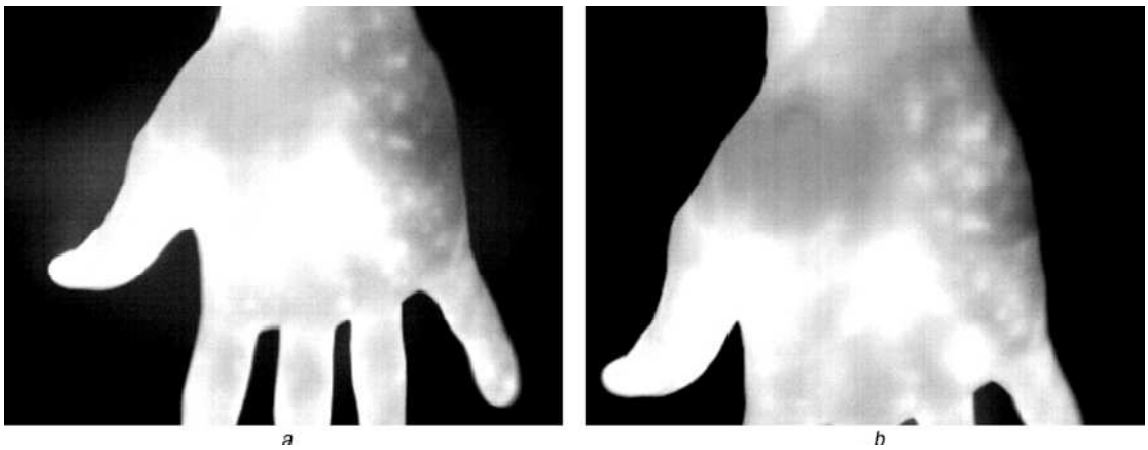

Figure 2.7: FIR images in a normal environment [14]

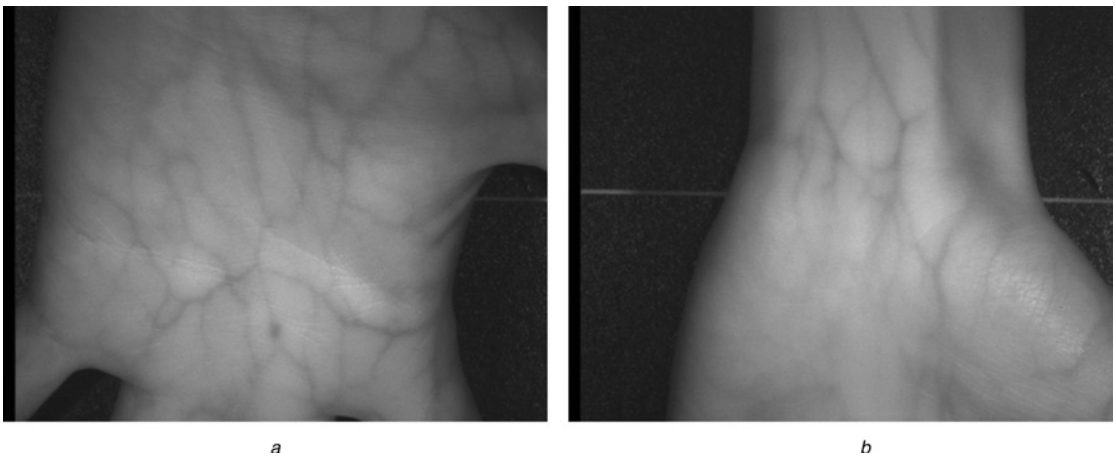

Figure 2.8: NIR images of palm and wrist of an hand.[14]

FIR imaging operates by detecting electromagnetic radiation emitted from the human body in wavelength range 8-14 μm and discern the presence of the veins near the surface of the skin by exploiting the fact that the blood in the veins is warm than the surrounding tissue.

NIR imaging operates quite differently by exploiting the fact that the haemoglobin in the blood absorbs incident IR radiation with wavelength in 700-900 nm range (just outside the visible light one, 300-700 nm).

FIR imaging can capture the veins in the back of the hand, is sensitive to the ambient temperature and humidity conditions and temperature variation of the human body.

Each image will result in flaring or ‘white-out’ of some parts of the image.

NIR imaging as observed to perform better by producing good quality images when capturing vein patterns in the back of the hand.

It is more tolerant to the changes in ambient environmental and body temperature conditions.

However, NIR imaging faces the problem of corruption from skin features such as hair, cuts, external marks and palm prints.

FIR does not suffers from these problems as images are not affected by the visible light.

2.1.3 Acquisition of the Images for Biometric Purposes

Usually a commercially available conventional charge-couple device(CCD) monochrome camera is used to obtain thermal image of the back of the hand [4].

Though principally designed for use in visible light, CCD cameras are also sensitive to near IR wavelengths of the electromagnetic spectrum up to about 1100 nm. This is an actinic IR range, which covers the near IR spectrum from 700-1400 nm.

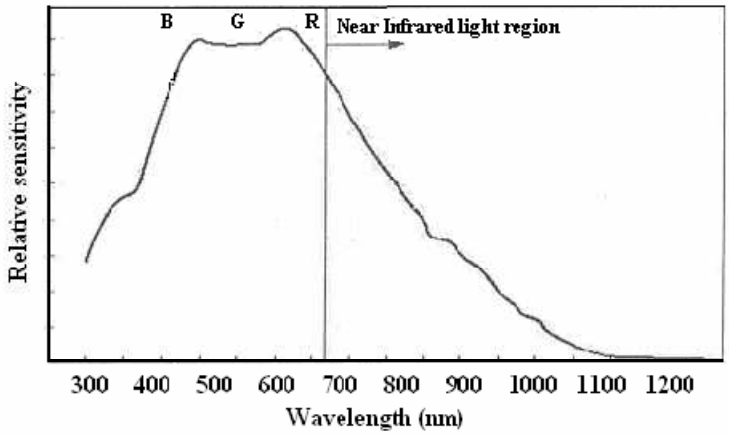

Figure 2.9: Spectral sensitivity characteristic of CCD sensor. [4]

The greatest intensity of IR radiation emitted by the human body is 10 mW/cm^2 and it's in the range of 3000-14000 nm.

Unfortunately CCD camera has no sensitivity in this region, consequently after experimentation with a variety of light sources, it was found to be necessary to irradiate the back of the hand using an IR cold (solid-state) source.

The reduced haemoglobin in venous blood absorbs more of the incident IR radiation than the surrounding tissue thus appearing darker.
The depth of absorption and radiation of actinic IR in biological tissue is approximately 3nm, and so thermal IR radiation provides information only about surface(skin) temperatures of biological objects.
In other words, only the subcutaneous vascular network is discernible in the image.
However, as sais before, the distinctiveness of the network depends on the thickness of the overlaying skin, on the degree of venous engorgement, conditions of vein walls and on the nearness of the veins of surface.
The steps studied by Shanin and Al (2007) [4] are the same, as the last diagram of Figure 1.3 explains.

2.1.4 Enhancement Algorithms for Infrared Images

Summarizing, the main problem of IR images is that [25] IR does not penetrate all kinds of tissue in the same manner and therefore images taken from various subjects may vary significantly in terms of clarity of the vein model and in some severe cases the resulting image may have connectivity problems, several regions could be blurred or even impossible to detect.
Vein model can be seen but the image is not clear enough for machine vision and pattern recognition.
Basically, these papers talk about median filters, Gaussian filters and normalization steps to enhance the images to deal with.
Other papers deal with other specific methods to enhance the IR images.
In [29], the main purpose is to investigate the performance of a three-step procedure for fingerprint identification and enhancement using CLAHE, the contrast limited adaptive histogram equalization, together with ‘Clip Limit’, standard deviation and sliding neighbourhood.
Firstly CLAHE with clip limit is applied to enhance the contrast of the small tiles existing in the fingerprint image and to combine the neighbouring tiles using a bilinear interpolation in order to eliminate the artificially induced boundaries.

'Clip Limit' is applied to avoid over saturation of the image, specifically in homogeneous areas that present high peaks in the histogram of certain image tiles due to many pixels falling inside the same gray level range.

Usually histogram equalization is applied to enhance the image's contrast by transforming intensity values of the image:

$$s_k = T(r_k) = \sum_{j=1}^{k} p_r(r_j) = \sum_{j=1}^{k} n_j/n$$

where s_k is the intensity value in the processed image corresponding to r_k in the input image, and $p_r(r_j)$= 1,2,3...L is the input image intensity level.

In other words the values in a normalized histogram approximate the probability of occurrence of each intensity pixel level in the image. Figure 2.10 displays how histogram equalization works.

Figure 2.10: Fingerprint before and after histogram equalization[29].

However by enhancing the contrast of an image through a transformation of its intensity values, histogram equalization can amplify the noise and produce worse results than the original image, due to many pixels falling inside the same gray level range.

Instead of that, CLAHE is used, Figure 2.11 shows the result.

Figure 2.11: Fingerprint before and after CLAHE.[29]

Second step, the image is decomposed into an array of distinct blocks and the discrimination of the blocks is obtained computing the standard deviation of matrix elements to remove the image background and obtain the boundaries for region of interest.
Finally, using a slide neighbourhood processing, an enhancement of the image is obtained by clarifying the endpoints and bifurcations in each specific pixel, thinning process.

Another recent paper that deal with histogram equalization in general is [26].
It talks about a combination of high-frequency emphasis filtering and histogram equalization; it overcomes the influence of luminous intensity and thickness of the back hand skin.
High-frequency emphasis filtering is used to give prominence to vein texture, and the histogram equalization is adopt to enlarge the contrast.
An image can be blurred by attenuating the high-frequency components of its Fourier transform, the opposite process, edges and other abrupt changes in gray levels are associated with high-frequency components, image sharpening can be achieved in the frequency domain by an high-pass filtering process, which attenuates the low-frequency components without disturbing high-frequency information in the Fourier transform.
It is well known that hand vein texture is associate d with abrupt changes in gray level of the image; they simply multiply a high-pass filter function by a constant and add offset so that high-frequency components of the image are enhanced and the gray-level tonality due to the low-frequency components is retained.

2.2 Vessel Tracking Techniques

When the enhanced image is obtained, the next step, as showed in all the block diagrams of Figure 2.3, is to extract the vessel network.
Lots of research projects have been carried out to develop automatic computerized systems for the extraction of the vascular structures[35] [38].

Techniques to automatically extract vessels may be divided into two families:

1. *Template-matching techniques*: they do not guarantee to work properly in presence of large variability in vessel calibre distributions since the template has to be turned into a reference vessel calibre. Computationally it's very demanding as they involve the processing of the entire image with a large number of filters.

2. *Tracking techniques*: analysis of local areas to trace the vessel. They start from a point on a vessel and move along it as far as possible by analyzing consecutive local areas, e.g. drawing scan, line across vessel. They can detect vessel centrelines or boundaries by analyzing pixels orthogonal to the tracking direction.
   Methods to identify vessel profile along the scan line are based on matched filters, morphological filters, optimization of Gaussian profiles, fuzzy c-mean classifiers, grouping of edge pixels, model based locally adaptive thresholding. A more sophisticated approach is the use of graph representation, so segmentation process is reduced to find the optimum path in the graph of the image.
   Typically start and end points have to be provided by the user.
   They only process pixels close to the vasculature adding the processing of every image pixels, for this reason, they are appropriately called 'exploratory algorithms' [33].
   A number of factors [35] and expected properties should guide the design of the tracking algorithm:
   - The tracker should obviously exploit the parallel nature of vessel borders;
   - It should be tolerant to broken edges, jump over gaps between edges ad still keep tacking a vessel;

- It should be tolerant to noise, degrade gracefully when following a wrong track induced by edge detection artifacts;
- It should not be stopped by bifurcations;
- It should extract most of the vascular network while minimizing user intervention.

2.2.1 Matched Filters

An example of matched filter is the paper of Chutatape (1998) [39] but they are still in use.

According to the known blood vessel feature, a second order derivative Gaussian matched filter is designed and used to locate the centre point and width of a vessel in its cross sectional profile. Together with the Extended Kalman filter is employed for optimal linear estimation of the next possible location of blood vessel segment by appropriate formulation of its pattern changing process and observatory model.

A blood vessel is considered to be a linking of many small segments, each vessel segment is defined by three parameters: direction (v_i), width of lumen (w_i) and centreline midpoint $t(c_i)$.

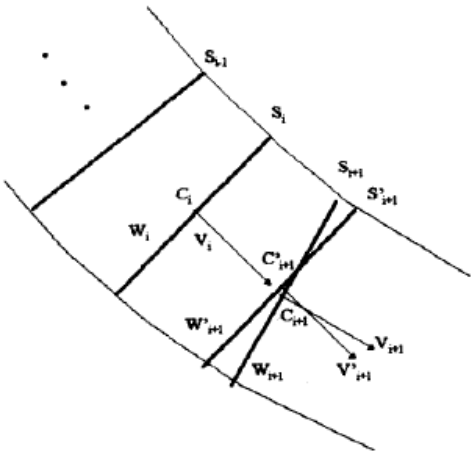

Figure 2.12: Estimate vessel segment and the actual one located by the matched filter.[39]

Given current and all previous vessel segments $S_1...S_i$, the estimation of S_{i+1} is obtained through the Kalman filter. Then the Gaussian filter locates the truly next vessel segment

based upon cross sectional density profile at the estimated position and direction and update the record.

For Can and Shen (1998) [33] the tracking method is based on adaptive exploratory processing of the image, directly at the image intensity level, without preprocessing, adding image wide pixel processing operation such as filters, edge operators, morphological filters and segmentation.
First step, algorithm explores image along a grid of one-pixel-wide lines, estimating frame contrast and brightness level and seeking out local grey-level minima.
Second step, sequence of exploratory searches initiated at each of the validated seed points.
The core of the tracing algorithm is based on the use of a set of 2D correlation kernels that act as low pass differentiations perpendicular to the direction of the vessels, and low-pass averaging filters along the vessel.

A fuzzy C-mean classifier is considered by Tolias et Al (1998) [38]. The theory of fuzzy sets allow the efficient manipulation of ambiguities by using linguistic variable to describe vague concepts like existence of a vessel. It uses only the fuzzy intensity information in order to track a vessel without any assumptions for shape of vessels sought and without utilizing edge information that is usually corrupted by noise.
The tracking algorithm starts letting vessel and non vessel be two linguistic values defined for the fuzzy variable 'vessel profile'. The fuzzy vessel tracking process is based on finding the membership functions of the two linguistic values.
Let p(s) be the set of pixels that belongs to a profile normal to the vessel direction v_p with $s_n = [l(n), j(n)]^T$ the pixel coordinates and n the number of pixels in the profile.
The number of pixels that constitute a profile is 3 times the vessel diameter calculated in the last valid profile, $n = 3Dp_1$.
Membership functions for non vessel $m_{nonvessel}(s)$ and vessel, $m_{vessel}(s)$, are defined on the universe of discourse $\{s|s \epsilon p(s)\}$ taking values in the range [0, 1].

Tracking terminates if one of the following conditions hold:

- vc_p vessel contrast, is lower than minimum contrast resolved by human eye $vc_p <$ 0.2 (Weber law);
- number of separate vessel regions found within a profile is greater than 2;
- the diameter calculated for a profile is lower than a threshold, or greater than 50% of the last calculated diameter.

In this case, the last valid vessel point is marked as a termination point and the algorithm starts tracking the vessel whose starting point is first in stack of the candidate start points.

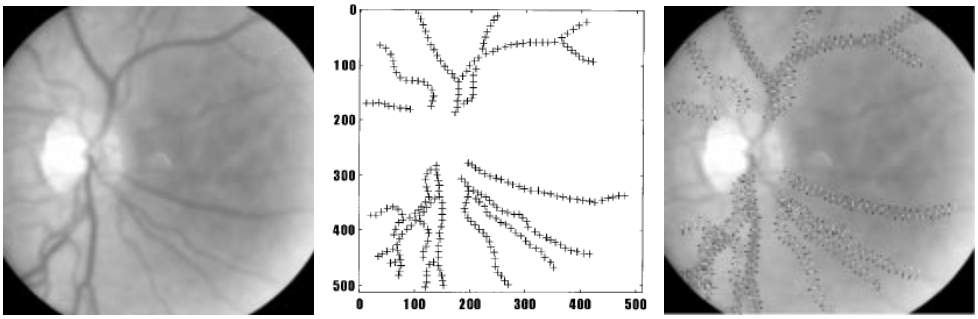

Figure 2.13: Result of the vessel tracking with the centrelines detected, and the vessel profiles and vessel memberships analyzed. [38]

Lalonde et Al. (2000) [35] faced the tracking steps with a non recursive paired tracking algorithm. It's designed to rack the borders of a vessel sequentially, following one border at a time while registering presence of 'twin' border, until one of the following events occurs: end of the line is reached; a junction is met as a consequence; a piece of vessel is analysed twice and both analyses should be in agreement.

Ability of the algorithm to jump over gaps and be beyond bifurcations is provided by a seed generation mechanism that analyses some properties of twin points and creates new starting points for subsequent tracking according to rules such as connectivity between twin points.

Tracking is performed in the edge map I(x,y) produced in edge direction phase, but it also makes the use of orientation map $\Theta(x,y)$ computed by the Canny operator. The orientation map is filtered before its use.

Each point in Θ(x, y) gives us an estimate of the orientation θ of the normal to the edge at (x, y).

A tracking attempt is initiated from a triple (c_o, $\overrightarrow{p}_o$, dir) called a seed: c_o is a point in I(x, y) called origin, $\overrightarrow{p}_o$ sets the progress direction and dir equal to 1 or -1 and specifies which direction to look at when searching for a twin point.

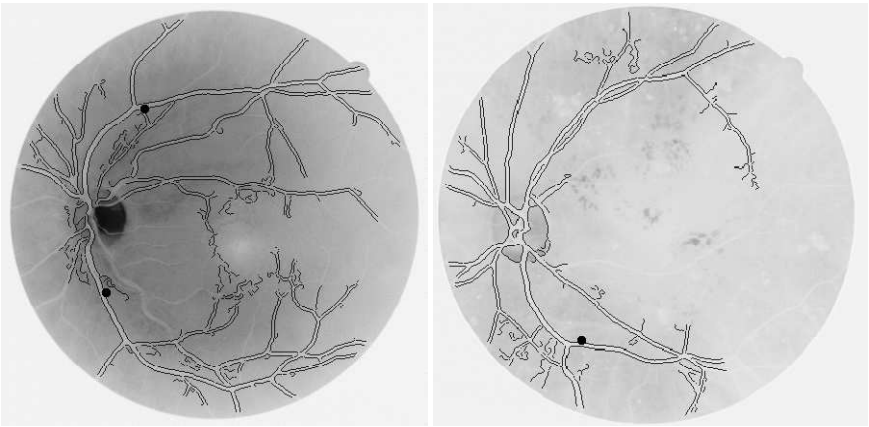

Figure 2.14: Tracking results, in black the seed points.[35]

Grisan et Al. (2004) [40] studied a fully automatic system for extraction of retinal vessel structure and related features. Based on sparse tracking techniques, exploiting a fuzzy c-mean classification for vessel across section identification. A subsequent refinement step eliminates false vessels and connects vascular network with a greedy algorithm; bifurcations and crossing are then identified.

The modules are:

- seed points extraction;
- bubble analysis module: for identifying vessel calibre and direction;
- tracking: moves along a vessel calculating at every step its varying direction, calibre and centre. When this procedure is not able to go on further along a vessel segment, it involves the bubble analysis, for a new seed points beyond the area that made the tracking process stop. When all the points have been analyzed, tracking of vascular structure is completed.
- False vessel elimination, correction, bifurcations and crossings.

The tracking is an analysis of consecutive cross sections of a vessel; a tracked point can be described by the quaternion $p_i = (x_i , y_i , \theta_i , d_i)$ containing the x and y coordinate, direction θ, calibre d of the i^{th} vessel point.

The versor $v = (\cos(\theta), \sin(\theta))$ represents the most likely direction for a new vessel point to be found, starting from p_i given a constant tracking step s:

$$(\hat{x}_{i+1}, \hat{y}_{i+1}) = (x_i, y_i) + s * \underline{v}$$

The cross section of a vessel can be very noisy, making the recognition of the vessel boundaries difficult. To have a better signal to analyze, and using the a priori information that an ideal vessel has an almost constant grey level pattern locally along its course, we can extract n cross sections of equal lengths, but with centre displaced along the new direction $\underline{v}$.

Pixels in the filtered cross section are classified with a fuzzy c-mean clustering applied to their gray-levels, and then defuzzified by applying a probability threshold, in order to obtain an hard classification into vessel and non vessel pixels.

Sequences of consecutive vessel pixels are interpreted as candidate profiles, whose mean is evaluated and compared to the mean of non vessel pixels. If the difference is lower than a constant threshold, the sequence is discarded as noise. The predicted vessel point is the redefined with the information a posterior.

The module takes care that a point belongs to one and only one vessel segment, avoiding overlapping vessels but also preventing crossover points to belong to two vessels at the same time.

The last, but more similar to the method used successively, is a paper of Miura et Al. (2004) [36].

As I said before, a cross sectional profile of a vein appears as a valley. The depth of the valley varies with the shading in the image, however the valley remains detectable. The profile is a robust method of finger-vein detection.

The line-tracking operation starts at any pixels of the captured image, the current pixel position id called the ‘current tracking point’ and it’s moved pixel by pixel along the dark line.

The depth of the cross sectional profile is checked around the current tracking point.

Direction of the dark line can be detected by checking depth of the valley by varying θ_i at which the valley is deepest. After that the current tracking point moves to the pixels closest to this direction. If valleys are not detectable in any direction θ_i, the current point is not on a dark line and a fresh tracking starts at another position

If only a single line tracking operation is conducted, only a part of veins within the image will be tracked. To solve, vein tracking sequences are started at various positions that are determined so that the line-tracking scan is conducted evenly across the image.

The number of times that each pixel has become the current tracking point is record in a matrix named the locus space.

Paths of the finger veins are obtained as chains of high-value positions in the locus space.

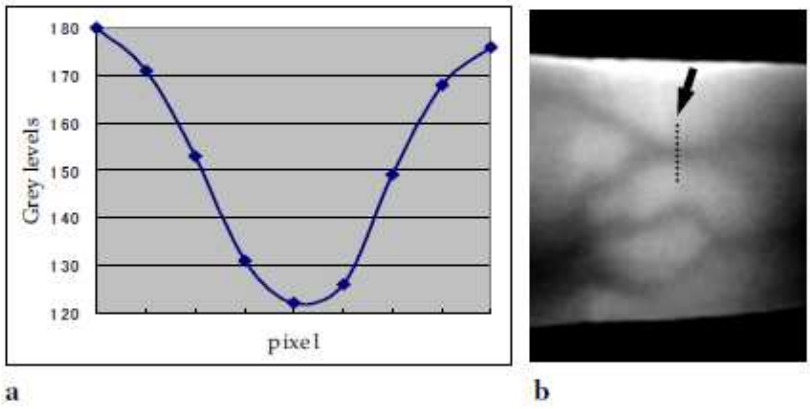

Figure 2.15: Cross-sectional brightness profile of a vein. a. Cross sectional profile, b. Position of cross section. [36]

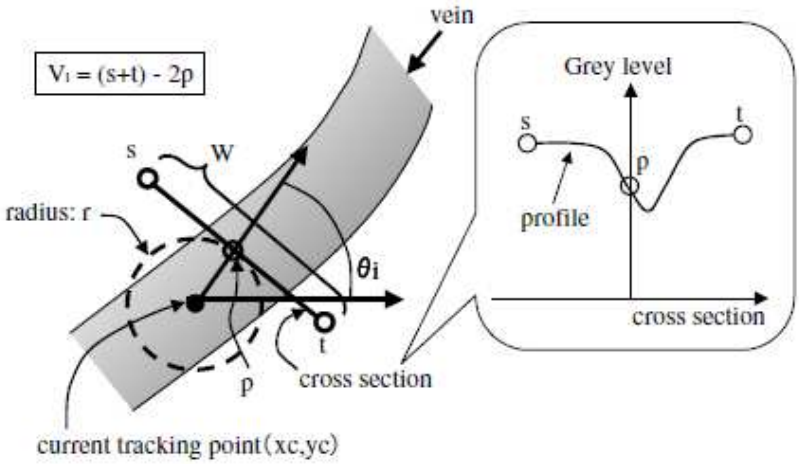

Figure 2.16: Dark line detection.[36]

2.3 Image Registration and Pattern Matching

2.3.1 Image Registration Techniques

After image acquisition [8], and hand vein pattern extraction sub stages, I have binary images containing the segmented back of the hand vein pattern.
The initial images are completely different one from each other in terms of initial resolution, and way of acquisition.
To compare them, for a subsequent pattern matching, or to determine the number of intersections, relative angles, length of vein segments and other relevant data according to the degree of the complexity set by the desired application,[25] the registration of the images is required.
Image registration [44] is the process to overalying two or more images of the same scene taken at different times, from different points of view and/or different sensors.
It geometrically aligns two images, the reference and the sensed one. The present differences between images are introduced due to difference in aging conditions.
Image registration is a crucial step in all image analysis tasks in which the final information is gained from the combination of various data sources like in the image fusion, change detection, multichannel image restoration.

Its applications can be divided into four main groups according to the manner of the image acquisition:

- *Different points of view*: images of the same scene are acquired from different points of view. The aim is to gain larger a 2D view or a 3D representation of the scanned scene;
- *Different times*: images of the same scene are acquired at different times, often on regular basis, under different conditions. The aim is to find and evaluate changes in the scene which appeared between the consecutive image acquisitions;
- *Different sensors*: images of the same scene are acquired by different sensors. The aim is to integrate the information obtained from different source streams;

- *Scene to model registration*: images of a scene and a model scene are registered. The model can be a computer representation of the scene, maps or digital elevation models, another scene with similar content, 'average' specimen. The aim is to localize the acquired image in the scene/model and/or to compare them.

Due to the diversity of the images to be registered and to various types of degradations, it is impossible to design an universal method applicable to all registration tasks.
Every method should take into account or not only the assumed type of a geometric deformation between the images but also radiometric deformations and noise corruption, required registration accuracy and application data characteristics.

Nevertheless, the majority of the registration methods consists of the following four steps:

1. *Feature detection*: salient and distinctive objects are manually or automatically detected. For further processing, these features can be represented by their point representatives (centre of gravity, line endings, distinctive points), called control points;
2. *Feature matching*: the correspondence between the features detected in sensed image and those detected in the reference image is established. Various feature descriptors and similarity measures along with spatial relationships along features are used for that purpose.
3. *Transform model estimation*: type and parameters of the so-called mapping functions, aligning the sensed image with the reference image, are estimated. The parameters of the mapping function are computed by mean operations established feature correspondence.
4. *Image re-sampling and transformation*: sensed image is transformed by mean of the mapping function. Image values in non integer coordinates are computed by approximate interpolation techniques.

The implementation of each registration step has its typical problems. First the decision of what kind of features is appropriate for the given task, those should be distinctive objects, which are frequently over images and are easily detectable, and their physical interpretability is demanded.

Detected features set in the reference and sensed images must have enough common elements, even in situations when the images do not cover exactly the same scene or when there are object occlusions or unexpected changes.

In the feature matching step, problems caused by an incorrect features selection or by image degradations can arise.

Matching algorithm in the space of invariants should be robust and efficient, single features without corresponding counterparts in other images should not affect its performance.

The type of the mapping function should be chosen according to the a priori known information about the acquisition process and expected image degradations. If no a priori information is available, the model should be flexible and general enough to handle all the possible degradations which might appear.

Moreover, the decision about which difference between images have to be removed by registration has to be done.

Registration methods can be categorized with respect to various criteria. The ones usually used are the application data, dimension of the data, type and complexity of assumed image deformations, computational cost and essential ideas of registration algorithm.

Two main approaches to feature understanding have been formed:

1. *Area-based methods:* correlation-like methods or template matching merge the feature detection step with the matching part. These methods deal with images without attempting to detect salient objects.
2. *Feature based methods*: in contrast with the previous methods, they do not work directly with image intensity values. They are suitable for situations when illumination changes are expected or multisensory analysis is demanded.

If the images are deformed with more complex transformations, there are other possible methods, like correlation methods, Fourier methods, mutual information methods and optimization methods.

The last ones deal with the research of the minimum of dissimilarity measure(penalty function) or the maximum of similarity measure, it is a multidimensional optimization

problem, where the number of dimensions corresponds to the degrees of freedom of the expected geometrical transformation.

The only method yielding global extreme solution is an exhaustive search over the entire image.

Although is computationally demanding, it is often used if only translations are to be estimated.

In case of transformations with more degrees of freedom or in case of more complex similarity measures, sophisticated optimization algorithm are required, which help to localize maxima or minima

2.3.1.1 Registration for Hand Vein Pattern Systems

Evaluating the papers that deal with hand vein pattern for biometric purposes, I found different ways of registration and subsequent matching techniques.

In Badawi et Al.(2007) [8] a rigid registration technique is used, since they already constrained the data acquisition system with the attachment in order to prevent any large translation or rotation.

One of the second images remained stationary while a 2D transformation is applied(x and y translation, rotation) on the other image in order to align it with the first pattern to find the maximum correlation percentage between two hand vein images. The scale is not counted.

The matching(similarity) percentage is calculated as the ratio of the count of overlapped white pixels between input images and the number of white pixels in one of the two input images (image with the minimum count of white pixels). They calculated the matching ratio for each transformation step then they choose the maximum ratio as the final matching ratio between two input patterns.

$$correlation(T_x, T_y, \theta) = Forall_{T_x,T_y,\theta}(|x \cdot T| * 100)/\min(|x|, |T|)$$

$$Maxcorrelation = \max(correlation(T_x, T_y, \theta))$$

where x is an image which contains the first test binary pattern, T is the second one, - is the AND, || is a summation of ones in the matrix.

Summarizing, image registration [48] is to determine a mathematical mapping that is the best match of two or more images. To register a float image I_F to a reference image I_R can be express mathematically as:

$$I_R(x,y) = \varsigma(I_F(T_\alpha(x,y)))$$
$$(x',y') = T_\alpha(x,y)$$

where ς is the intensity or radiometric calibration function, T_α is the transformation function, which maps two spatial coordinates a and y, to the new spatial coordinates x' and y' by the set of parameters α.
Intensity based image registration [49] can be mapped as a typical optimization problem:

$$\alpha^* = argoptima_{T_\alpha}(S_{T_\alpha}(I_F, I_R))$$

α^* is an optima estimation by the optimization algorithms.
Local optimization techniques such as the gradient descent method are frequently used for medical image registration. But these methods need good initial values for estimation in order to avoid the local minimum.

2.3.1.2 PSO: Particle Swarm Optimization Technique

The optimization considered is the PSO, particle swarm optimization, technique originally designed by Eberhart and Kennedy (1995) [50]. It is a computational intelligence technique it's not largely affected by the size and linearity of the problems and can converge to the optimal solution in many problems where most analytical methods fail to converge.
It is a concept originated as a simulation of a simplified social system [53], the original intent was to graphically simulate the graceful but unpredictable choreography of a bird flock or a fish school.

PSO [54] is initialized with a group of random particles (solutions) and then searches for optima updating generations. After finding the best values, the particle updates its velocity and positions with particular equations.

Each particle(individual) adjusts its 'flying' according to its own flying experience and its companions' flying experience instead of using genetic operations.

Each particle is treated as a point in a D-dimensional space; the i^{th} particle is represented as $X_I = (x_{i1}, x_{i2}...x_{id}...x_{iD})$.

The best previous position (position giving the best fitness value) of the i^{th} particle is recorded and represented as $P_I = (p_{i1}, p_{i2}...p_{id}...p_{iD})$. Index of the best particle among all the particles in the population is represented by symbol g.

The rate of the position change (velocity) for particle i is represented as $V_I = (v_{i1}, v_{i2}...v_{id}...v_{iD})$.

The particles are manipulated according to:

$$v_{id} = w * v_{id} + c_1 * rand() * (p_{id} - x_{id}) + c_2 * Rand() * (p_{gd} - x_{id})$$

$$x_{id} = x_{id} + v_{id}$$

Those are the d^{th} dimensional component of the position and velocity of the i^{th} particle at time step t. *Rand()* and *rand()* enhance the exploratory nature of PSO, p_{id} is the d^{th} component of the best(fitness) position that the i^{th} particle has accomplished by t.

p_{gd} is the d^{th} component of the best global position achieved in the population.

c_1 and c_2 are known as cognition and social factors as they control the relative strengths of individualistic and collective behaviour of each particle.

w is the inertia weight, it was developed to better control exploration and exploitation.

Suitable selection of it, provides a balance between global and local exploration and exploitation and results in fewer it on average to find a sufficiently optima solution.

A large value of the inertia weight facilitates global exploration while a small inertia tents to facilitate local exploration in the current search area.

For implementing a global version of the PSO the process is as follows [53]:

- Initialize a population (array) of particles with random positions and velocities on a D-dimension in problem space;
- For each particle, evaluate the desired optimization fitness function in d variables;
- Compare particle's fitness evaluation with particle's *pbest*, best solution that it's achieved so far. If the current value is better than *pbest*, then set *pbest* value equal to the current value, *pbest* location equal to the current location in the D-dimensional space;
- Compare fitness evaluation with population's overall previous best. If the current value is better than *gbest* (overall best value achieved so far by any particle in the population), then resets *gbest* to the current particle's array index and value.
- Change the velocity and the position of particle according to Formula ()
- Loop to the second step until a criterion is met, usually a sufficiently good fitness or a maximum number of iterations (generations).

The performance of PSO is depending on setting of control parameters: inertia weight, acceleration constants, maximum number of iterations, initialization of population. The inertia is usually a monotically decreasing function of the number of iterations.
The goal of image registration is to find the optimal parameters which determine the relative position and orientation of the two sensed images.

2.3.2 Pattern Matching for Biometric Purposes

When we are talking about biometric purposes, we are interested in determine the similarity between images. The crux of a matcher is a similarity function which quantifies the intuition of similarity between two representations of biometric measures [10] [45].

There are four best known for pattern recognition:

1. *Template matching*: matching, in general words, is used to determine similarity between two entities (points, curves or shapes) if the same type. Here, a template

(2D shape) or a prototype of the pattern to be recognized is available. The pattern to be recognized is matched against the stored template while taking into account an allowable pose (translation, rotation) and scale changes.

2. *Statistical classification*: each pattern is represented in terms of features or measurements and is viewed as a point in a D-dimensional space. Features points are like line endings and bifurcations, so the goal is to choose those features that allow pattern and vectors belonging to different categories to occupy compact and disjoint regions in a D-dimensional feature space.

3. *Synthetic or structural matching:* adopt a hierarchical perspective where a pattern is viewed as being composed of simple sub patterns which are themselves built from yet simpler sub patterns. These sub patterns to be recognized are called primitives and the given complex pattern is represented in terms of interrelationship between these primitives.

4. *Neural networks:* massively parallel computer systems consisting of an extremely large number of simple processors with many interconnections.

Miura et Al. [36] a mismatch ratio is calculated to examine whether or not two sets of data have a correlation with each other.

The ratio R_m is defined as the difference between two sets of data to be matched . R(x, y) and I(x, y) ate the values at position (x, y) of the registered and input matching data, w and h are the width and height of both sets of data, c_w and c_h the distances in which motion in the vertical and horizontal directions, is required to adjust the displacement between the two sets of data, and the template data are defined as the rectangular region within R(x, y) whose upper-left position is R(c_w, c_h) and lower-right position is R(w – c_w, h - c_h).

Value of mismatch N_m(s, t) which is the difference between the registered and input data at the positions where R(c_w, c_h) overlaps with I(s, t) is defined as:

$$N_m(s,t) = \sum_{y=0}^{h-2c_h-1} \sum_{x=0}^{w-2c_w-1} \{\phi(I(s+x,t+y), R(c_w+x, c_h+y))\}$$

$$\phi(P_1,P_2) = \begin{cases} 1 & if|P_1 - P_2| = 255 \\ 0 & otherwise \end{cases}$$

Parameter that indicates whether a pixel labeled and part of the vein region overlapped with each other. The minimum value of N_m can be defined as

$$N_m = min_{0\le s<2c_w, 0\le t<2c_h} N_m(s,t)$$

So:

$$R_m = N_m / \left\{ \sum_{j=t_0}^{t_0+h-2c_h-1} \sum_{i=s_0}^{s_0+w-2c_w-1} \phi(I(i,j),0) + \sum_{j=c_h}^{h-c_h-1} \sum_{i=c_w}^{w-c_w-1} \phi(0,R(i,j) \right\}$$

The member at the denominator is the number of pixels that are classified as belonging to the vein region in the two data sets.

Wang, Leedham and Cho [28] achieved the vein pattern matching by measuring the Hausdorff distance between a part of the vein patterns; it is a distance measure for comparing similarity of shapes; and between two point sets.

For two point sets $M^P = \{m_1^P, m_2^P ... m_k^P\}$, $T^P = \{t_1^P, t_2^P ... t_k^P\}$:

$$H(M^P, T^P) = \max(h(M^P, T^P), h(T^P, M^P))$$

$$h(M^P, T^P) = 1/N_m^P \sum_{m_i^P \in M^P} min_{t_j^P \in T^P} \left\| m_i^P - t_j^P \right\|$$

where the first equation is the undirected formula, the other one is the directed, and N_m^P is the number of points in M^P.

Using spatial information of an image, lacks of local structures such as orientation come when there are shapes of curves to compare.

LHD, line segment Hausdorff distance, is calculated to match the shape of vein patterns, because it incorporates structural information of line segment orientation and line-point association.

Given two finite line segment sets $M^l = \{m_1^l, m_2^l ... m_p^l\}$ and $T^l = \{t_1^l, t_2^l ... t_p^l\}$, LHD is built on the vector $\vec{d}(m_i^l, t_j^l)$ representing the angle distance, the parallel distance and the perpendicular distance:

$$\vec{d}(m_i^l, t_j^l) = \begin{bmatrix} d_\theta(m_i^l, t_j^l) \\ d_{||}(m_i^l, t_j^l) \\ d_\perp(m_i^l, t_j^l) \end{bmatrix}$$

Numerical value of the distance is given by:

$$d(m_i^l, t_j^l) = \sqrt{(w_a * d_\theta(m_i^l, t_j^l))^2 + {d_{||}}^2(m_i^l, t_j^l) + {d_\perp}^2(m_i^l, t_j^l)}$$

The directed and undirected LHDs are defined in Formula (), where $l_{m_i^l}$ is the length of the line segment m_i^l:

$$h_l(M^l, T^l) = \frac{1}{\sum_{m_i^l \in M^l} l_{m_i^l}} \sum_{m_i^l \in M^l} l_{m_i^l} * min_{t_j^l \in T^l} d(m_i^l, t_j^l)$$

$$H_l(M^l, T^l) = \max\left(h_l(M^l, T^l), h_l(T^l, M^l)\right)$$

Skeletons of each vein patterns are firstly broken at each junction points and resulting in number of curve segments. For each individual curve segment, points are sampled in a 5-pixel interval to represent the curve segment.

Using these sample points as end points, a set of line segments representing the shape of the vein pattern are obtained.

As I said before, another interesting paper is that of Badawi et Al. [8]
Determining an appropriate similarity metric is a very difficult problem since it should be able to discriminate between the representations of two different identities despite noise, structural and statistical variations in the input signals, aging and artifacts of feature extraction module.
In light of operational environments mentioned above, the design of similarity functions and matching algorithm needs to establish and characterize a realistic model of variations.

2.4 Features Selection and Shape Indicators

For statistical and biometric purposes, I mean, to find shape descriptors for statistical pattern recognition, processing algorithms are then used in order to determine number of intersections, relative angles, length of vein segments and other relevant data according to the degree of complexity set by the desired applications.

The software used is based on the work of Di Ruberto et Al. [55], that describes a method to automatic 2D shape recognition, based on finding a skeletal representation of a shape which resumes its geometrical and topological features, useful for indexing in a database of shapes.
In general, recognition approaches fall into two classes: the first one, feature-based methods that represent each object as collection of line segments, curves, corners and regions; the second one, a number of approaches consider an object as a single feature in high-dimensional space.
The goal of that paper is both to find the global information suitable to guide matching and create a model that summarizes the shape of an object to use for indexing in a database of objects.

A version of the object that is as thin as possible is created, the skeleton of medial axis, the thinnest representation of the original object that presents the topology and its geometric properties adding synthesis and understanding.

The medial axis of an object is the locus of the centres of the maximal disk that can be inscribed within the object.

The detection of the end points, junction points and curve points of medial axis is important for a structural description that captures the topological information embedded in the skeleton.

Formally the definition of end point is a point of 1-pixel width digital curve with a single pixel among its 3x3 neighbourhood.

Junction point is a point of 1-pixel width digital curve with more than two curve pixels among its 3x3 neighbourhood.

Curve point has two curve pixels among its 3x3 neighbourhood.

The thin line can be converted into a graph associating the curve points with the edges , the end and junction points with the vertices.

Such a skeletal graph can then be used as an input to graph matching algorithm.

In this case, an algorithm for detecting skeleton characteristic points based on a morphological approach is introduced.

The skeleton has been pruned in an adaptive way in order to achieve a more regular and effective representation for a percent indexing. A parametric morphological pruning is applied to eliminate short branches on a skeleton, till stability is reached; it removes the end points of an image.

All the pixels belonging to a chain of the skeleton and laying within a distance of less than 5% of the skeleton's length from an end point are removed.

This structural representation is particularly suited to effective and generic shape matching.

To extract end points, they perform erosion transform with the complement of each structuring element SE, defining an end point $\bar{A}$ and its rotation $\theta_i(\bar{A})$, on the complement of the skeleton X, $\bar{X}$, the union of all the results is taken and then it's intersected with X:

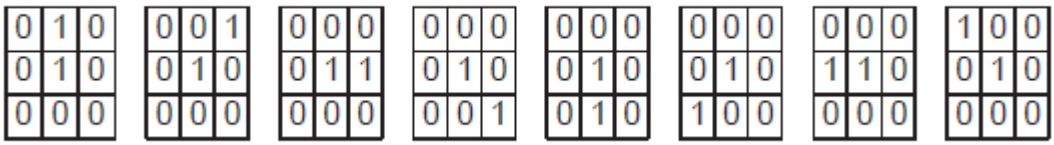

Figure 2.17: SEs for the end points: the fundamental A (in bold) and its rotations $\theta_1(A)$; $\theta_2(A)$; ... ; $\theta_7(A)$ in order. [55]

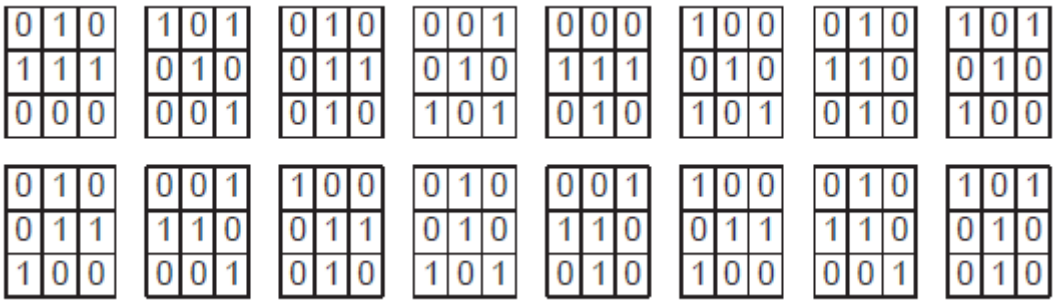

Figure 2.18: SEs for the junction points: B (in bold) and its rotations (θ_1 (B); ... ; θ_7(B)) in the top row and C (in bold) and its rotations. [55]

$$ENDPOINTS(X) = \left[\bigcup_i \varepsilon_{\theta_i \bar{A}}(\bar{X})\right] \cap X$$

$$JUNCTIONPOINTS(X) = \left[\bigcup_i \varepsilon_{\theta_i B}(X)\right] \cup \left[\bigcup_i \varepsilon_{\theta_i C}(X)\right]$$

where ε is the erosion operation.

The filtered skeleton, with end points and junction points as vertices and the skeleton parts as links, can be interpreted as a graph.

Figure 2.19: A wrench binary shape and its morphological skeleton before pruning[55]

Figure 2.20: The skeleton after pruning short external branches and after eliminating short internal branches.[55]

From the skeleton an attributed skeletal graph is built (ASG) to organise in a structured way information about object shape and topology embedded in its thinned representation. This graph can used as a structural object model allowing comparison of different objects by means of a graph matching algorithm.

The attributed skeletal graph defined allows to discriminate different shapes in a database, producing comparable results, but demonstrating its robustness in presence of scale, reflection and rotation transformations and showing ability to handle noise and occlusions.

Chapter 3

Acquisition and Enhancement of Infrared Images

This pilot study is a collaboration done at the University of Dundee, between the School of Computing and the Centre for Human Anatomy and Identification.

I was collaborating with Helen Meadows, a PhD student at the Centre for Human Anatomy and Identification.

Miss Meadows provided me with pictures and information on her project, and kept me up to date, throughout the year with weekly meetings.

Miss Meadows has been working on this project titled “Limb Vein Pattern Analysis: a Biometric for Human Forensic Identification” [11] for two years now, with the supervision of Prof. Sue Black and Dr Roger Soames.

Prof. Sue Black and the NPIA (National Police Improvements Agency via the National Injuries Database) introduced vein pattern recognition in the forearm to the courts in a ground breaking criminal trial where, for the first time, this concept is being used to address issues pertaining to the identification of a suspect from images associated with a case of alleged child abuse.

Her project will improve the work that has already begun in this area, examine and analyze the superficial venous pattern of the upper and lower limbs to determine the veracity of such pattern analysis to a forensic environment.

Infrared images have been recorded and assessed to determine whether a positive identification can be established on the basis of feature and model prediction data contained within the superficial venous pattern of the limbs and whether this information has a viable forensic application with regards to stability of data.

This is the first time that work of this nature has been linked to an anatomy department and it represents a growing realization by commercial firms that their technology must be predicated on sound anatomical fact and biological understanding.

The collaboration with the School of Computing was made because the main goal is to characterize in an automatic way the detection of superficial venous pattern in general anatomical parts of the human body, instead of their manual way to find it.

The principal motivation of this project is to automated the tracing of the vessel network, that was performed before with the use of Photoshop CS4, drawing the venous pattern manually. An example of the vessels pattern obtained is in Figure 3.1, comparisons between the vessels networks detected by Miss Meadows and the ones detected at the end of the project are shown in Appendix.

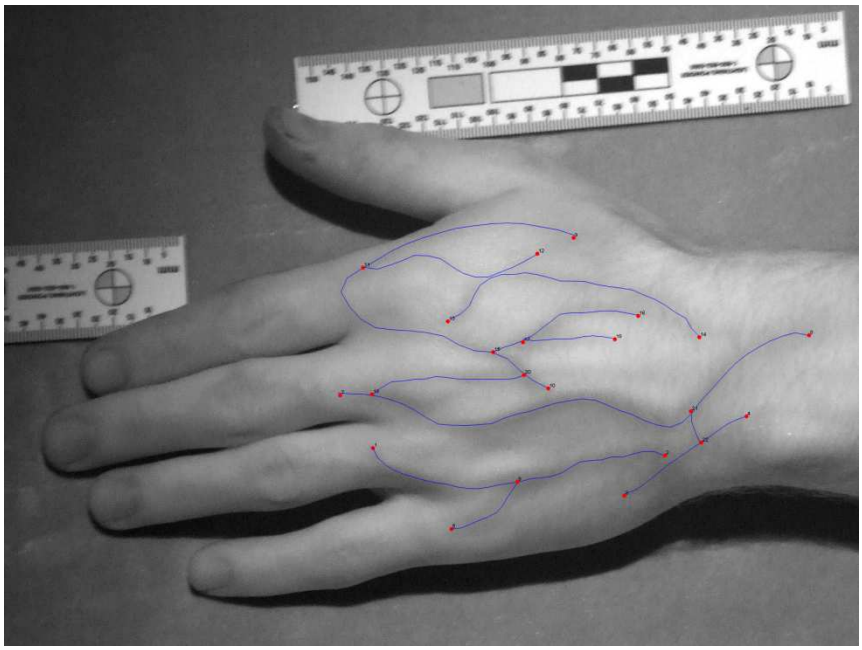

Figure 3.1: Tracing of the veins with Photoshop.

In particular the pilot study handles with the back hand images (Figure 3.2).

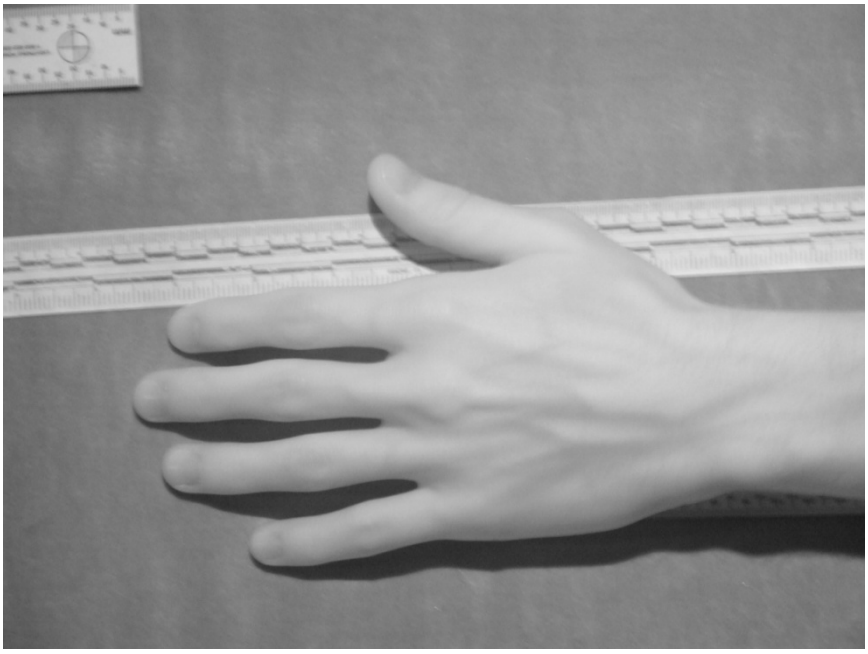

Figure 3.2: Example of infrared back hand image.

The starting set of images was formed by arms, legs, feet images; some examples of these images follow in Figure 3.3, 3.4 and 3.5.

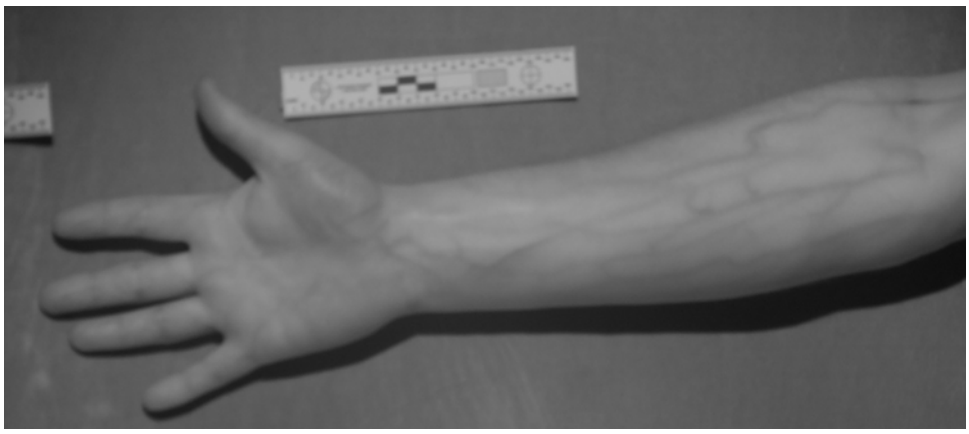

Figure 3.3: Example of arm image.

Figure 3.4: Example of feet image.

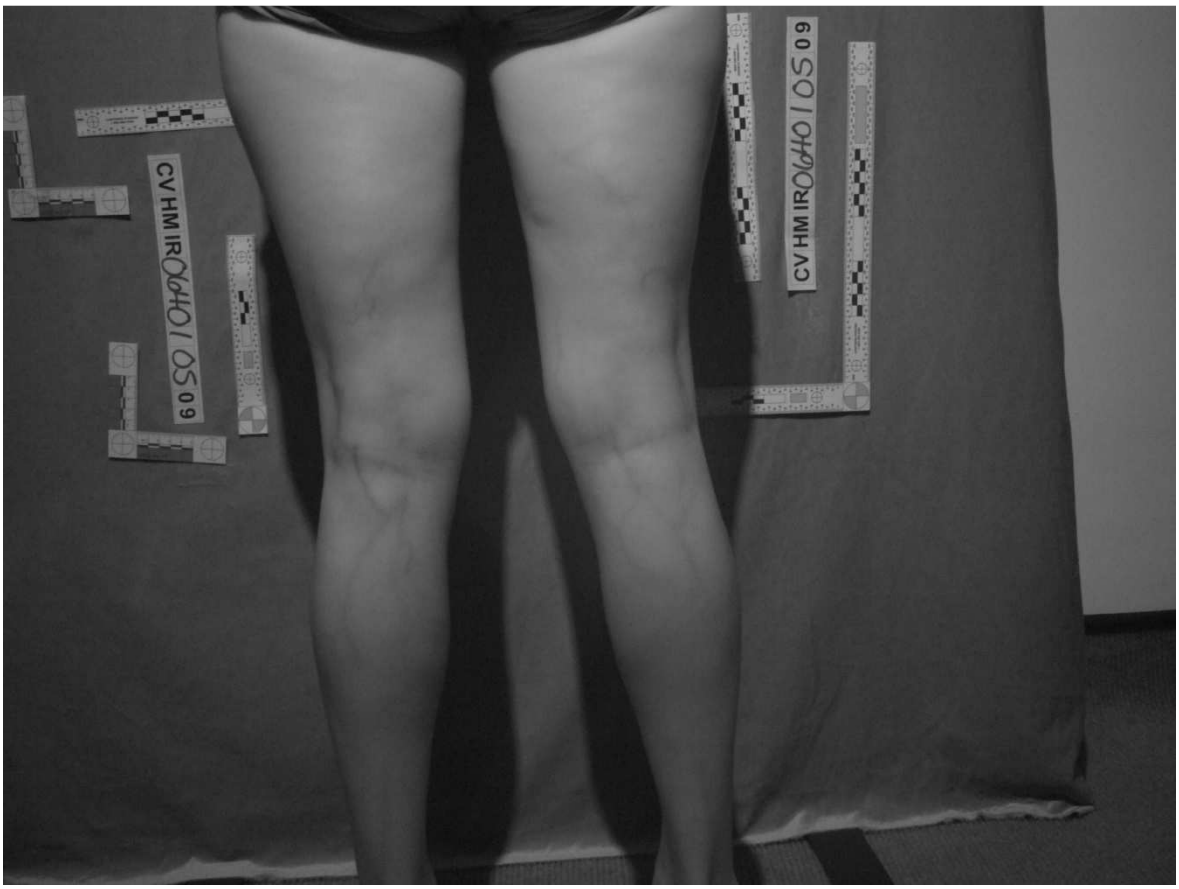

Figure 3.5: Example of legs, the infrared image is not clear enough to work with.

3.1 Infrared Images: Contrast Problems and Application of Enhancement Algorithms

At the beginning of the research, I observed different kind of images that I was going to work with and I started to analyse the characteristics of each one.
A major problem that came up with working with the infrared images was the lack of contrast. As can be seen in the lack of difference between the Fig. 3.6.

Figure 3.6: Visible image (left) and infrared image(right) of a back hand.

The main problem for those, and also in general, infrared images that I am going to use it is the lack of contrast, for example, making a comparison with the correspondent visible images, the difference between them is not a lot. This comes out not only in a visible way but also from a computer vision point of view.

The detection of the vessels network is done through the application of algorithms working on the depth of the profile of a vein, that appears in this way:

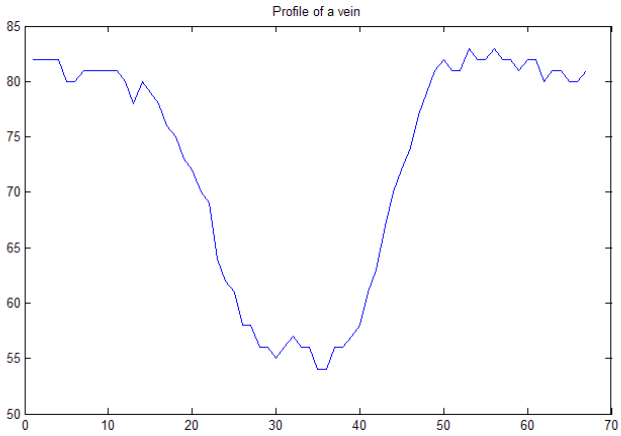

Figure 3.7: Profile of a vein, with good contrast.

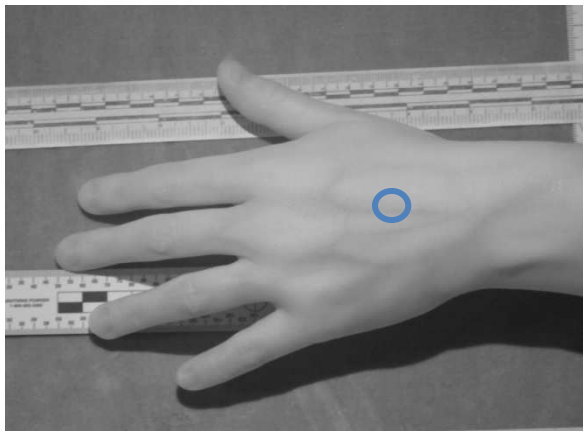

Figure 3.8: A low contrast back hand image with a circle indicating the vein of interest.

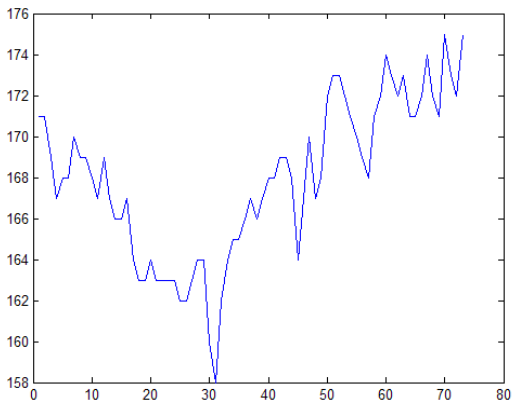

Figure 3.9: Profile of the vein from a low contrast image.

In many medical practises X-ray and ultrasonic scanning are used to obtain vascular images. Although these methods can produce high quality images of blood vessels, they are invasive techniques as they require injection of contrast agents into the vessels.
Obtaining vein pattern images in a non invasive manner is the key challenge in a vein pattern biometric system. Infrared imaging provides a non contrast data acquisition method and requires no injection of agents into the blood vessels.
It is potentially a suitable non invasive method to acquire vein pattern images.
The interest in the use of IR imaging has grown considerably, due to the non ionizing aspect of the IR radiation.

As noticed in my case, there are two aspects that limit the application of infrared radiations.
The first aspect is the reduced and different penetration of the radiations in the tissue of the human body, it is different because the rays do not penetrate all kinds of tissue in the same manner.
The second aspect is the low thermal contrast of the subject, which manifests itself as low image contrast. Generally the temperature difference between target objects and their background is small, and the temperature of the background is high, which results in IR images with highly bright background and low contrast between background and target.
The degree of accuracy of a IR image is given by factors, such as the depth of veins' model beneath the skin, the flow of haemoglobin, the veins' thickness, the specular reflection and the high scattering effect.
As said previously, the veins' model can be easily seen, but the image is not clear enough for machine vision and pattern recognition.

It is for these reasons that a good enhancement algorithm, or more, must be applied before starting the approach to the analysis of the vessels network.

3.1.1 Enhancement Algorithms

3.1.1.1 First Design: Manta-Ray Function

The first aim would be to find a method to enhance the contrast of the two images. This was quite time consuming as the contrast was very low and the images were quite different one from the other one, for example Figure 3.10 and 3.11.

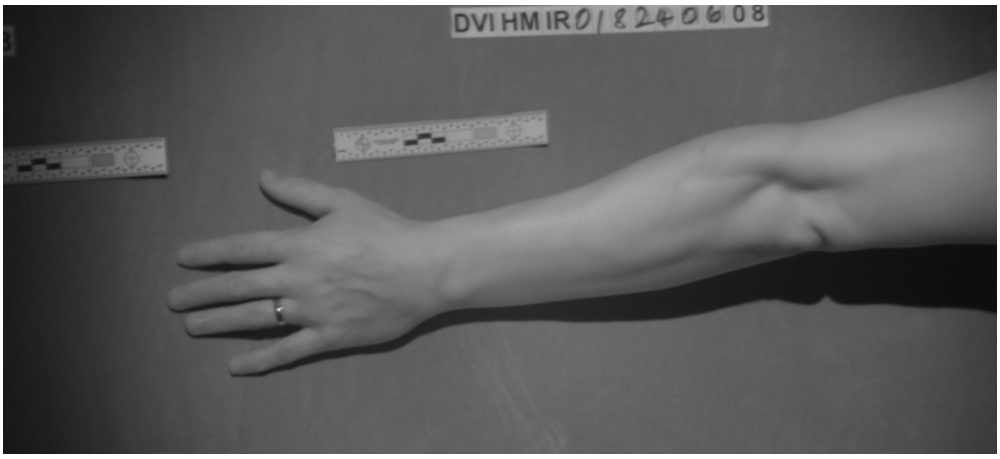

Figure 3.10: Infrared image of a dorsum of the hand.

Figure 3.11: Infrared image of a dorsum of the hand.

In order to begin with the application of the various enhancement functions, I normalized all the images, in other words taking them to the same resolution.

The first design was a function called MANTA, which received its name from the similarities it shares with the animal called “Manta Ray”, as shown in Figure 3.12.

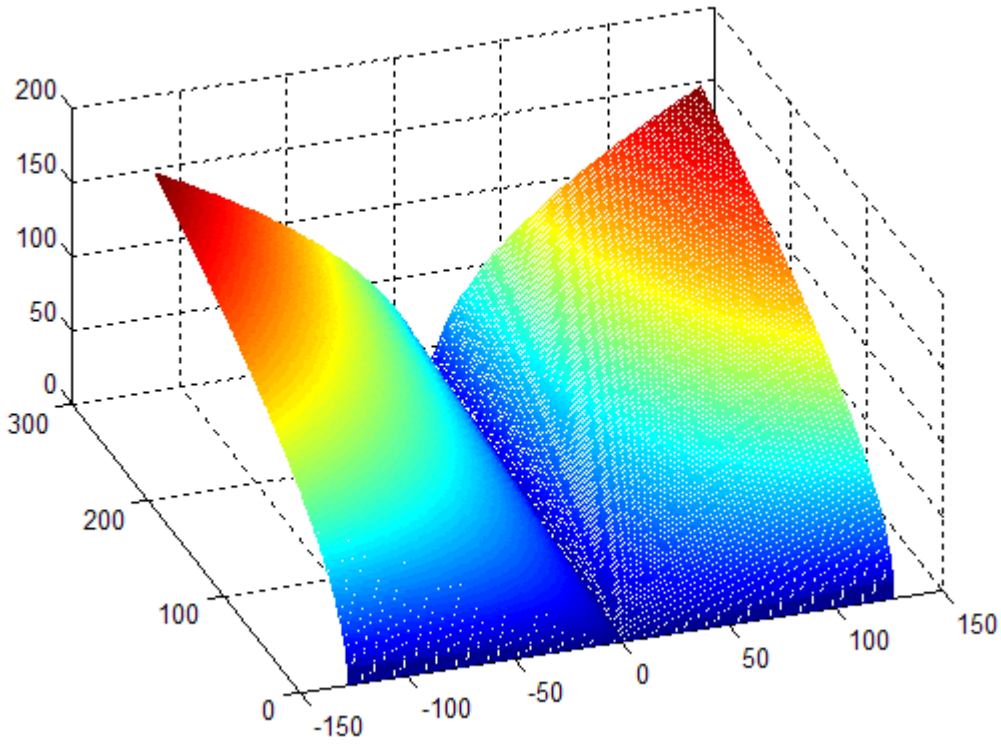

Figure 3.12: Plot of the first function for the enhancement.

The function is based on a kind of ‘dark test’, because I am interested in the evaluation of the absolute brightness and the homogeneity of the image. In other words the main point is to test the intensity and the standard deviation of local areas of the specified image.
After the evaluation, the idea was to modify the dark and homogeneous regions (veins), putting them darker, and to modify the bright and homogeneous areas (background, skin), in a brighter way.

As I shown in Figure 3.9, the veins are not enough contrasted in comparison to the background, so the next step of the recognition process is not applicable because the vessel detection algorithm can't work without a strong contrast.

In other words, the gap is not enough to work on it, so the main goal is to modify the image to obtain a bigger gap.

I developed a function which analyses the entire image, works on local areas, chooses a neighbourhood of pixels, of a desired size. In general, a pixel's neighbourhood is some set of pixels, defined by their locations relative to that pixel, which is called the centre pixel. The neighbourhood is a rectangular block, and moving from one element to the next in a image matrix, the neighbourhood block slides in the same direction.

This is a spatial domain method [34], because it operates directly on the pixels of the image. Spatial domain processes are denoted by the expression:

$$g(x,y) = T[f(x,y)]$$

where *f(x, y)* is the input image, *g(x, y)* is the processed image, *T* is an operator on *f*, defined over some neighbourhood of *(x, y)*.

The principal approach in defining a neighbourhood about a point (x, y) is to use a square of sub-image area centred on (x, y), as Figure 3.13 shows.

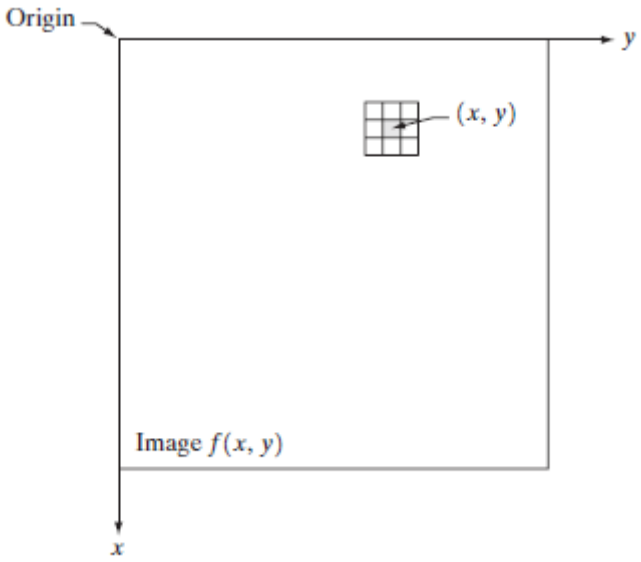

Figure 3.13: A 3x3 neighbourhood about a point (x, y) in an image [34].

The centre of the sub-image is moved from pixel to pixel starting at the top left corner. The operator T is applied at each location (x, y) to yield the output at that location.

The process utilizes only the pixels in the area of the image spanned by the neighbourhood.

The size of the mask of pixels is a parameter to choose, evaluating the result a posterior of the transformation.

In my case, the average of the intensities of this square of pixel, size 5x5, and the standard deviation is calculated, and their values are used as numbers to pass to the function that modify the pixel.

The choice is on these parameters because I need to characterize this neighbourhood, to decide if it belongs to the background (skin, background of the image, etc) or to the superficial venous pattern. I need a measure of intensity and one of homogeneity, that could be the standard deviation.

The main function of the algorithm contains the realization of the function shown in Figure 3.12, that using the two numbers said before, it returns a multiplying factor:

$$I' = f(I, \sigma, \bar{I})$$

where I is the original image, σ is the standard deviation of the square of pixels, $\bar{I}$ is the mean of the intensities of the square of pixels and I' is the image processed by the function f.

The number obtained by the function is multiplied with the pixel of the original image actually analyzed. Each pixel of the original image will modify in this way, to gain the new enhanced image.

The function was built in this way.

First of all, the need for a particular shape, function, with as x the mean of the intensities and as y the standard deviation, that grows on the diagonals, because when the values of the intensity is high or low, and the value of the standard deviation is high, it means that the local area that I'm analyzing is dark or bright and homogeneous. These are the requirements that I need to enhance the region, in other words to put darker the dark and homogeneous regions and brighter the bright and homogenous regions.

The function is as follows:

$$f = \sqrt{|\bar{I}|} * \sqrt{|\sigma|}$$

where $\bar{I}$ is the mean of the intensities and x $\in$ [-a, a], the interval of the intensities centred in that mean and σ is the standard deviation, with y $\in$ [0, b].

Second, the need to satisfy another requirement, the function has to increase diagonally but it has to be a steep increase, cause I am looking for a big contrast between the two main regions, veins and background.

$$f = k * \left(\sqrt{|\bar{I}|} * \sqrt{|\sigma|}\right)$$

where *k* is the parameter that could satisfy it.

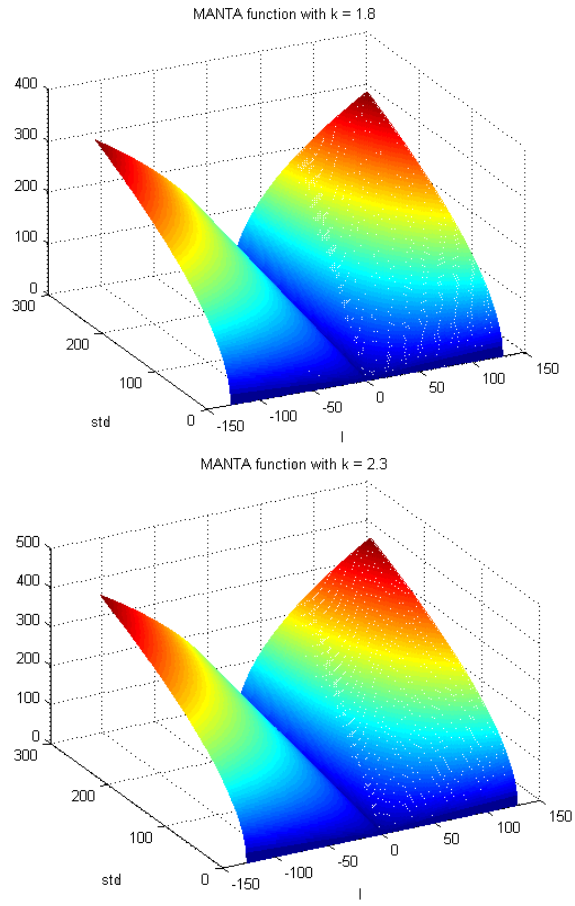

Figure 3.14: MANTA function with different values of k.

The main problem of this design was the choice of *k* because from its value depends the final result.

I need also a general value of it to apply to all the images of the database, but a problem raised, because changing the image, different values of k were needed.

A general value of k would not work for each of these images, a problem not suitable for a large database of images.

The images obtained, also after more than one iteration, are not useful, they are too dark, there is not a divided contrast between the background and the veins as I would have hoped.

The following figures explain why I cannot use this algorithm to enhance the images, even if I tried different values of k.

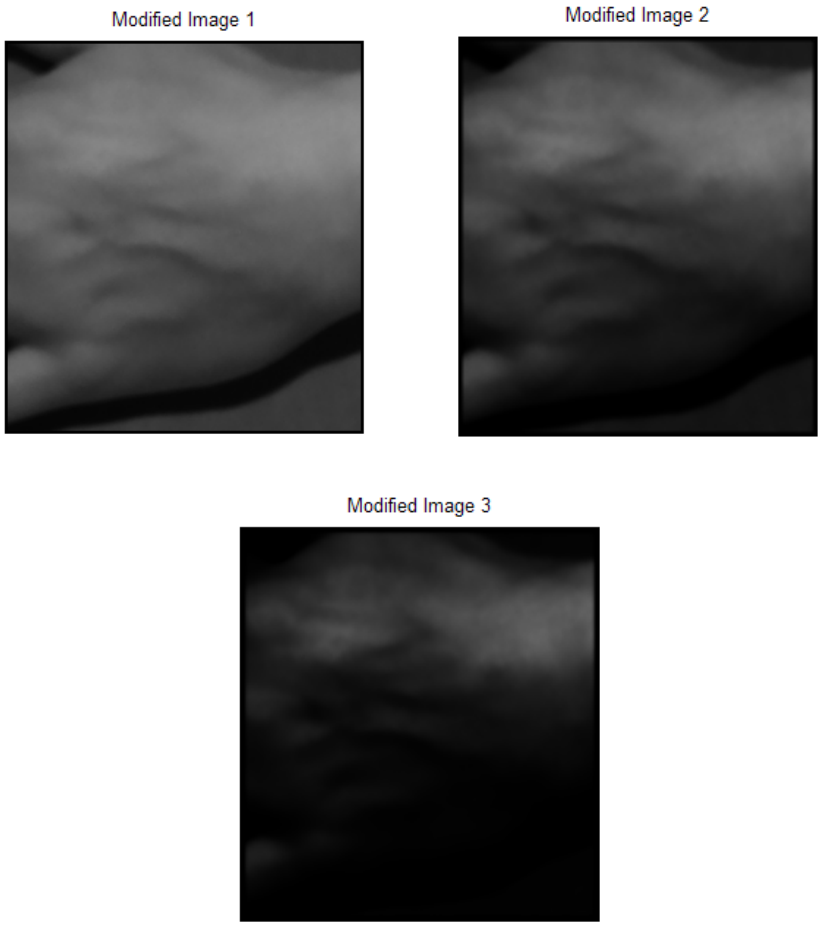

Figure 3.15: Modified images after three iterations of the algorithm.

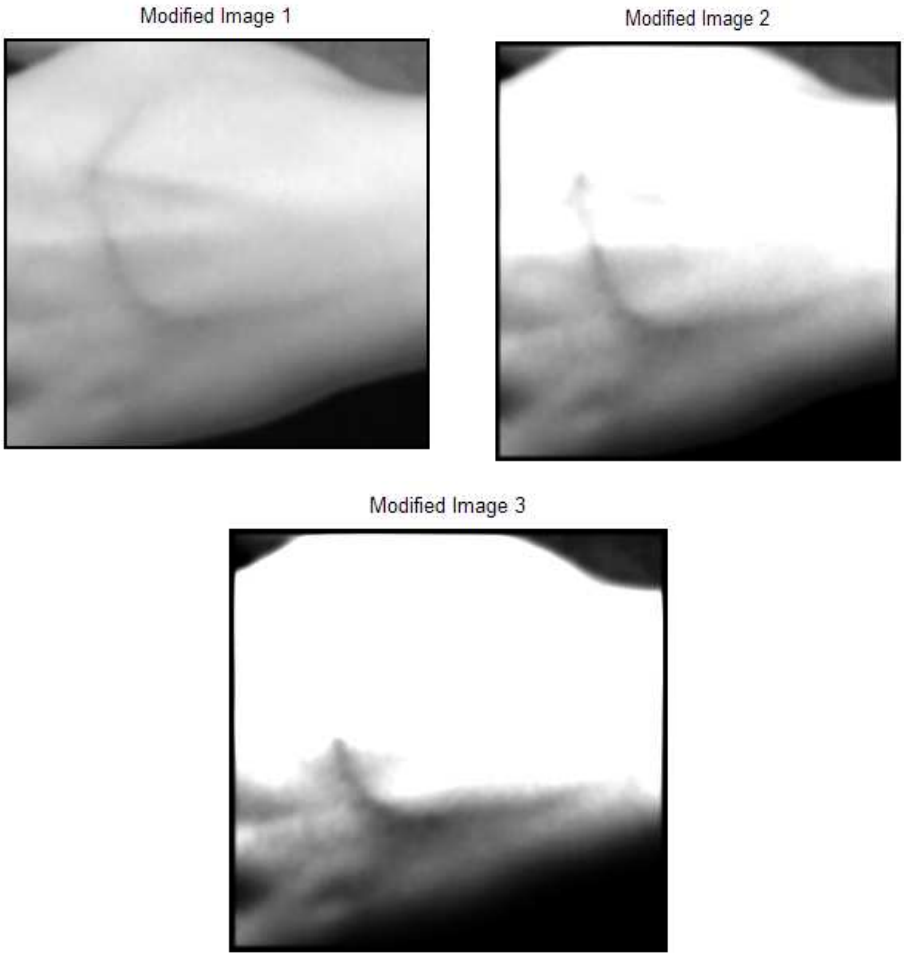

Figure 3.16: Modified images after three iterations of the algorithm.

As it is visible from Figure 3.15 and Figure 3.16, the lack of contrast is not resolved, plus the final result is worse than the original image, because the image is too dark and/or saturated.

The next step is to design an other function that can solve the problem, always focusing on the main requirements that I would like to obtain from the algorithm.

3.1.1.2 Second Design: the Polynomial Function

Always keeping the structure of a spatial domain enhancement method, a change in the main transformation function was required.
Thinking about simple math functions, related to my requirements of well separated dark and bright regions, I found the third degree polynomial function, a right way to achieve them.
The idea of the MANTA function was wrong, because the function grows in both side, when it is dark and also when it is bright, wrong choice, cause if the pixel is dark, I need to change it in a darker way, so its value has to be lower, and if it is brighter, vice versa. One side has to increase, the other side to decrease.
The shape of the polynomial of third degree should satisfy the requests.

I need other parameters, characteristic of the image considered, and a value that will keep the multiplying factor, result of the transformation function, between boundaries.
So, 1 is a fixed value to keep without any changes, then the polynomial is built based on our parameters and eventual boundaries.

$$\begin{bmatrix} I_m^3 & I_m^2 & I_m \\ I_M^3 & I_M^2 & I_M \\ \bar{I}^3 & \bar{I}^2 & \bar{I} \end{bmatrix} \begin{bmatrix} \alpha \\ \beta \\ \gamma \end{bmatrix} = \begin{bmatrix} 0 \\ 2 \\ 1 \end{bmatrix}$$

The values to be fixed are 1, 2 and 0: the minimum intensity I_m is 0; the maximum intensity I_M is 2, because I do not want to obtain values bigger than 2, I am working with multiplications, and it could provoke saturation of the intensities, with bright zones; and the average intensity $\bar{I}$ has to be always fixed to 1.
It is important to preserve the last value, instead of the other two that I can change, in a posterior way, checking the final result of the enhancement.
The third degree polynomial function is designed in this way:

$$f(x) = \alpha x^3 + \beta x^2 + \gamma x + \delta$$

$$\begin{cases} f(I_m) = \alpha I_m^3 + \beta I_m^2 + \gamma I_m + \delta = 0 \\ f(I_M) = \alpha I_M^3 + \beta I_M^2 + \gamma I_M + \delta = 2 \\ f(\bar{I}) = \alpha \bar{I}^3 + \beta \bar{I}^2 + \gamma \bar{I} + \delta = 1 \end{cases}$$

I have to take into consideration another equation to add to the previous system:

$$f'(\bar{I}) = 3\alpha \bar{I}^2 + 2\beta \bar{I} + \gamma = 0$$

The following system has to be solved to find the parameters of the polynomial for each image and for each iteration for the same image, because it is working on the proper characteristics of the image.

At the end the set of parameters $p = [\alpha\ \beta\ \gamma\ \delta]$ to solve the previous system of equations is found, and it is passed to the main transformation function.

In this case I am not considering a measure of homogeneity, the parameters which I am considering are only values linked to the intensity of the image.

At the end, the multiply factor is evaluated with this equation:

$$f_m = p(1)Im^3 + p(2)Im^2 + p(3)Im + p(4)$$

where Im is the mean of the intensities of the squared of pixel considered at that point.

Another parameter k is added to control the range of the intensities, and it is chosen a posterior, looking at the processed image. It joins the polynomial in this way:

$$b = [1 - k \quad 1 + k \quad 1 \quad 0]$$

Instead of

$$b = [0 \quad 2 \quad 1 \quad 0]$$

As Figure 3.17 and Figure 3.19 shows, changing the parameter k, the result is different: for example if I choose a value of k = 0.1, the set value, and k = 0.6, the result are

different from each other. The modified image with k = 0.6 presents changes in intensities that I cannot use to work in the next steps, plus it does not give me the possibility to understand the vessels network.

To understand better if the algorithm is giving me useful result to detect the vasculature, I can compare the profile of a vein of the two images. The result is shown in Figure 3.18 and Figure 3.20.

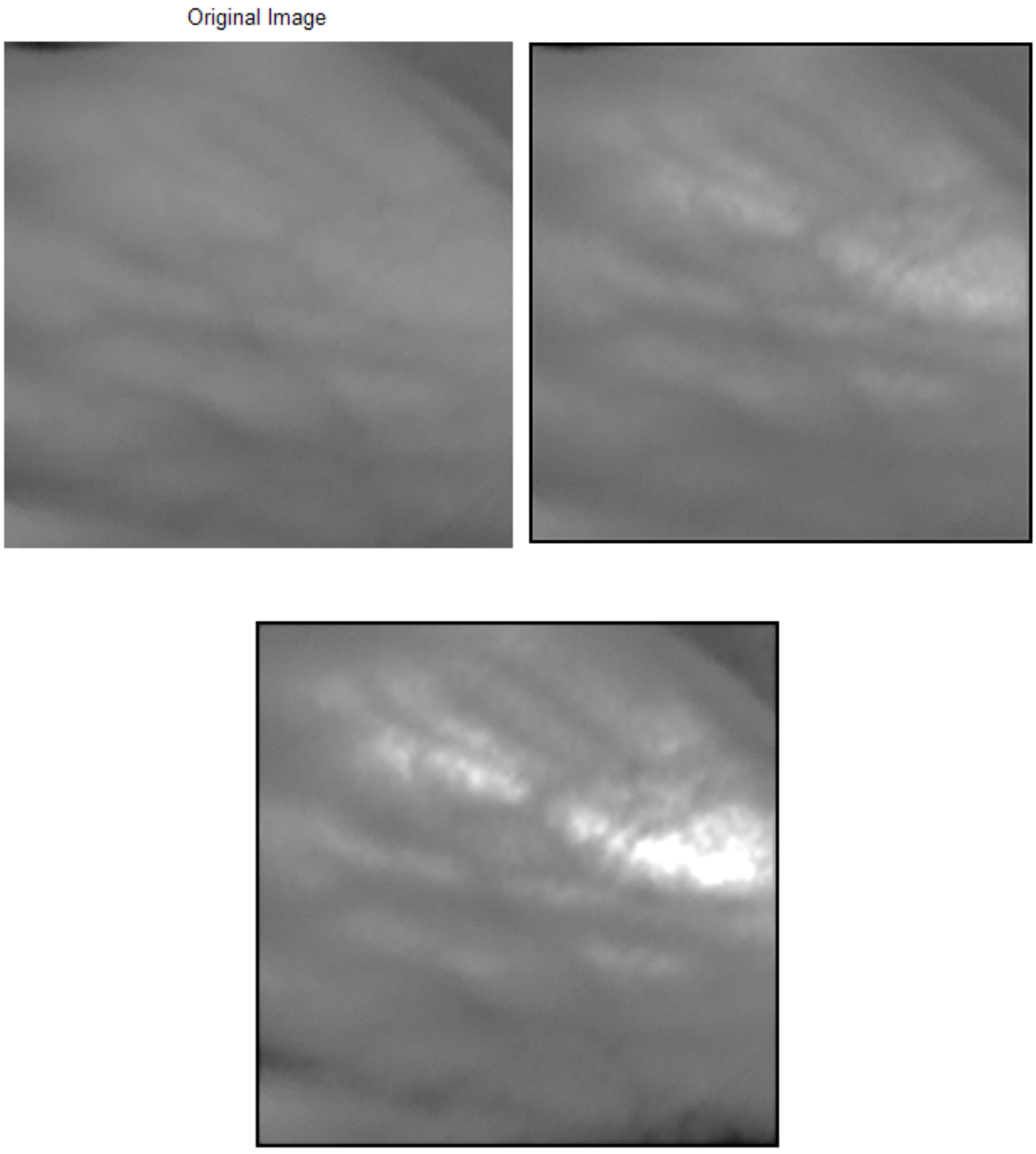

Figure 3.17: Original image (left corner), modified image after one iteration (right corner) and after two iteration (last image) with k = 0.6.

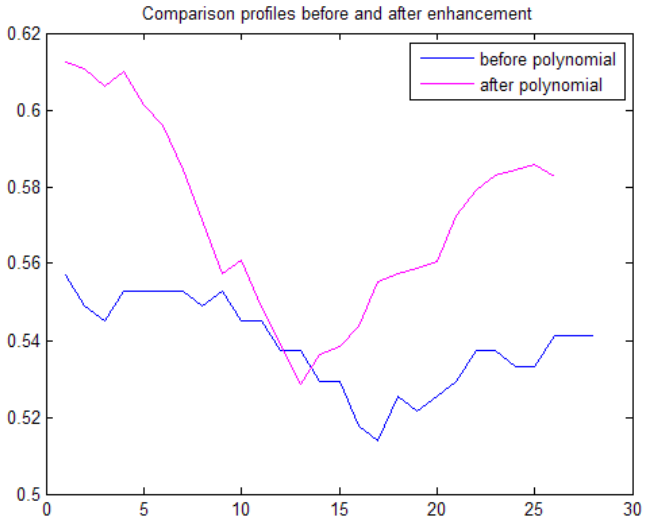

Figure 3.18: Comparison of profiles of a vessel in the original and processed image.

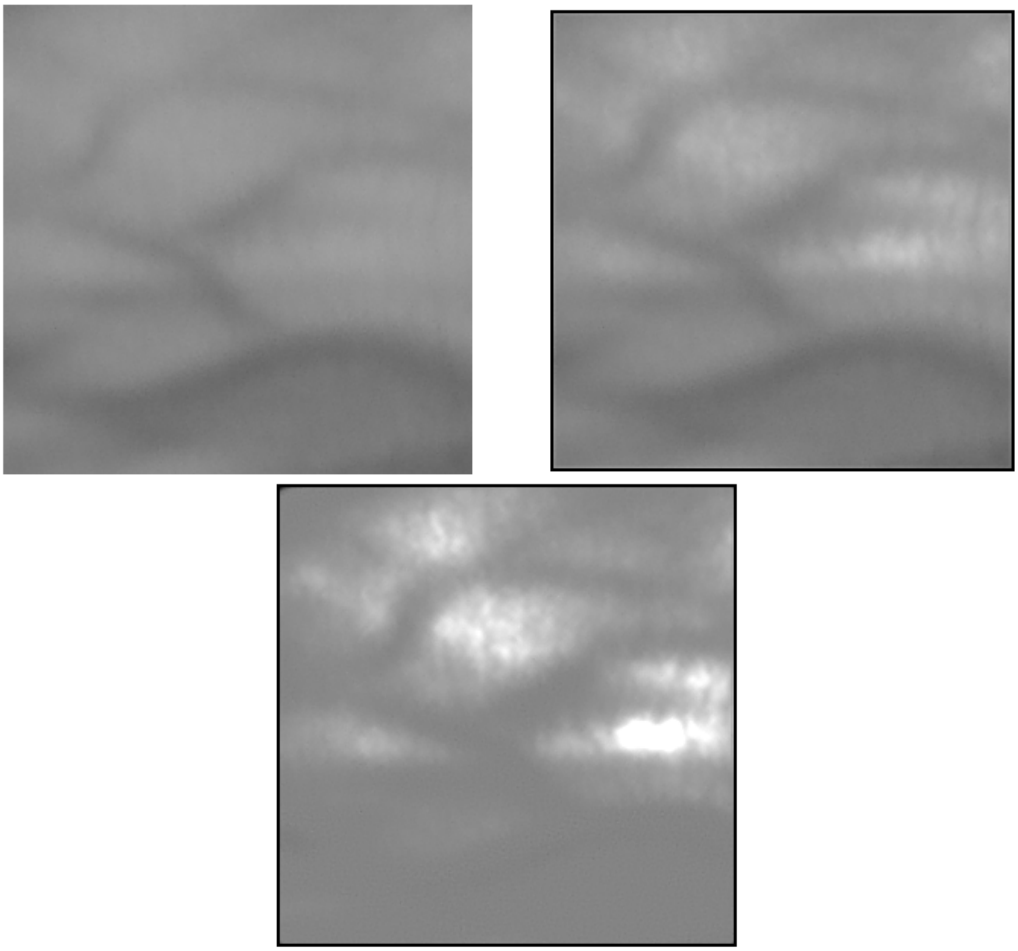

Figure 3.19: Original image(left corner) and modified images after one (right corner) and two iterations (last image) with k = 0.1.

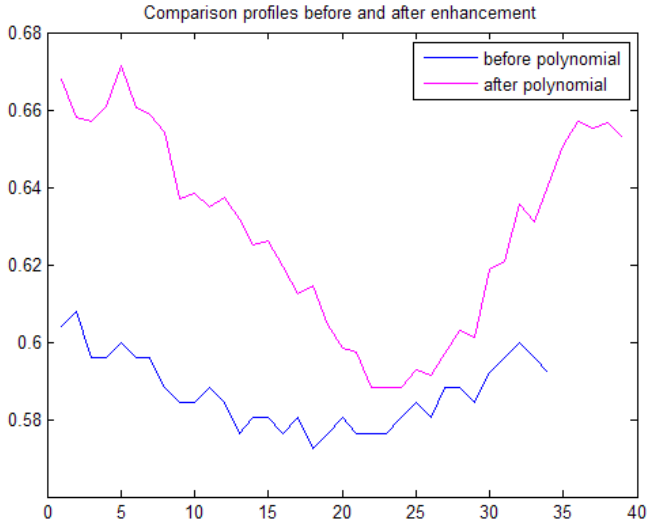

Figure 3.20: Comparison of profiles of a vessel in the original and processed image.

Figure 3.18 and 3.20 shows how the algorithm works from a point of view of depth in the vein's profile. It is the main characteristic that I want to change, because the software for the vessels segmentation works following the valley of a vein, the difference in contrast between the background and the veins.

The problem of the uniqueness for all the images of the parameter k is solved, because I keep a singular value for it, ranging between 0.1 and 0.2.

3.1.1.3 CLAHE: Contrast Limited Adaptive Histogram Equalization

Observing the images and researching on the enhancement and various problems of the infrared images, I found a paper [29] that deals with the histograms of those images and uses the transformations based on these.

For example, the histogram of one of the image is as follows, in Figure 3.21.

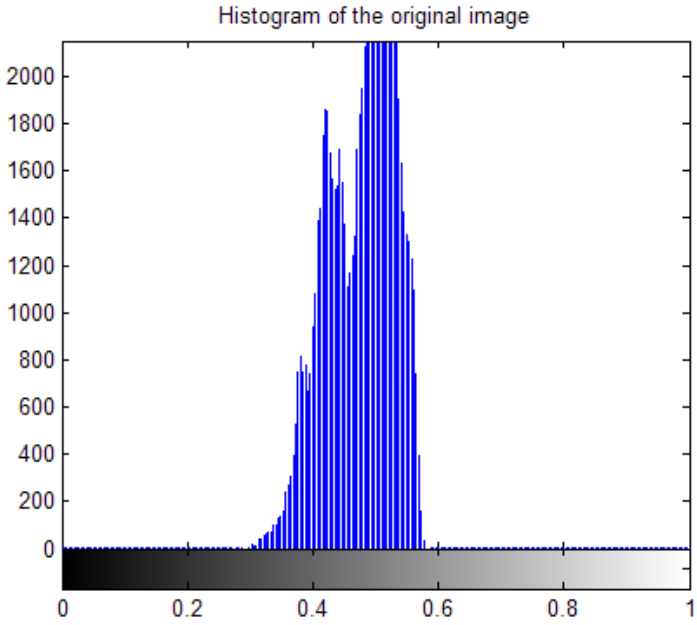

Figure 3.21: Example of histogram of the original image.

Usually the histogram equalization is used to enhance the image's contrast by transforming intensity values of the image.

In other words the values in a normalized histogram approximate the probability of occurrence of each intensity pixel level in the image.

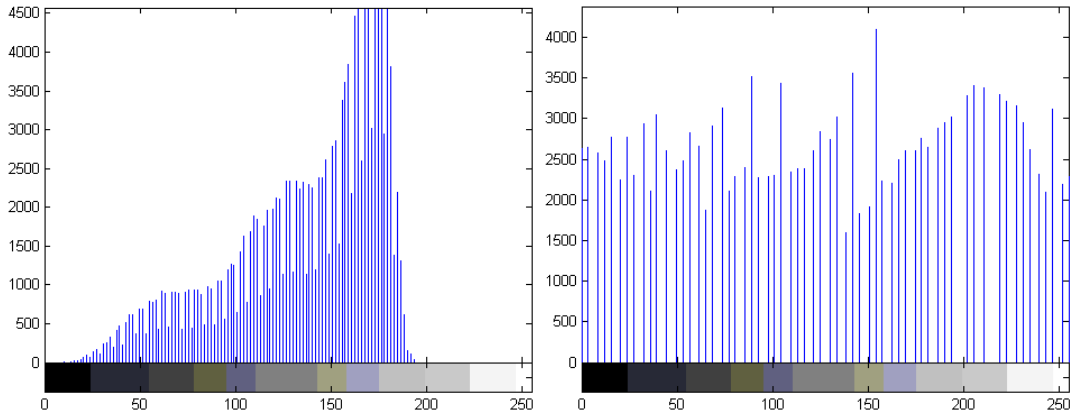

Fig 3.22: Histogram and equalized histogram of a fingerprint image [29].

However, by enhancing the contrast of an image through a transformation of its intensity values, histogram equalization can amplify the noise and produce worse results than the original image, due to many pixels falling inside the same gray level range.

The CLAHE, Contrast Limited Adaptive Histogram Equalization is used.

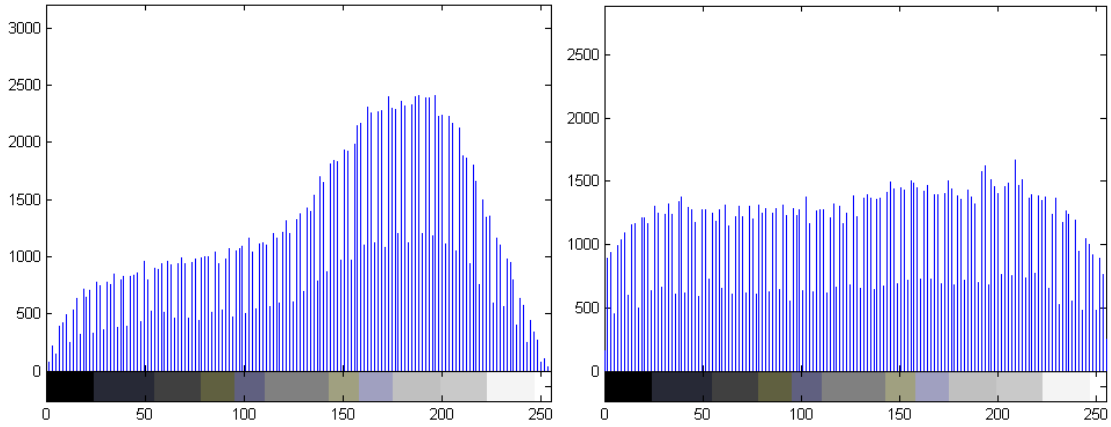

Figure 3.23: CLAHE and CLAHE with clip limit of a fingerprint image [29].

I have to handle with images with small features, such as veins, junctions, branching angles; CLAHE should work better.

The histogram equalization works in small regions in the image, called tiles; each tiles contrast is enhanced so that the histogram of the output region approximately matches the histogram specified by a parameter that deals with a kind of distribution, the desired shape for the image tiles.

After performing the equalization, *adapthisteq*, function built-in of Matlab (R2008a, version 7.6.0.324) to run the CLAHE, combines neighbouring using bilinear interpolation to eliminate artificially induced boundaries.

There is another parameter, called 'Clip Limit', that specifies a contrast enhancement limit. It is a contrast factor that prevents over-saturation of the image specifically in homogeneous areas.

These areas are characterized by a high peak in the histogram of the particular image tile due to many pixels falling inside the same gray level range.

Each time an image is acquired, window and level parameters must be adjusted to maximize contrast and structure visibility.

It partitions the image into contextual regions (tiles) and applies the histogram equalization to each one.
This evens out the distribution of used grey values and thus makes hidden features of the image more visible. The full grey spectrum is used to express the image.

Each values of the possible parameters is chosen always a posterior, trying to find the best compromise.
This is not a simple choice because all the images which will be used are completely different from each other.
I have tried with a lot of combinations, at the end I choose 8 tiles and 0.02 as parameter for the clip limit value. An example follows in Figure 3.24.

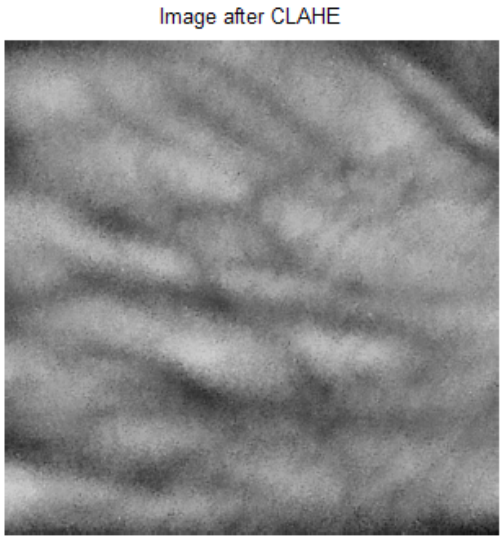

Figure 3.24: Image after CLAHE operation.

Finally I have decided to join the two functions, first applying the CLAHE function, and second applying the polynomial function.
The lack of contrast is solved partially, because the images are completely different from one other, but generally, with the standard images, it works well, giving me the possibility to go on with the next steps of the pattern recognition.
The results are shown in the following pictures, Figure 3.25 and Figure 3.26.

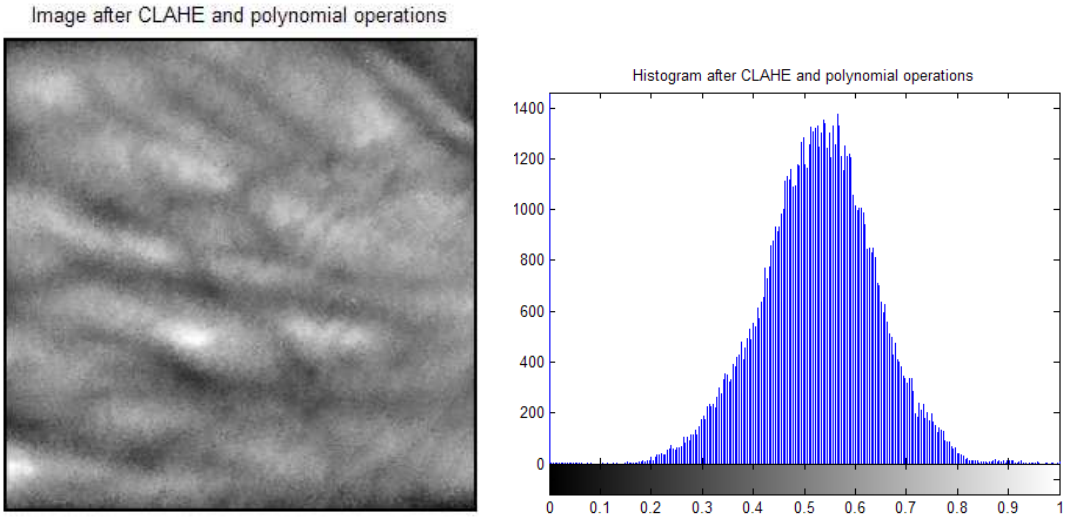

Figure 3.25: Processed image and relative histogram after enhancement operations.

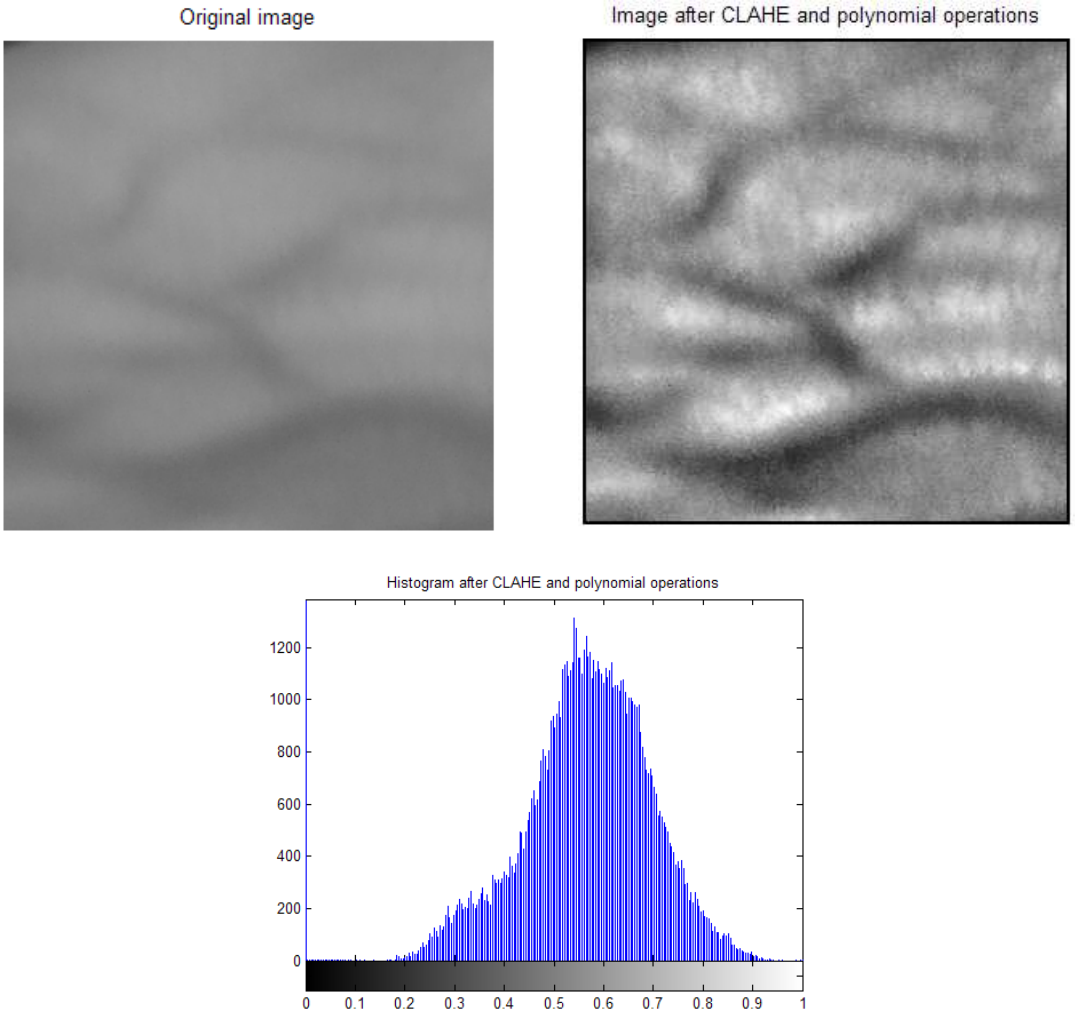

Figure 3.26: Comparison between original and processed image and relative histogram.

Chapter 4

Detection of the Venous Pattern

The next step, which is the main step, is the detection of the vessel network and the extraction of the tree vein pattern.

A lot of methods working on the extraction of the vascular structure network were and are developed, with different principle and way to work, to detect the vasculature and obviously different algorithms.
Techniques to extract and obtain automatically the vessels of an anatomical part of the human body can be divided into two groups:

1. *Template-matching techniques*: the template has to be turned to a reference vessel calibre, these techniques do not guarantee to work properly in presence of large variability in vessel calibres. Plus, they use a large number of filters working on the entire image, so it is very demanding from a computational point of view.

2. *Tracking techniques*: instead of processing the entire image, they analyze local areas of small size to trace the vessel step by step. The method to identify its profile along the scan line is not unique, but different ways to do it are studied.
   Basically they have the same principle, as they start from a point, entered by the user, on the vessel and move along as far as it is possible, until the meeting of an end condition, that can be automatic, user-provided, etc.

They process the pixel close to the vasculature, this is the reason because they're called 'exploratory algorithms'[33].

4.1 Vessel Tracking Technique

After a quick explanation of the vessels algorithm detectors, I can say that the tracking technique is the best choice for my images, because I cannot use algorithms that need fixed properties of the vasculature, as the calibre, although I am in presence of a large variability of vessel calibre distributions, and not only.

I analyzed and worked with a software from a fellow PhD student, Adrià Perez-Rovira, that implements a vessel tracker algorithm.

I found also a paper called "*Feature extraction of finger-vein patterns based on repeated line tracking and its application to personal identification*", Miura et al., 2004 [36], that works on the same principle used by this software.

The tracking starts at various positions, starting points, user provided in the way that, if a tracking operation is finished, I will point another start on a vessel in the image so another tracker can start to work.

The algorithm works locally, so dark lines are identified step by step analyzing local areas and the line tracking is executing along lines, pixel by pixel.

When an end condition, that can be user provided or not, is found, the tracking line is stopped, the area of the vessel is drawn and a new starting point can be chosen.

As it is known, the cross sectional [36] profile of a vein appears as a valley. The depth of the valley is the main characteristic to work with, because it causes the detectability of the vein; the depth varies with the shading in the image, contrast, and so on.

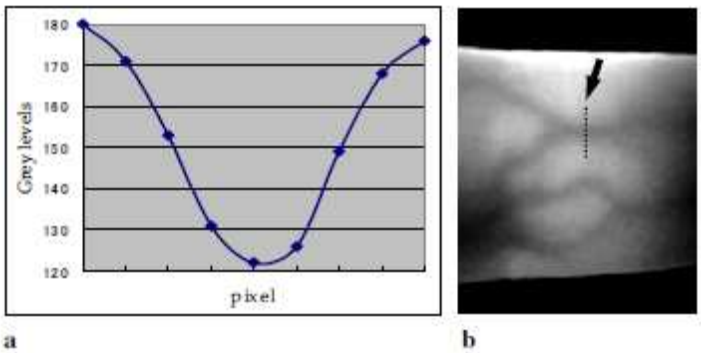

Figure 4.1 a, b: Cross-sectional profile of a vein in the finger: a. cross sectional profile; b. position of cross section.[36]

This is the main reason because I spent a lot of time in the enhancement of my images.

The profile can give us a robust method to find if the tracking area that it is going to be analyzed, belongs to a vein or not.

The line tracking operation starts when I point the mouse; this is the current tracking point and it is moved pixel by pixel along the scan line, and the depth of the valley is continuously checked.

The direction is another important step to evaluate and it can be done by checking the depth of the valley by varying an angle θ, gaining the direction where the valley is still deepest.

Proving that, the next pixel is where the angle θ points. Figure 4.1 a, b gives a clear explanation.

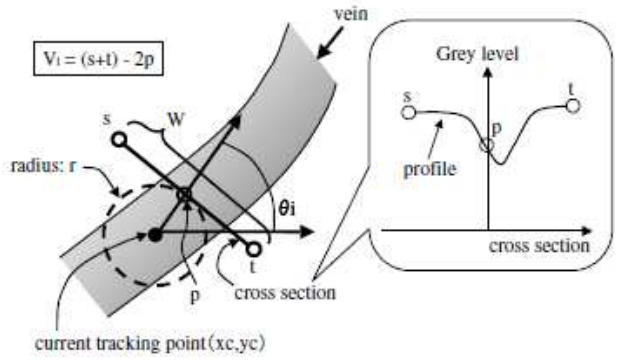

Fig 4.2: Dark line detection. [36]

The algorithm works on a continuous check of the conditions around a pixel, and explores the space close to it, this is why it is called, in general, exploratory algorithm.

Referring to the software used for my project, it checks the vessel orientation using the gradient of the image, around the starting point.

This part of the image is used to compute the eigenvectors, first of them is the orientation and the other one is the stability or confidence.

After that the section is cut, the orientation of that is obtained and the cross sectional profile of the vein along this section line is evaluated. Then the vessel borders are detected and the tracking operation can start, working on the vessel centreline, orientation, distance of the centre from the borders, the direction of the tracking.

First of all the tracking line analyzes one side, and if it finds an end condition, it changes direction, checking the other side, till the final end condition is reached. A visible

clarification of the procedure is in the Figure 4.3, where the red points are the vessel centrelines, the green section is the section of the starting point, and the yellow sections are the ones of the next steps of the tracking, showing step by step the tracking line.
I need also the confidence parameter, calculate with the eigenvectors, that is the relation between the eigenvalues of the region surrounding the point evaluated, and the residual, error fitting section with previous one.

The main steps are summarized in the following points:

1. Move forward to another section, given the previous step, or status;
2. Get the orientation of the next section;
3. Get the borders of the section;
4. Recomputed the centre;
5. Save the new status.

The end condition is reached if the tracking line goes out from the window of the image or arrives to a previously marked vessel, or if the width of the consistency, done by the difference between the confidence and the residual of the previous step and the next one is more than a precise number.
At the end, when apparently all the vasculature network that I need is detected, I obtain a figure with all the areas that the tracking line scanned, as Figure 4.4 shows.

Figure 4.3: Tracking line during the operation.

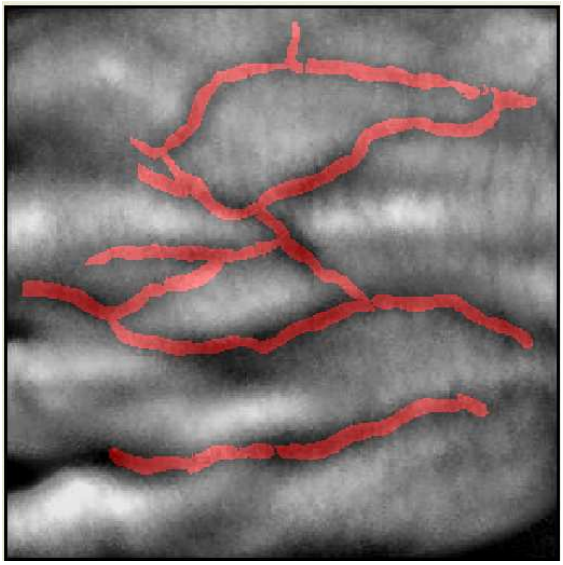

Figure 4.4: Complete tracking operation in a selected back hand image.

Running the software, I can work with a graphics user interface called *vesselSegmentation* where I can start the detection of the vessels network with the algorithm explained before.

4.1.1 Problems in the extraction of the vessels network

The main problem was the nature of my images, infrared images and the lack of contrast. This is why I have tried to obtain the best possible image designing algorithms for the enhancement. If the contrast is high, the vessel tracker is faster and does not require a lot of user-provided starting points, a characteristic that a good vessel tracker algorithm should have.

Anyway with the algorithms applied to improve the contrast, explained in the previous chapter, I was able to work in a good way with the vessel tracking technique proposed previously.

I changed the values of the main parameters, like the box size, that is the side of the image to cut, because it depends from the resolution of the specified images, for example the resolution of a retinal image, generally used with this software, is 2000x3000, instead of one of my images, where the selected ROI is 300x300.

I have also changed the parameter that handles with the maximum width of a vessel in the image, setting it to 18 pixel. The obvious differences between the usual images used with the software and the back hand images used in the project are shown in Figure 4.5 and Figure 4.6.

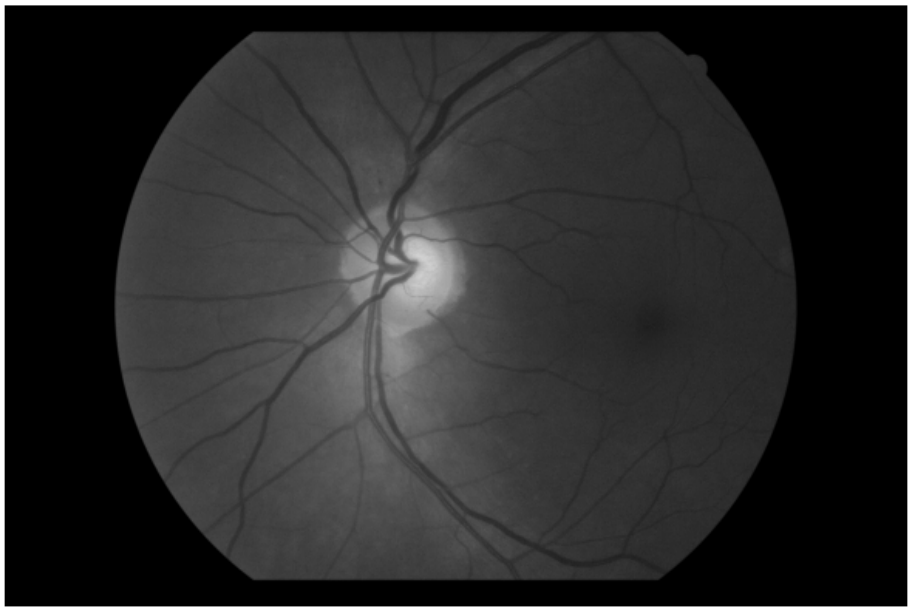

Figure 4.5: Retinal image, usually used with the vessel segmentation software.

Figure 4.6: example of a back hand image.

If the lack of contrast is too high, the detection of the vessels network is impossible, because the tracking line is going to stop after few track steps , or in the worse case, it does not start at all. The vessels network cannot be detected and the next steps cannot be reached.

In addition the user has to provide a high number of starting points, so the user intervention is maximized.

This goes against another property that is expected for a vessel tracking algorithm, that is, to extract most of the vascular network while minimizing the user action.

Another thing to be aware of, is the anatomical parts of the hand, Figure 4.7 shows an image of the back hand with tendons and veins and Figure 4.8 shows one of the IR images with evidence of the tendons that can provoke artifacts in the detection of the vessels network.

These problems could arise from the way the back hand images are acquired, such as with the hand stretched and the fingers open.

Applying the vessel enhancement algorithm, all the dark parts of the images are contrasted, so they become darker.

In these case, the tendons of the hand are a problem, because their shadow is a linear structure, and the vessel tracking line running on the vessel, can assume them as part of the network.

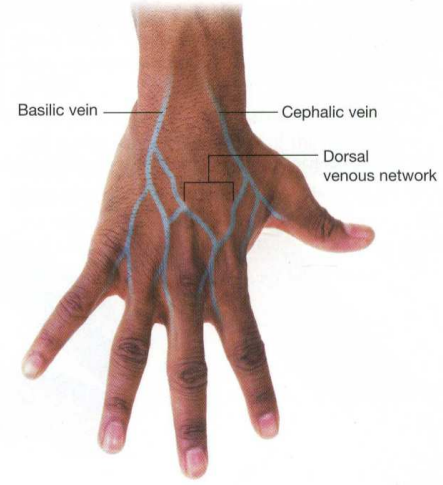

Figure 4.7: Back hand image and its structures, veins and tendons.

Figure 4.8: Back hand image with tendons visualized as vessels, dark lines: the selected part in the image shows a tendon.

I need to be careful when the scan line is moving.

In my opinion, it will be better with the hand closed in a fist, because in this way the tendons are not noticeable, and the superficial venous pattern is visible in a better way, Figure 4.9.

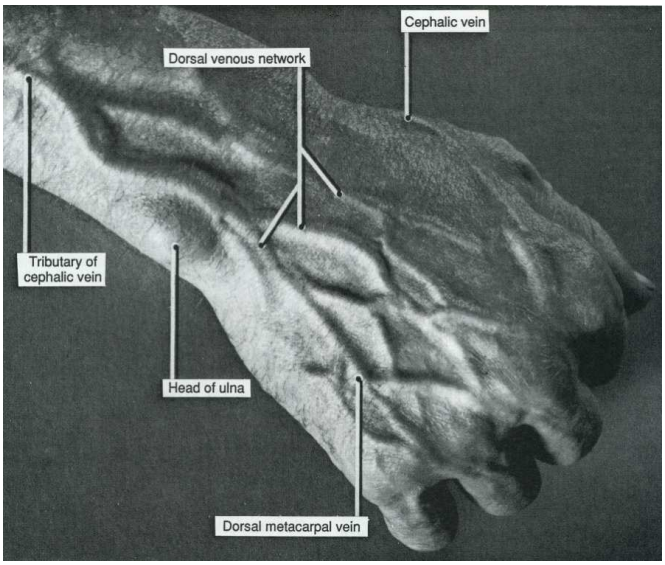

Figure 4.9: Hand closed in a fist.

Hence, a lot of artifacts can raise in the final result of the vessel segmentation.

A way to avoid it, is by making comparisons while doing the detections, with the original IR image, cropped in the same way as the enhanced one.

The hairs on the dorsum of the hand could prove to be an eventual problem, as Figure 4.10 shows:

Figure 4.10: Back hand with hairs in the dorsum.

But it is not a real problem for the algorithm because the hairs are too thin to be detected with the vessel tracker.

Finally, the status of the tracked images is saved, as Figure 4.4 shows, the binary mask (Figure 4.11) of the vascular network is stored in a folder, ready to be processed.

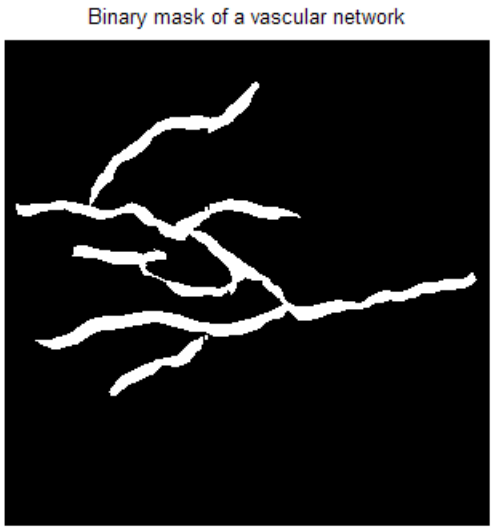

Figure 4.11: Binary mask resulting from the detection of the vessel network with the vessel tracking algorithm.

Chapter 5

Skeletonization and Feature Detection

5.1 Skeletonization of the binary mask

As first step after the accomplishment of the binary mask of the superficial venous pattern of the back hand images, the skeletonization of the mask is required, because a good representation of the pattern's shape is via extracting its skeleton, or topological skeleton.
The shape is important because, after the size of the veins grown as human begins to grow, only the shape of the vessel pattern is used as the sole feature to recognize each individual.
The skeleton is the thin version of a specific shape that is equidistant from its boundaries, and usually it emphasizes the geometrical and topological properties of the figure, such as its connectivity, topology, length, direction and width, and it contains all the information necessary to reconstruct the original shape.
Keeping these properties in my mind, it would be first thing that I can find useful as feature to characterize an individual, as the main goal of this study is to search for unique characteristics different for each individual, is the estimation of the widths of the veins.

After the application of the morphological operation called *thinning*, I started to evaluate the width of the vessels.

The function built-in of Matlab *bwmorph* has two options to do the morphological skeletonization, *thin* and *skel*.

The thinning algorithm is a procedure applied for an infinite number of times, because it's repeated until the image no longer changes.

It removes pixels so that an object without holes shrinks to a minimally connected stroke and an object with holes shrinks to a ring halfway between the hold and outer boundary.

Another option is *skel*, it performs its result in an infinite number of times, and removes pixels on the boundaries without allowing objects to break apart.

The best result obtained was with the first option, as Figure 5.1 explained:

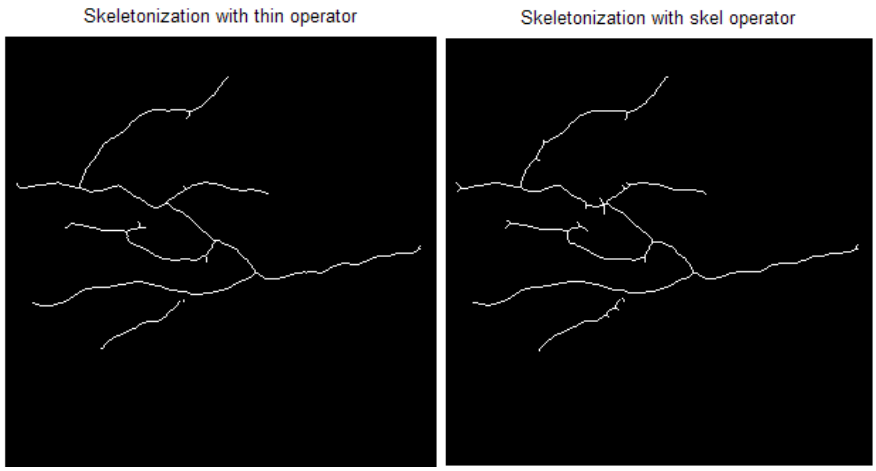

Figure 5.1: Skeleton obtained with thin operation(left) and skel operation(right).

A morphological operation useful to fill isolated interior pixels can be applied, such as 0's surrounded by 1's, to obtain a continuous skeleton.

5.2 Evaluation of the width of the veins

The widths are estimated locally, e.g. every 5 pixels of the skeleton. At the beginning I need to estimate the Euclidean distance transform of the binary image, considering the diameter, not the radius.

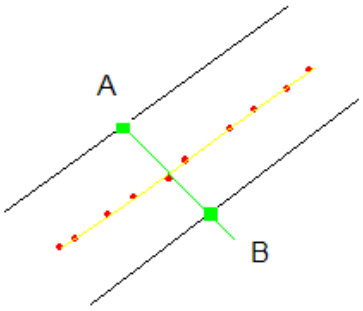

Figure 5.2: Evaluation of the width with the Euclidean distance, in yellow the skeleton, A and B are two points on the borders of the vein.

The width of the vein is evaluated in this way:

$$w = \|A - B\|$$

where w is the value of the width, and A, B are two points of the vein in the binary image, as Figure 5.2 displays.

Figure 5.3 shows the vessels' width for the entire image:

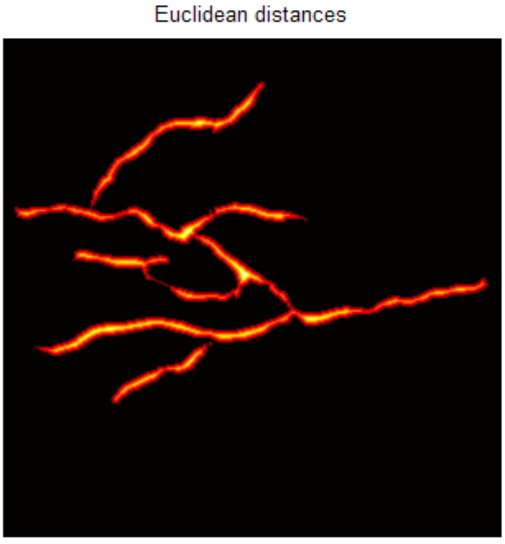

Figure 5.3: Widths of the vessel network.

For a pattern recognition study, the successive step could be pattern matching or research for shape's descriptors, a set of numbers that are produced to describe a given shape. The choice of the features is very important because the better is the descriptor, the greater is the difference in the descriptions of different shapes and the lesser is the difference for similar shapes.
I started the research on possible features, as the width in the previous case. The final step after the choice of them is the statistic study on their values.

5.3 Pattern Matching and Particle Swarm Optimization

This pilot study is a collaboration between the School of Computing and the Centre for Human Anatomy and Identification.
The pattern matching is one of the main goals for the forensic group; a way to realize it was researched, considering a registration for the images.

5.3.1 Registration of the images

The images are completely different one from each other, e.g. in term of resolution and acquisition(Figure 5.4, 5.5).

Figure 5.4: Example of an image of the database.

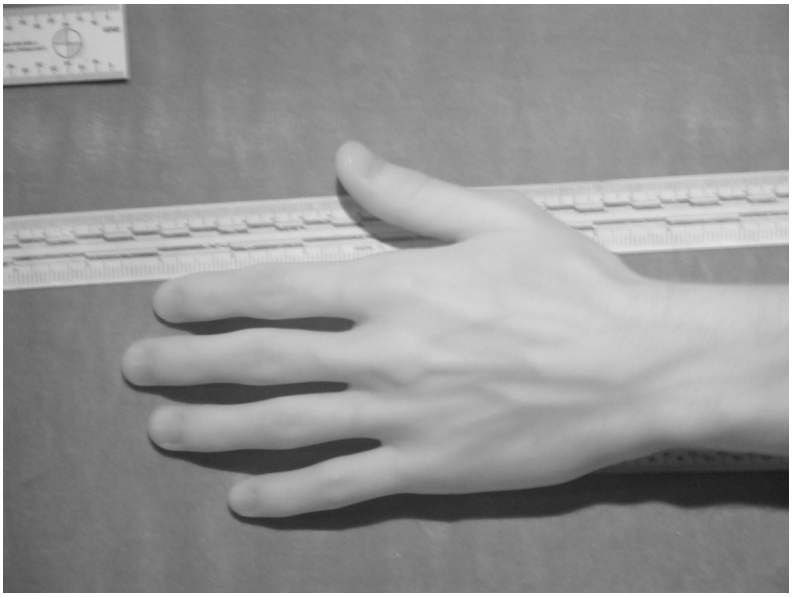

Figure 5.5: Example of an image of the database.

The relative binary masks are scaled in a different way, rotated and translated, as Figure 5.6 displays.

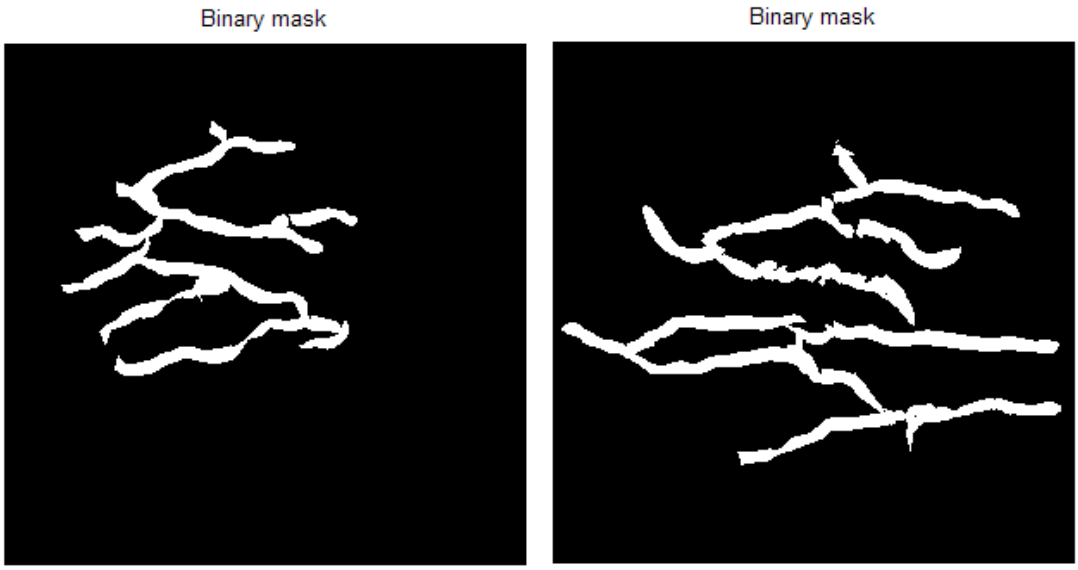

Figure 5.6: Binary masks of the two different images.

In the matching step, the extracted vascular pattern from the feature extraction step is compared against a pre-registered pattern in the database, to obtain a matching score, or overlap of the two vessel binary network.

There are two typical methods of pattern matching:

1. *Structural matching*: comparing locations of features points such as line endings and bifurcations extracted from two patterns being compared to obtain the matching score. For fingerprint images is largely used, hand vascular patterns have fewer minutiae-like feature points. The goal is to choose these features that allow pattern vectors belonging to different categories to occupy compact and disjoint regions in a d-dimensional feature space.

2. *Template matching*: comparison of pixel values of two vascular pattern images(matching like shaped pattern), it is a robust method. A template(2D shape) or a prototype of the pattern to be recognized is available. The pattern to be recognized is matched against the stored template while taking into account all allowable pose (translation, rotation) and scale changes.

Hence, as said before, if I would like to do further comparison, I need to register the binary masks.

Image registration is a crucial step in all image analysis tasks, in which the final information is gained from the combination of various data sources.

The purpose is to determine a mathematical mapping that is the best match of two or more images.

To register a float image, called for example I_F, to a reference image I_R, can be expressed mathematically as:

$$I_R = \varsigma(I_F(T_\alpha(x, y)))$$

where ς is an intensity or radiometric calibration function, T_α is a transformation function, which maps two spatial coordinates x and y to new spatial coordinates x' and y' by a set of parameters α.

$$(x', y') = T_\alpha(x, y)$$

Intensity based image registration can be mapped as a typical optimization problem:

$$\alpha^* = argoptima_\alpha(S_{T_\alpha}(I_F, I_R))$$

where S_{T_α} is a certain metric, α^* is the optima estimated by the optimization algorithm.

The optimization methods find the minimum of dissimilarity measure(penalty function) or the maximum of similarity measure. It is a multidimensional optimization problem, where the number of dimension corresponds to the degrees of freedom of the expected geometrical transformation.

Summarizing the goal of the image registration is to find an optimal set of parameters which determine the relative position and orientation of two images.

5.3.2 Particle Swarm Optimization

Local optimization techniques such as the *Gradient descent method* are frequently used for medical image registration. But these methods need good initial values for the estimation in order to avoid local minimum or maximum.

I still do not know how to deal with the images and what kind of initial values I can set.

Another technique is the PSO, Particle Swarm Optimization technique, designed and developed by Eberhart and Kennedy (1995) [50]. It is a technique that it is not largely affected by size and linearity of the problem and it can converge to optimal solution in many problems where most analytical methods fail to converge.

Its design was inspired by social behaviour of bird flocking or fish schooling.

PSO is initialized with a group of random particles, solutions and then searches for optima updating generations.

Each particle keeps track of its coordinates in the problem space, which are associated with the best solution (fitness) it has achieved so far, the fitness value is stored.

Another 'best' value is tracked by the PSO, it is the best value obtained so far by any particle in the neighbourhood of the particles.

Each particle in the population is manipulated according to:

$$v_{id} = w * v_{id} + c_1 * rand() * (p_{id} - x_{id}) + c_2 * Rand() * (p_{gd} - x_{id})$$

$$x_{id} = x_{id} + v_{id}$$

Those are the d^{th} dimensional component of the position and velocity of the i^{th} particle at time step t. *Rand()* and *rand()* enhance the exploratory nature of PSO, p_{id} is the d^{th} component of the best(fitness) position that the i^{th} particle has accomplished by t.

p_{gd} is the d^{th} component of the best global position achieved in the population.

c_1 and c_2 are known as cognition and social factors as they control the relative strengths of individualistic and collective behaviour of each particle.

w is the inertia weight, it was developed to better control exploration and exploitation.

Suitable selection of it, provides a balance between global and local exploration and exploitation and results in fewer it on average to find a sufficiently optima solution.

5.3.2.1 PSO Design

The starting point is the binary mask of each image, e.g. of Figure 5.6, and referring to my database of images, each binary masks is completely different one from the other one, and they need a set of geometrical transformations.
The geometrical transformations, that are required to be applied, are the horizontal and vertical translation, rotation and scale.
The set of parameters is made of four values:

$$\underline{x} = [\,\theta\ x\ y\ s]$$

where θ is the rotation parameter, x and y are the translation parameters and s is the scale.
The research for a function is based on the fact that a specified shape has to be modified in relation with a reference shape, applying the transformation done with the optimal set of parameters obtained:

$$f(I, \underline{x}) = I'$$

with I' as the modified image.
It is an optimization problem, because the best set of parameter is required to determine the best alignment of the two masks, the best match.
The PSO is the optimization technique that I used to achieve the optimal set:

$$\hat{\underline{x}} = argmin_{\underline{x}}\, e(I_1, I_2, \underline{x})$$

I_1 is the reference image, I_2 is the image to be registered and e is a cost function, designed in a precise way, focusing on my purpose, the overlap of the two binary masks.
The images, on which I am working, are logical images, so logical operators can be easily used.
A possible form for the cost function is:

$$e(I_1, I_2, \underline{x}) = \sum_i^N \sum_j^M (XOR(I_1, f(I_2, \underline{x})))$$

where N and M are the number of pixels in the image, the size, XOR is the OR exclusive and it works in this way:

0 0 0
0 1 1
1 0 1
1 1 0

The result is true if the inputs are different and false if they are equals.
The intermediate step obtained by the logical operation is displayed in Figure 5.7:

Figure 5.7: Result of the XOR operation: after the white pixel are counted.

The value passed to the PSO algorithm is the sum of the 1's pixels obtained by the application of the cost function. The optimization algorithm will evaluate the smallest sum of 1's for each particle and then for each iteration, the best set of values correspondent.

That number is the fitness of the swarm evaluate, it is the weight.

I_2 is the new image after the geometrical transformation, done by another particular function.

A point $\underline{x}$ is considered, that is the coordinate of a point in the vein pattern.

The first step is to compute the centre of gravity of the moving pattern, I_2, because a change in the coordinate system is required from that of the entire image to that of the moving pattern, because the transformation has to be referred to it.

The centre of the gravity is

$$\underline{c} = \frac{1}{N}\sum_{k=1}^{N}\begin{bmatrix} x_k \\ y_k \end{bmatrix}$$

where x_k and y_k are the 1's coordinates, because it's computationally less expensive working only with the moving pattern, N is the number of points.

After the decision to make is the order of the geometrical transformations:

1. Rotation;
2. Translation;
3. Scaling.

Firstly the translation of the moving pattern in the new coordinate system is applied:

$$\underline{p_T} = \underline{p} - \underline{c}$$

$$\begin{bmatrix} m' \\ n' \\ 1 \end{bmatrix} = \begin{bmatrix} m \\ n \\ 1 \end{bmatrix} - \begin{bmatrix} c_1 \\ c_2 \\ 1 \end{bmatrix}$$

with $\underline{p}$ old coordinates and $\underline{p_T}$ new coordinates.

Secondly, following the order for the transformations, a rotation r is applied, and thirdly a x and y translation.

The rotation matrix r is defined as:

$$r = \begin{bmatrix} \cos\theta & \sin\theta \\ -\sin\theta & \cos\theta \end{bmatrix}$$

All together with the translation operation:

$$R = \begin{bmatrix} \cos\theta & \sin\theta & x \\ -\sin\theta & \cos\theta & y \end{bmatrix}$$

where x and y are the parameter values of the translation. The new coordinates are:

$$\underline{p_T^{'}} = R_{\underline{p_T}} - \underline{t}$$

After all, the old coordinate system is restored:

$$\underline{p_T^{''}} = \underline{p_T^{'}} - \underline{c}$$

Finally, the application of a *scale* parameter is required because, as Figure 5.4 and 5.5 displays, the distance between camera and hand is not fixed, and after that the new modified image is passed to the evaluation function.

5.3.2.2 Evaluation of the Values of the PSO Parameters

As explained before, the PSO is subjected to different parameters.

PSO is a stochastic optimization technique, it requires more than one iteration to run, a value that has to be set in an accurate way, because increasing the number of iterations, the algorithm is slower.

Another important choice is the number of particles: PSO utilizes a population of particles, random solutions that fly through the problem hyperspace with assigned randomized velocity. At each iteration, the velocity of the individual particle is stochastically adjusted according to the historical best position for particle itself and neighbourhood best position.

The movement of each particle naturally evolves to an optimal or near-optimal solution.

The term ‘swarm’ comes from the irregular movement of the particles in the problem space.

The inertia weight is employed to control the impact of previous history of velocities on current velocity, thus to influence the trade-off between global (wide-ranging) and local (nearby) exploration abilities of the flying points.

A large inertia facilitates global exploration while a small one tends to facilitate local exploration.

The acceleration parameters c_1 and c_2 are known as cognition and social factor as they control the relative strengths of individualistic and collective behaviour of each particle.

Low values allow particles to roam far from target regions before being rugged back, while high values result in abrupt movement toward or past target regions.

The performance of PSO depends largely on settings of the control parameters: inertia weight, acceleration constants, maximum number of iterations, initialization of population (comprising the initialization of the velocity), the number of particles.

The setting of the range of the values used to find the optimal set of parameters is very important, and related to the images of the database on that I am dealing with.

The set of them is a posterior study, because I need to try a lot of times, which is the best range, looking at the result.

At the beginning I worked only with a mask, modifying the same one with different translations and rotations, to see if the PSO was working, seeking for an overlap of the reference and the processed images.

The final ranges of the values for each parameter is:

$$\theta = \left[-\frac{\pi}{6}, \frac{\pi}{6}\right] \qquad Xtrasl = [-40,\ 40] \qquad Ytasl = [-40, 40] \qquad scale = [0.8, 1.4]$$

The latest result is shown in Figure 5.8:

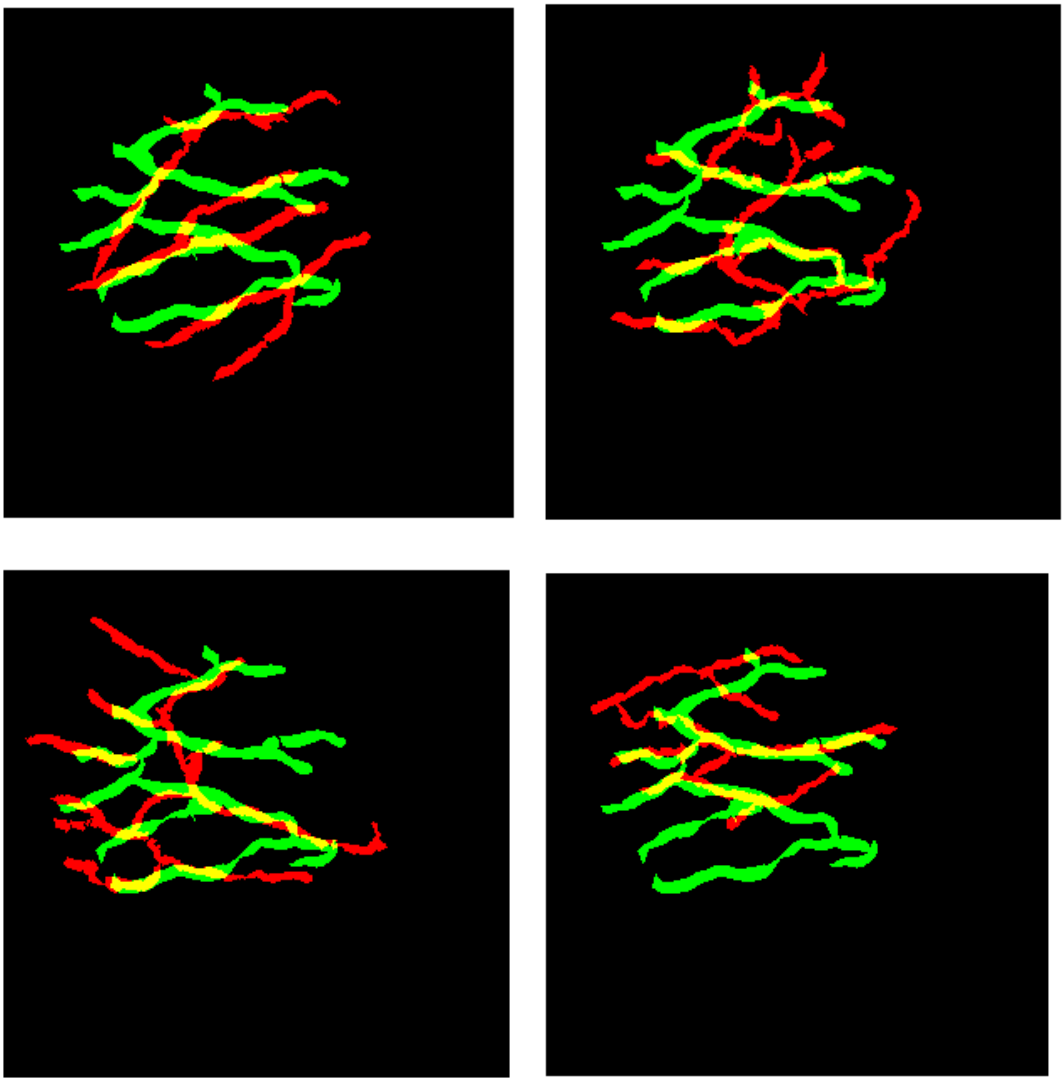

Figure 5.8: Various results of the PSO: in green is the reference mask, in red is the registered image, in yellow the overlapped points between the two masks.

The next choice is the number of particles, sets to 20, because the number of parameters is only 4, so a small number of particles is the right one.

The parameters, such as inertia weight, c_1, c_2 and initialization of velocity, were set as follows: $c_1 = c_2 = 2$ and inertia weight = 0.4.

The values of the two acceleration parameters was changed a lot of time, starting from 1.2 to 2, but the last value fits well for my application.

A way to see how to choose the various values and make a final decision, was to print a matrix with the best global states of each iteration, such as the four best values of the set of parameters, at the beginning and a number of best local states for each iteration.

If the values change too much, the range is wrong, and the values of the acceleration has to be changed, and vice versa, if the values are quite the same.

Hence, I need a compromise, that allow changes in the value but not in a rapid way. Along the first four column of the matrix, I can evaluate if I have to change the number of iterations, indeed, along the rows, I can check how the accelerations work.

The search for an optimal set of parameters is a repeated process, and the stop criteria is the maximum number of iterations that is reached.

The number of iterations is set to 50, because trying to get a higher number is useless, the best global states for half of the iterations remained the same.

As the number of iterations affect the velocity of the problem, in a computationally manner, it is better to keep it low.

About the initial value of the velocity of the particles, the choice is a zero value.

Figure 5.8 displays the final result, in addition Figure 5.9, 5.10 explain how the registration changes the image to be registered.

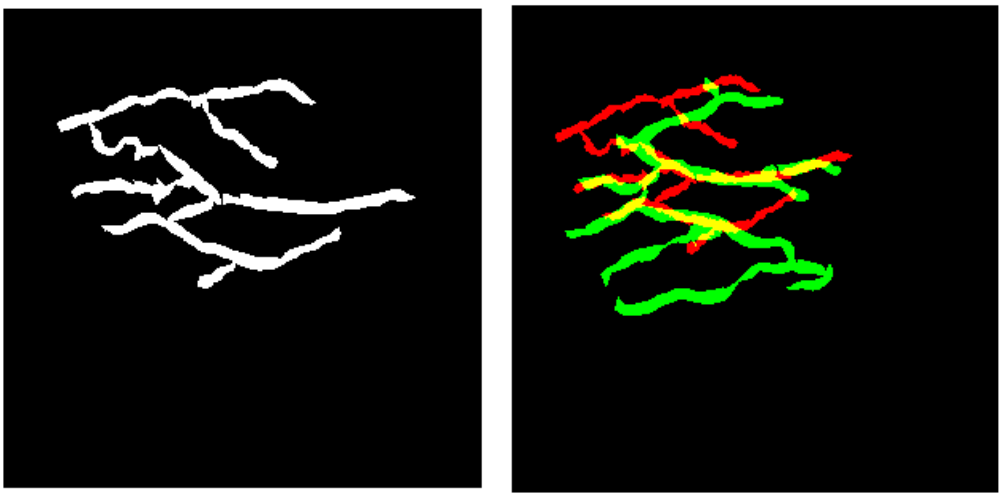

Figure 5.9: Before and after the registration, the white mask is the original one and the red one is the registered.

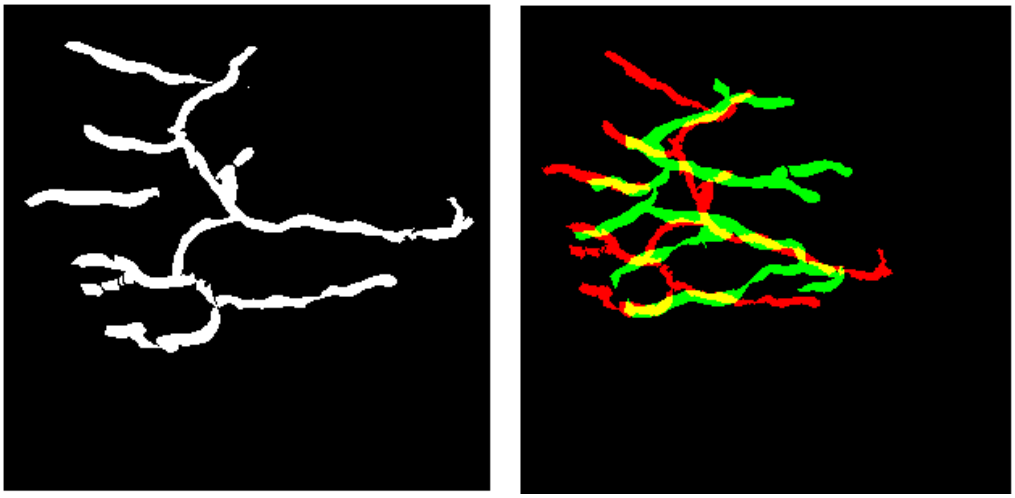

Figure 5.10: Another example of the result obtained after the registration.

5.4 Creation of the Graph and Characteristics of the Vessel Tree

In the previous chapter I talked about the structural matching, that is summarizing, a comparison of locations of feature points such as line and endings, bifurcations extracted from different patterns being compared to obtain the matching score.

The main goal is to choose the appropriated set of those features, that allow us to characterize a specific vascular network.

The shape descriptors are a set of numbers, produced to describe a given shape. The better is the descriptor, the greater is the difference in the descriptors of different shapes and the lesser is the difference for similar shapes.

Shape indicators are chosen simply observing the images and wondering about the main characteristics of these kind of images.

Firstly, the junctions, in particular the minimum angles between the branches of a junction, is treated as a possible indicator. Their position could be another characteristic, but for the nature of the images, I cannot consider them to take any kind of conclusion.

Secondly, following the idea of the junctions, the length of the vessels, precisely, of the vessels segments between junction and junction, junction and end point can be considered.

To obtain in an automatic way all these features, I applied and modified on my images, a software of a PhD student of School of Computing, Adrià Perez-Rovira, designed on retinal images.
As I said in the previous chapter, I need to apply changes in the software because I am dealing with images completely different, without any link with the retinal images.
First of all I would like to explain, from a theoretical point of view, how it works, considering the paper [55] "*Recognition of shapes by attributed skeletal graph*", Cecilia Di Ruberto, on which the software is based.

5.4.1 Recognition of Shapes by Attributed Skeletal Graph

The main purpose of this research is the seeking of features, that could help me to achieve the main goal of this pilot study, the characterization of an individual, and make statistics on the indicators.
The shape of the subcutaneous vascular tree of the dorsum of the hand could contain information that are capable of authenticating the identity of an individual, so the main step is to find something that confirm this definition.
A processing algorithm is used in order to determine the number of intersections, relative angles, length of vein segments and other relevant data according to the degree of complexity set by the desired application.
Calculating the skeleton of the binary mask, it gives a potential tool to find and study features of an object.
In other words, it resumes geometrical and topological features useful for indexing in a database of shapes.
In particular finding information on a shape, it could address the next matching step and create a model that summarizes the characteristics of an object.

Detection of the end points, junctions and curve points of medial axis is important for a structural description that captures topological information embedded in the skeleton.
The thin line is converted into a graph associating the curve points with the edges, the end and the junction points with the vertices.
To detect the characteristic points of the skeleton based on morphological approach, the skeleton has been pruned in an adaptive way in order to achieve a more regular and effective representation for a percent indexing.
From the cleaned skeleton, an attributed skeletal graph is built to organize in a structured way the information about an object shape and topology embedded in the medial axis.
Unfortunately the skeleton of an object often contains many spurious branches that are due to boundary irregularity. To eliminate short branches on a skeleton, a parametric morphological pruning transformation conditioned to the skeleton length, has been applied.
The pruning removes the end points of an image and proceeds until stability is reached.
It is a very important step because it can delete junctions that are not real, artifacts that do not allow a good classification of the feature.
At the end, the skeleton obtained with end points and junction points as vertices and the skeleton parts as links, can be interpreted as a graph with its adjacency matrix.
The vessels are extracted and other high level corrections are done, such as the merging, instead of the only pruning.

Finally a configuration structure is needed, as starting point.
This configuration parameters depend from the type of binary mask required for the study, thereafter I changed all the values used to find a correct graph of the vessel network in the back hand images.

Specifically, the variables passed to the software are:

1. *Junction weights*: the weight of the incoming vessel pixels to compute the incoming direction;

2. *Apply morphology*: a closing operation, to apply it or not is a decision to take;

3. *Radius of the closing*: the value is set 1, it depends strictly from the images treated.

4. *Morphological operation*: ‘thin’ or ‘skel’, as I said in the previous chapter, the ‘thin’ operation is working better with the type of the images.

5. *Remove all the spots*: remove small spots in the input binary image before the skeletonization;

6. *Spots minimum area*: value is set to 10, because the resolution of the image is 303x303, so the area chosen is enough, it’s the minimum area of a spot to be not removed;

7. *Ending weights*: to compute the end direction for merging;

8. *Maximum distance*: set to 10, it is a small number always for the resolution of the images, it is the maximum distance to consider for a merging;

9. *Reliability*: for the merging operation, a value of 0.25 is quite conservative, so the set value is 0.20;

10. *Minimum vessel length*: set to 5, it is the minimum length of a vessel which is not a junction-junction.

After the specific choice of the values, a set of images is displayed, showing visually the steps described with the parameters and done to obtain the final graph.
Step by step, the various passages are shown in Figure 5.11, 5.12, 5.13.
First of all it removes small spots on the binary mask, then an operation of closing is performed, it is a dilation followed by an erosion, because it removes islands and thin

filaments of background pixel. It is shown also how it performs, so I can decide the size of the spots, the minimum area to be not removed.

The skeletonized image is evaluated and after different operations on the vessels tree, the entire graph of the veins, with the proper junctions, is realized.

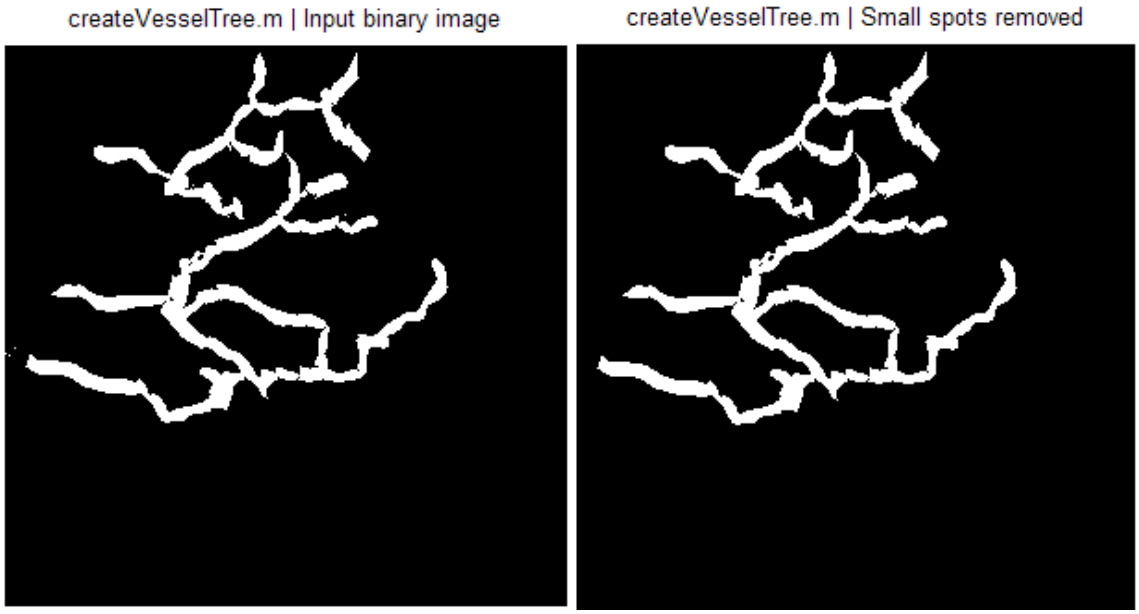

Figure 5.11: Original binary image (left) and small spots removed from it (right).

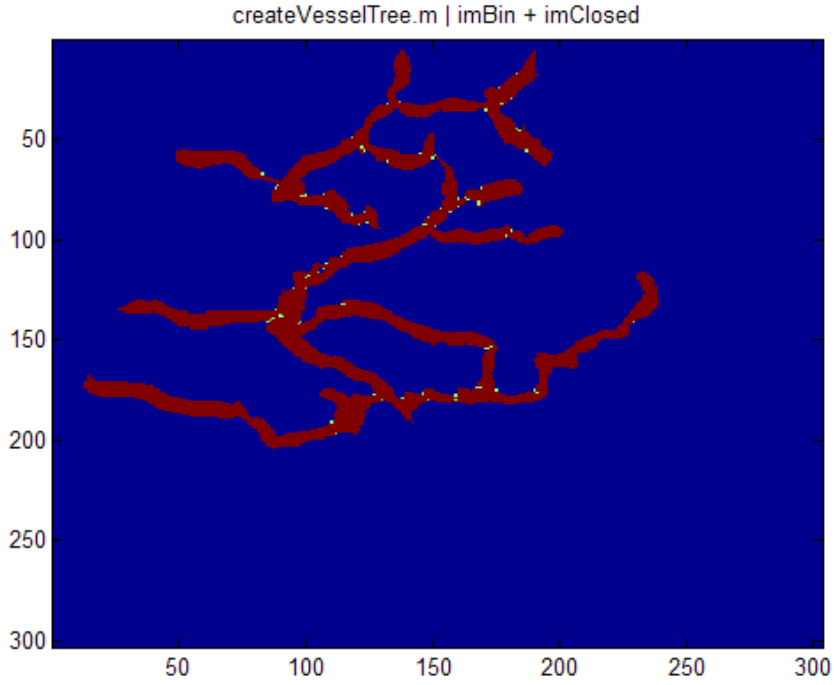

Figure 5.12: Binary mask (red) and the operation of closing (green).

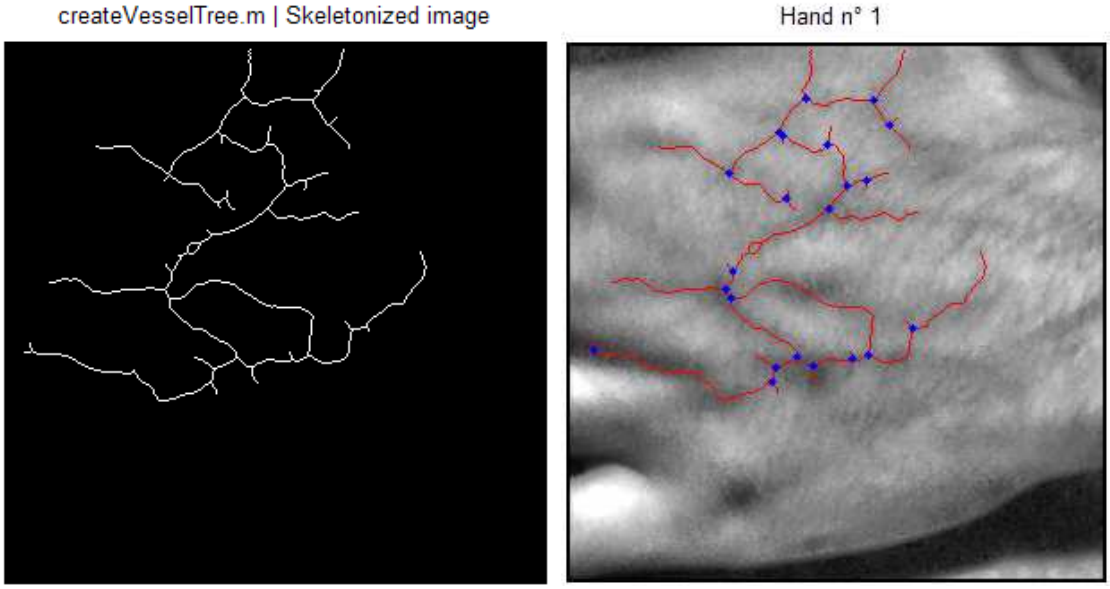

Figure 5.13: Skeleton(left) and final vessels graph with relative junctions displayed (right).

A lot of values are stored in a structure of data after the establishment of the graph, that might be interesting and contain eligible features for the images treated.
The number of nodes and vessels is detected. For each node, it is known the position, not useful because the masks are derived from different images acquired in different manners.
If a node is a junction or not, it is an important information and step, because I decided to use the branching angles as possible feature, so I need to handle only with the junctions, the end points are not considered.
The descriptor structure contains three numbers that are the values of the angles between branches of a junction.
The angles in the vascular tree descriptor are the orientation of the vessels, being 0 when they point and move clockwise. Before to store them and choose the smallest one, the evaluation of their value in degrees is required, applying a simple algorithm.
I have to subtract them but paying attention because the distance between 350 and 10 is 20 and not 340.

An easy way to cope with that problem is doing the subtractions between pair of angles and checking the difference a posterior with two rules:

1. If the angle α is negative $\longrightarrow \alpha = -\alpha$;

2. If the angle α is over 180 degrees ⟶ α = 360 – α.

Instead the vessel structure contains the start and the end nodes, with their orientation, the number of pixels, the length calculated with the Euclidean distance.
This is the reason that the number of pixels and not the length, is a better feature, while the Euclidean distance is only an approximation.

All the requirements are given by this analysis, and storing the parameter of interest, the statistical evaluation can be done by choosing the appropriate way to do it, seeking for a way to study the discriminative power of certain features.

Chapter 6

Experimental Results

6.1 Database of Images

At the beginning the set of images was made by random pictures, such as upper and lower limbs, legs, feet, collected by Miss Meadows in the past few years.

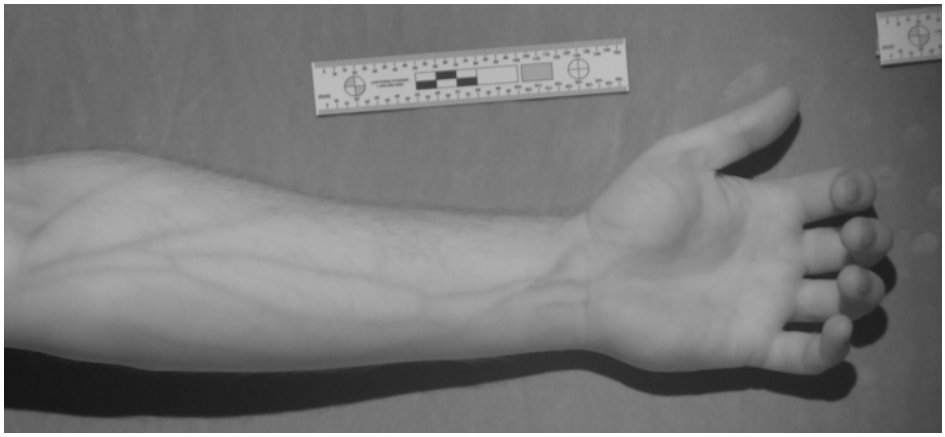

Figure 6.1: Examples of infrared images collected.

The initial database was formed of folders with arms, legs, feet, hands. The first idea was to search for a method of improvement of the contrast.

The pictures of legs were too big and quite impossible to deal with them, because the visible area of the vessel network was covered by different factors, as light, shadows, as Figure 6.2 shows.

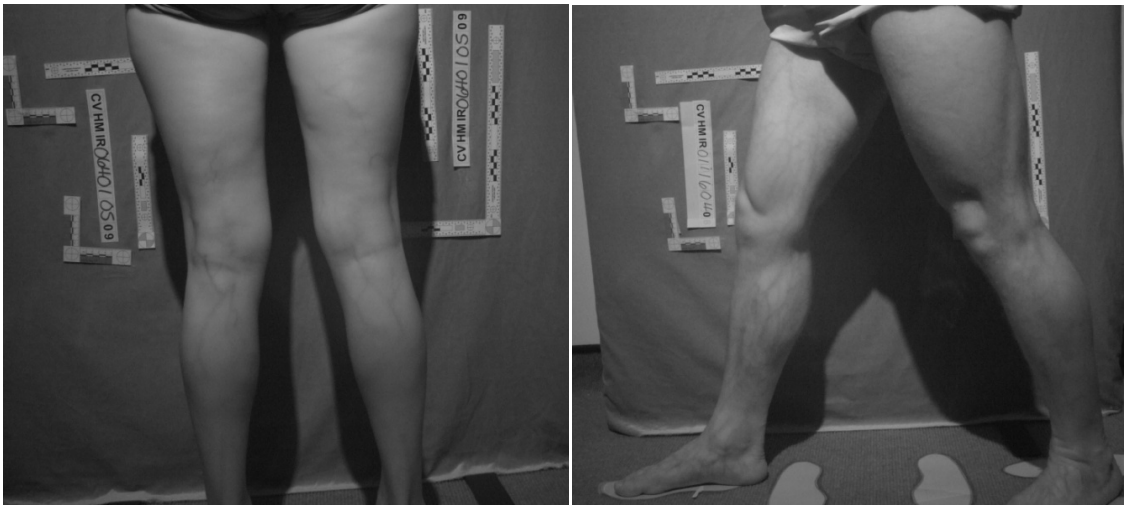

Figure 6.2: Infrared images of legs showing difficulties to find the venous pattern.

First of all, I tried to apply the enhancement software to the pictures of feet, the best contrasted images, Figure 6.1(feet).

After the first set, the real set of images was selected and it consisted in sixteen folders with two folders inside respectively with the IR images, left and right hand, and the visible light images.

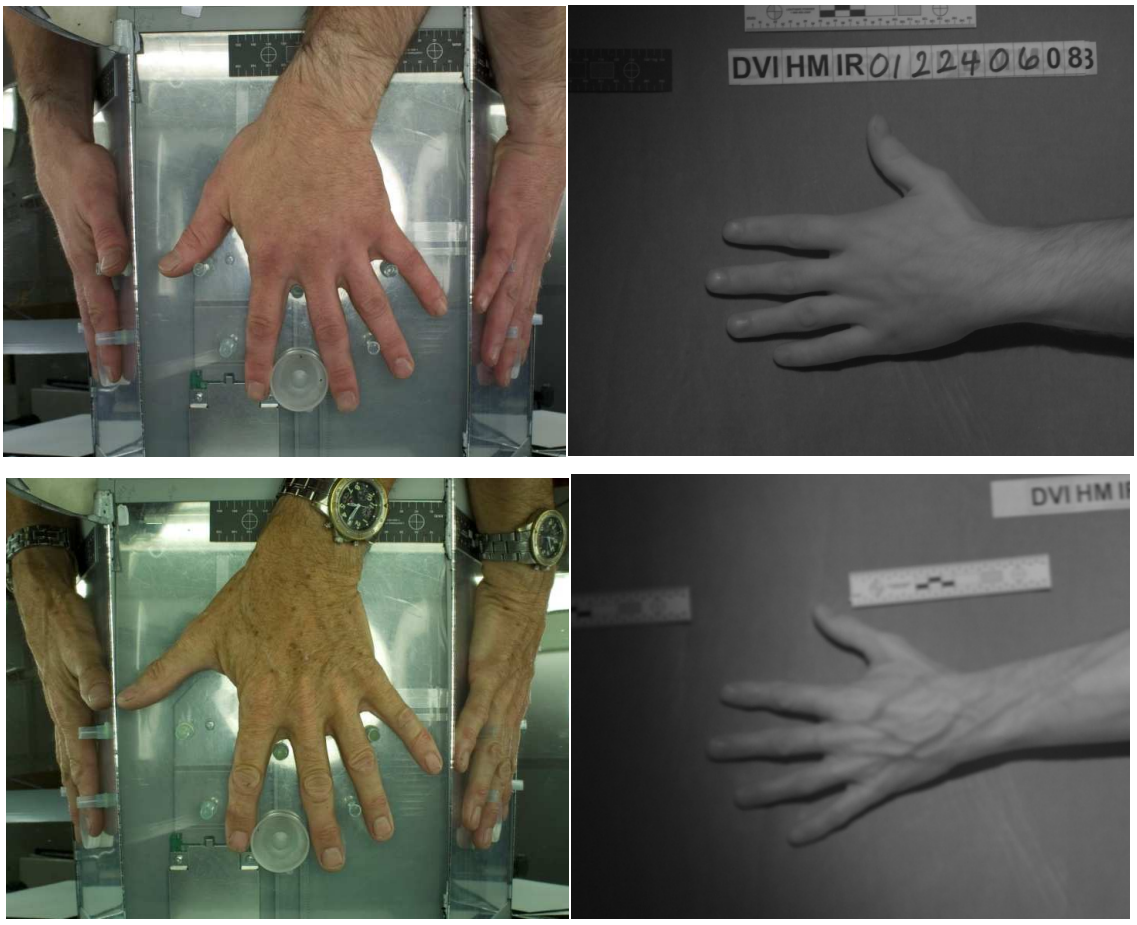

Figure 6.3: Visible(left) and infrared images of two back hands.

After the application of the developed software and the various steps studied to achieve the main goal of the pilot study, another set of images was received, added to the other images.

Other fifty folders were evaluated, selecting the images on which a pattern recognition study could be applied.

A study of utility of the images was needed, because in various images the lack of contrast was too high to be able to work with them, e.g. Figure 6.4 displays.

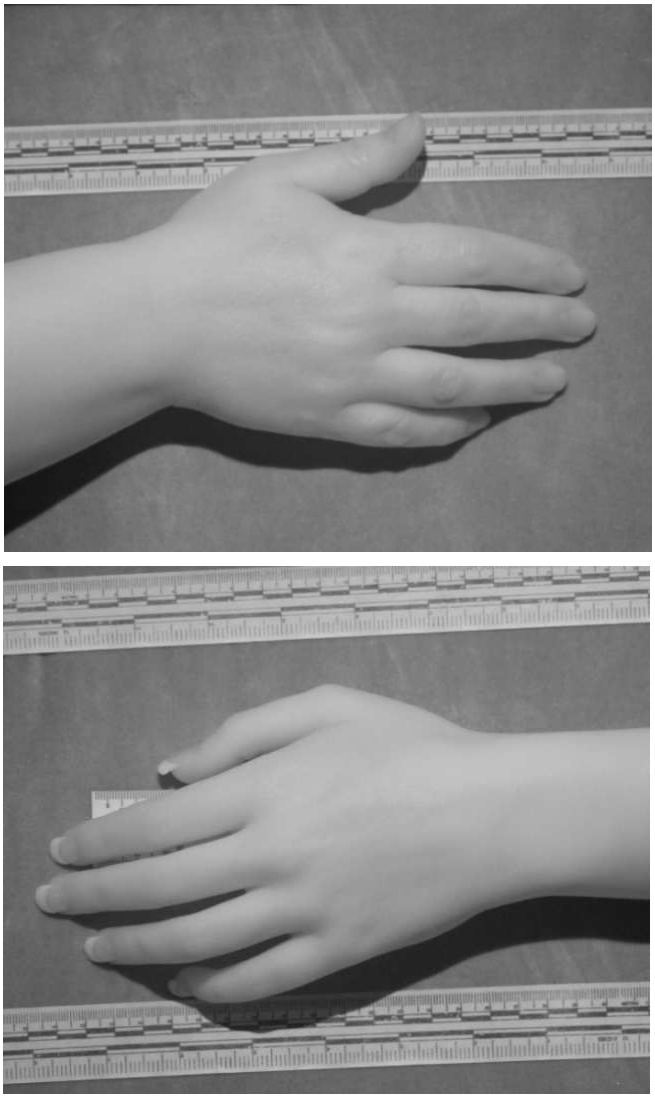

Figure 6.4: Examples of lack of contrast in two infrared images.

Trying to apply the enhancement functions to the IR images of Figure 6.4, the results were useless, without any sign of improvement.

The number of folders of the database was decreased to thirty-six folders.

The images are infrared images, with resolution of 2000x3000, RGB with three channels, but analyzing them, the channels are equals, the image is monochromatic, so only one channel was chosen.

The images were cropped to select a specified ROI, region of interest, because the part of the back hand with the vessel network is a small region in the centre of the dorsum.

The background, the fingers and the wrist are useless for the detection of the main network.

Figure 6.5 shows the difference between the whole image and the cropped area.

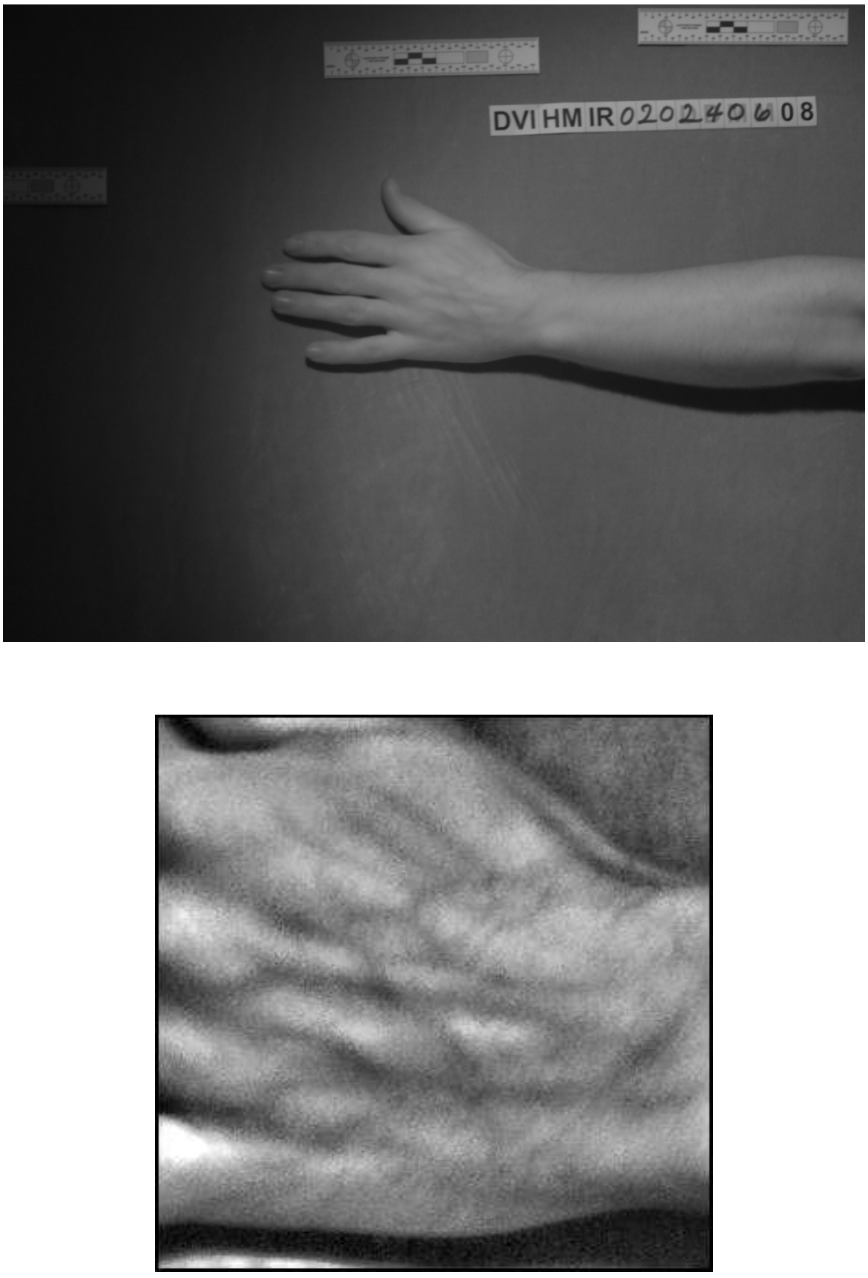

Figure 6.5: Original image (up), cropped and enhanced image (down).

The resolution of the cropped image is 300x300, the database is set with the same properties, Figure 6.5 (low) is an example.

The denomination of the images has been changed, with a specified order.

6.2 Acquisition of the Images

6.2.1 Introduction to IR Photography

Veins can be identified using near-infrared light, whereby reflected or transmitted images of blood vessels can be detected via the reaction between light and the deoxygenated blood in the subcutaneous vessels.

Near-infrared rays generated from a bank of light emitting diodes(LEDS) penetrate region of interest and are absorbed by the deoxygenated haemoglobin.

Due to differences in absorbance between the veins and other tissues, the reflected near-infrared rays produce an image in which regions of high absorbency(i.e. veins) appear as dark lines in an image captured by a charge-coupled device (CCD).

The image can be processed and manipulated to construct the venous patter from the captured image.

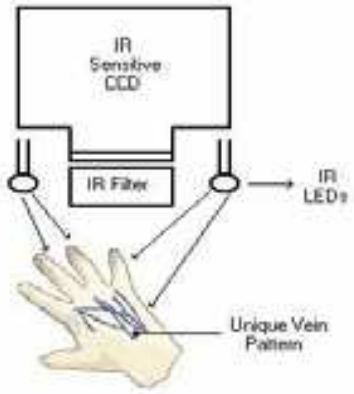

Figure 6.6: CCD camera [8]

When capturing an image under infrared light the film or image sensor used must be sensitive to infrared light, distinguishing these types of sensor from those that are

sensitive to visible light. The region of the spectrum available for image capture in this case is referred to as near-infrared to distinguish it from far-infrared, which is the domain of thermal imaging. Wavelengths used for photography range from about 700 nm to about 900 nm. An infrared filter is also required to allow infrared (IR) light pass through to the camera to the sensor, whilst blocking all or most of the visible light spectrum (these filters appear black or deep red to the naked eye).

When these filters are applied to an infrared sensor on a digital camera, a variety of effects can be obtained. These include false-colour or black-and-white images with a dreamlike or sometimes lurid appearance known as the "Wood Effect" in artistic photography. This effect s mainly caused by plant life strongly reflecting IR light in the same way visible light is reflected from snow.

Modern digital camera sensors are inherently sensitive to infrared light. Under normal light conditions this would interfere with the standard image capture by disturbing autofocus capability or by softening the image as infrared light is focused differently than visible light. Oversaturation of the red channel may also occur. Under precise lighting conditions some clothing is transparent in the infrared. This has, in the past led to unintended (at least to the manufacturer) uses of these types of camera. Thus, to improve image quality and protect privacy, many digital cameras employ infrared blockers.

An alternative method of digital SLR infrared photography is to remove the infrared blocker in front of the CCD and replace it with a filter that removes visible light. This filter is behind the mirror, so the camera can be used normally - handheld, normal shutter speeds, normal composition through the viewfinder, and focus, all work like a normal camera. Metering works but is not always accurate because of the difference between visible and infrared reflection. When the IR blocker is removed, many lenses which did display a hotspot cease to do so, and become perfectly usable for infrared photography. Additionally, because the red, green and blue micro-filters remain and have transmissions not only in their respective colour but also in the infrared, enhanced infrared color may be recorded.

Fuji have produced digital cameras for use in forensic and medical investigation which have no infrared blocking filter. The first camera, designated the S3 PRO UVIR, also had extended ultraviolet sensitivity (digital sensors are usually less sensitive to UV than to IR). Optimum UV sensitivity requires special lenses, but ordinary lenses usually work well for IR. In 2007, FujiFilm introduced a new version of this camera, based on the

Nikon D200/ FujiFilm S5 called the IS Pro, also able to take Nikon lenses. Fuji had earlier introduced a non-SLR infrared camera, the IS-1, a modified version of the FujiFilm FinePix S9100. Unlike the S3 PRO UVIR, the IS-1 does not offer UV sensitivity.

6.2.1.1 Human Tissue as an Optical Medium

The effect of infrared light on skin largely depends upon the three factors of absorption, reflection and scatter (Bryson, 2005 [21]). As the wavelength of light used for illumination is increased so the surface texture that can be photographed is progressively decreased. The scattering of light increases greatly with depth of tissue. The amount of visible light reflected from the surface of the skin is similar for all skin colours.
Most of the light which penetrates dark skin is absorbed in the first two layers. This leads to higher contrast in surface detail as there is less scatter and less reflected light from deeper layers of the skin. Darker skin tones reflect more infrared that lighter skin tones, and any light that does penetrate is almost completely absorbed by the melanin bearing layers. This leads to an extreme lack of contrast between infrared absorbing veins and surrounding tissues as less light reaches that far.

6.2.1.2 Fuji IS-1 Camera

A Fuji IS-1 digital camera with nine Mega Pixel Fujifilm Super CCD sensor and ISO 80-1600 capabilities was used for all image capture. The camera has a high sensitivity range to capture images under visible and infrared light (approximately 400nm –900 nm) conditions.
Power Source – batteries and charger.

6.2.1.3 Lens Filtration

Lens filtration can be applied to the Fuji IS-1 to isolate specific wavelengths. An 850nm Visually-Opaque, toughened glass Infrared filter was applied to the lens of the Fuji IS-1 using a standard step-down ring.

6.2.1.4 Infrared Light Source

The 88mm (L)x 95mm (W) x 68mm (H) structure consists of painted steel and reinforced glass. Internal to the casing are 48 Infrared LEDs at a 60° angle, which respond to a night (on) and day (off) detector facility. The infrared light source emits infrared light at a wavelength of 850nm, has an operating current of 600mA. And a maximum irradiation distance of 15m.

6.2.1.5 Infrared Light Source Mount

Fully adjustable wall bracket with 1/4 inch Whitworth screw for the Infrared Light Source, as shown in Figure 6.6.

Figure 6.7: Infrared light source.

6.2.1.6 Material Used

This is a list of the materials used for the acquisition of the IR images:

- *Infrared Light Source Adaptor*
- *Duck Tape*
- *Black Velvet Sheet* (Figure 6.9)

- *Screen*
- *Pre-printed Adhesive Labels* (Figure 6.9)

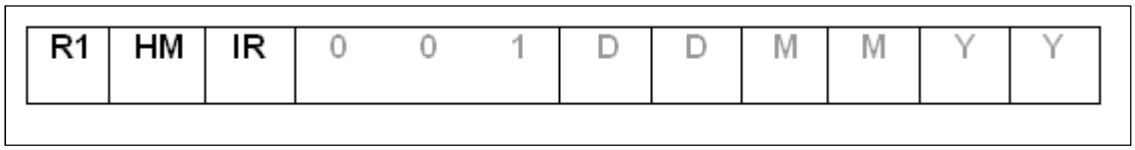

- *Pre-laminated markers*
- *Height Scale*
- *Weight Scale*
- *Blood Pressure Monitor*
- *DCIM MEMORY*
- *Belkin card reader*
- *Dell laptop*
- *Recordable DVD*
- *Microsoft access*

Figure 6.8: Studio: camera with tripod, black velvet sheet.

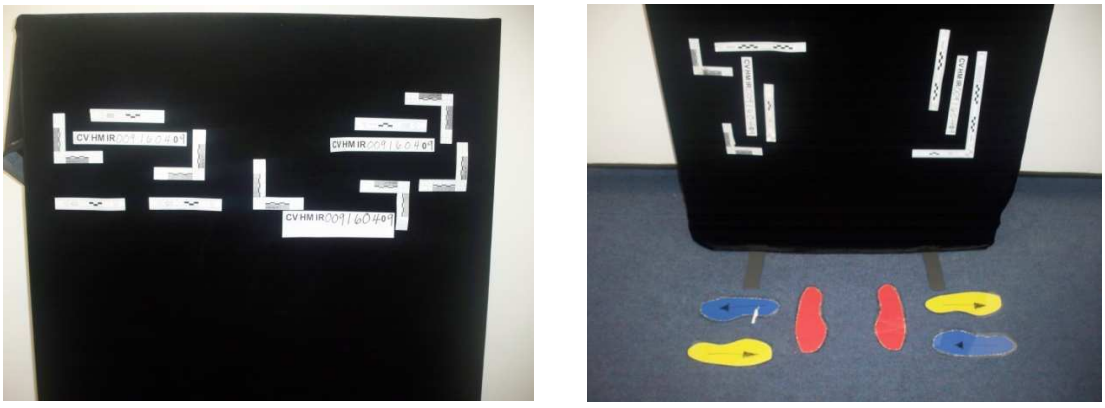

Figure 6.9: Black velvet sheet and positions.

Figure 6.10: Distance from:
Camera – scale centre – black feet = 54cm

Camera – screen = 210 cm

Camera – Red feet = 182.9 cm

Between Blue feet = 63.5 cm

Between Yellow feet = 63.5 cm

Figure 6.11: View of the studio.

Figure 6.12: View of the studio.

Figure 6.13: Camera and infrared light source.

6.3 Feature Detection

After the general explanation on what I am working, the main goal of the pilot study is to find possible discriminative features, and ways to proof their power in the identification of people.
A biometric feature is the highest level of security that we could achieve, but the tight characteristics of a particular biometric has to be found to confirm it.
The uniqueness of quantifiable features found automatically from a superficial venous pattern has to be proved with statistical tests and evaluations with histograms, across a population of individuals.
This is a pilot study, of a brief period of time; the entire process wants only to address a way to follow, to achieve the wanted result.

A careful evaluation of the possible discriminative features is required, starting from the main characteristic and material of the project, the infrared images, and the properties of the vessel network.

6.3.1 Width of the Veins

The width of the veins was the first feature considered, Figure 6.14 .

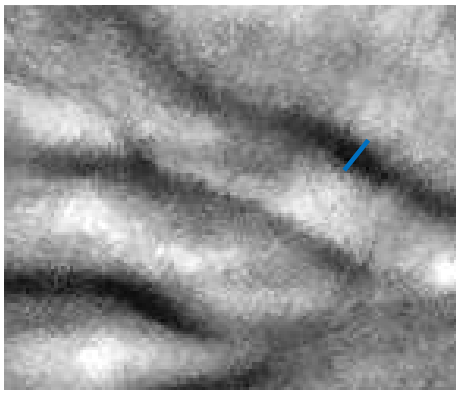

Figure 6.14: Image of a vein with a blue line that indicates its width.

The value of the widths were calculated with the Euclidean distance of the binary mask of the vessels network, Figure 6.15 displays the range of the widths for the entire vasculature detected.

Figure 6.15: Range of the widths in a back hand image.

The range of the values of the width of a vein pattern image is narrow, therefore the number of bins for the relative histogram is small; the choice is eight bins.
The resultant histogram for each image is shown in the following page, Figure 6.16, 6.17 respectively for the left hand and for the right hand.

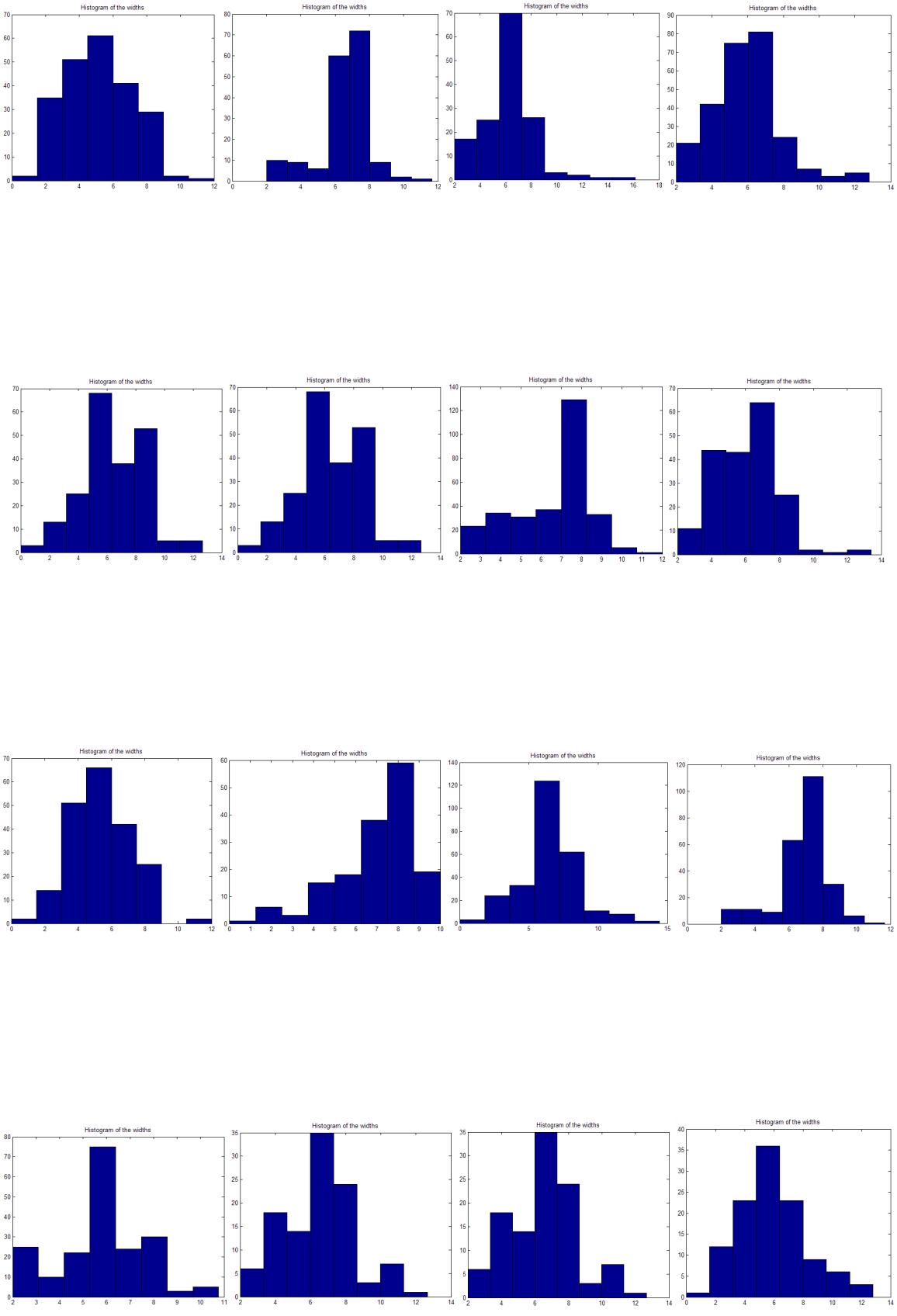

Figure 6.16: Histograms of the widths for the left hands.

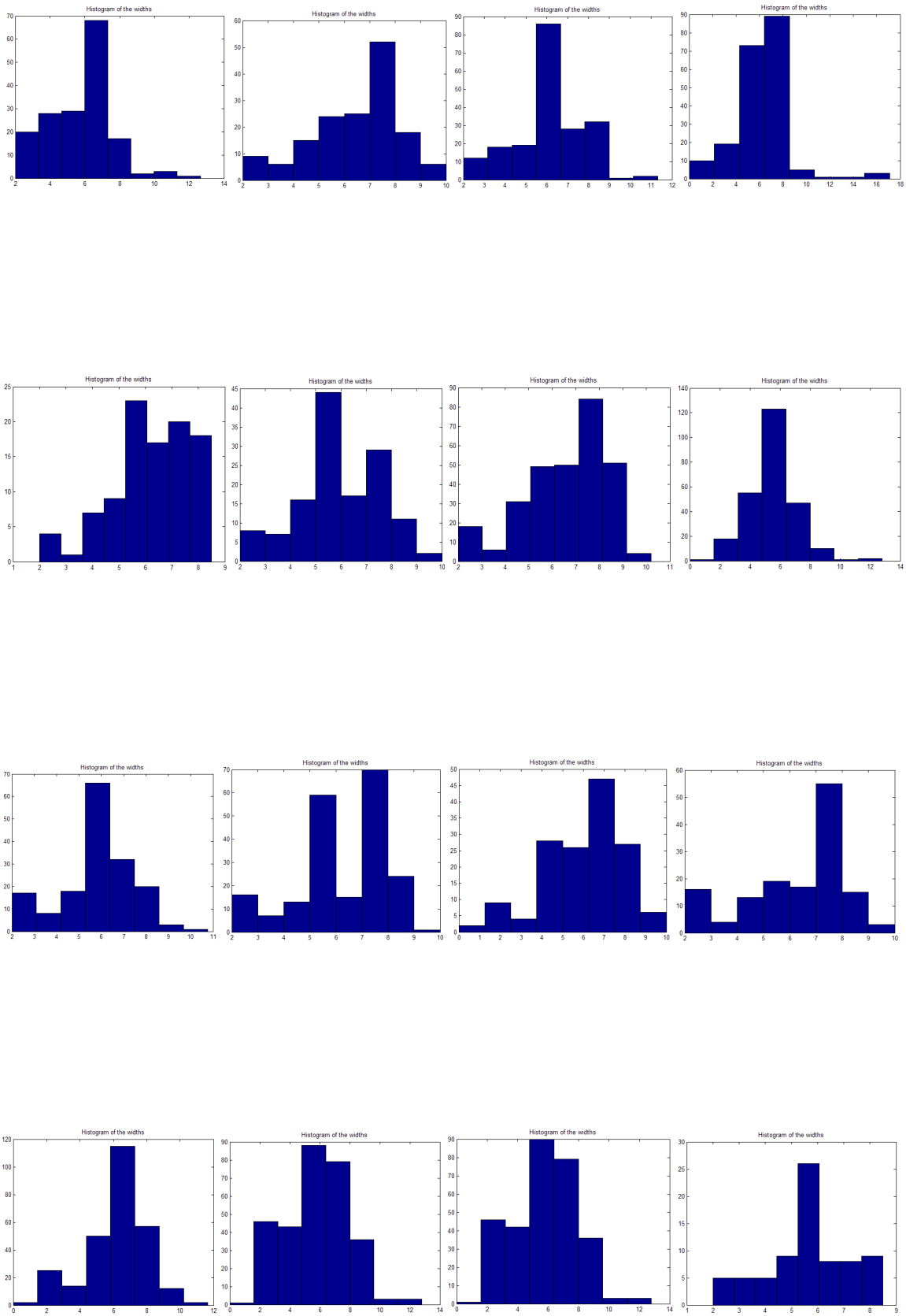

Figure 6.17: Histograms of the widths in the right hands.

6.3.1.1 Discussion

The results in the various histograms do not show a discriminative power of the considered feature, the width of the veins.

The feature selected is only one, taken singularly, the amount of information is not enough to perform any kind of evaluation.

Intuitively the histograms do not present noticeable differences. Considering a real venous pattern in the hand, in a visible way, great changes in the hand from another one cannot be noticed, all the widths have a maximal value.

Evaluating small regions of interest, such as the cropped image of the dorsum of the images, the widths cannot vary in a big range.

This characteristic of the vessel network is not enough performant to focus the attention only to it, and a singular feature cannot help us to give any kind of conclusions.

Other features were discovered and classified.

6.3.2 Branching Angles

The most important characteristic of a vascular network could be the junction point.

Junctions characterize the vessels tree in the back hand in the same way, because the number and the angles of them could be an appropriate way to describe an image.

The number of junctions is not a discriminative feature by itself.

The branching angles, i.e. the angles between the branches of a junction (Figure 6.18) could be a distinctive feature for the processed image.

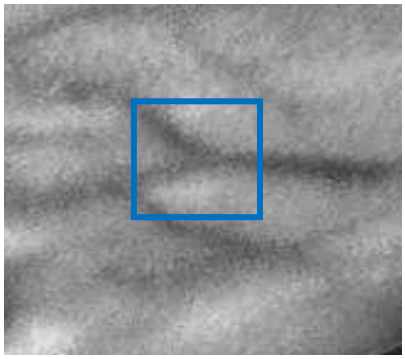

Figure 6.18: Branching angle selected with a blue square.

The analysis of the power starts from the choice of the angle to consider, in the triplet of the angles of a junction.

The choice has been the minimum value of the three angles, after the elaboration of the values with an algorithm, to obtain the value in degrees, explained in the previous chapter.

The minimum angle is considered as a candidate for the statistical study, wondering if it could be an identifiable feature.

First of all, an histogram of the angles found in the skeleton of the binary mask for each image, after various morphological operations, is plotted.

Thirty-six histograms for the left hands and thirty-six histograms for the right hands are obtained (Appendix), the first set of sixteen images is considered in the following pages, Figure 6.19 and Figure 6.20.

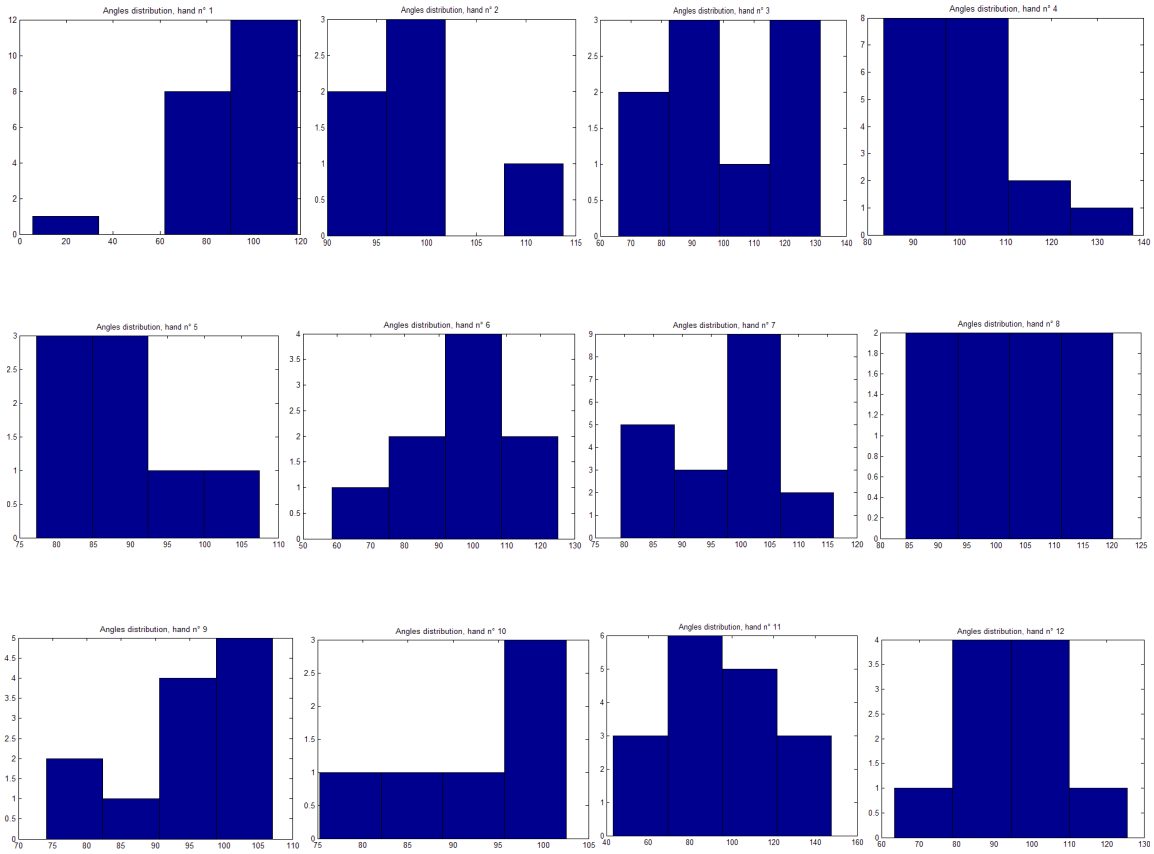

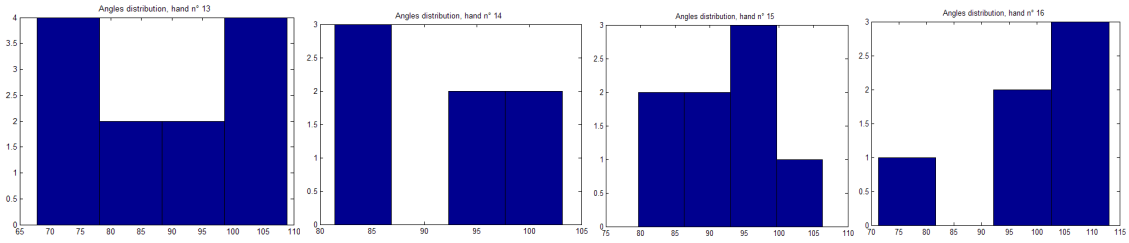

Figure 6.19: Histograms of the branching angles for the left hands.

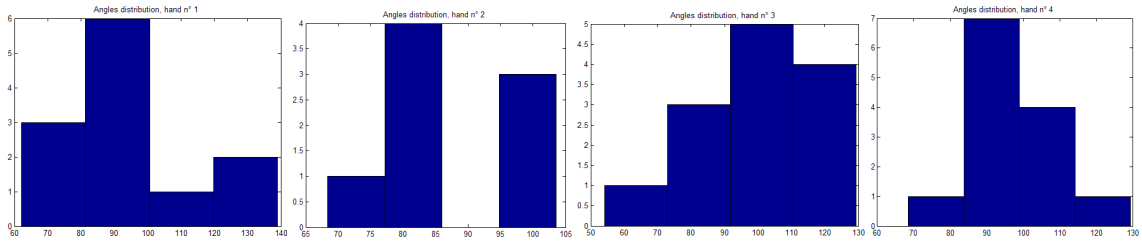

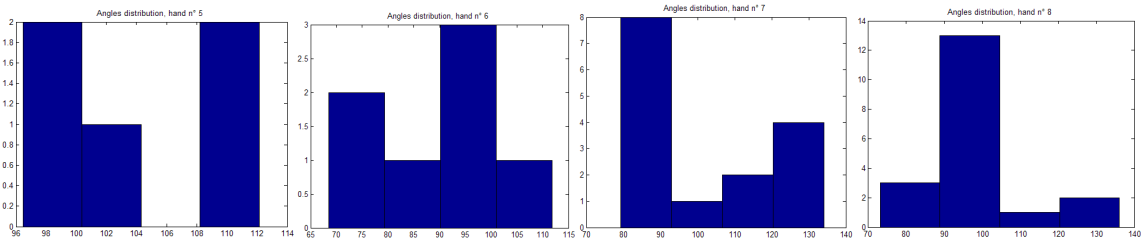

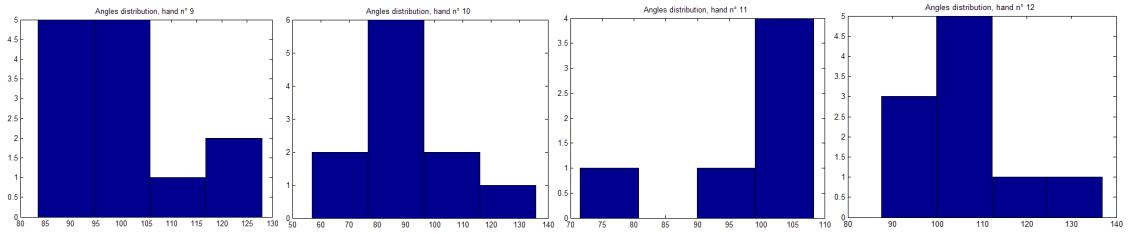

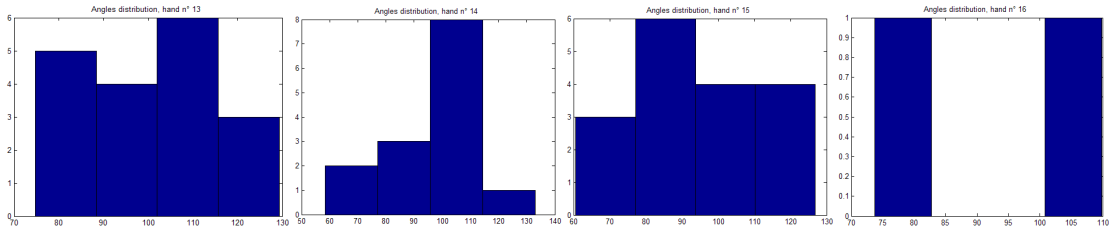

Figure 6.20: Histograms of the branching angles for the right hands.

The number of angles for each image is less than fifteen-twenty, at maximum.
The number of bins chosen for the histograms is four, related to the small number of angles in a back hand image.

6.3.2.1 Discussion

The singular histogram is not informative, for an eventual discussion on the characteristic power of a feature.
The only comment that I can do, is about the range of variability of each histogram.
The values shown by the histograms, x axis, are almost the same, in the range of 90-120; therefore there is not great variability in the range of the values of all the angles present in each skeleton of the binary masks.
The result was expected to be in this way, because the feature considered is alone, without any comparison. The ROI is quite small, anatomically as the hand, so the angles cannot vary in a wide range of values.

From another point of view, intuitively, looking at the histograms, considering only the shapes of the distributions, I can notice that all the shapes are different.
Some kind of conclusions could arise from this note.

6.3.3 Vessels Length

Another feature, linked with the junctions, can be noticed: the length of a vessel between junction-junction points or junction-end points.

Two types of results are given by the algorithm applied to obtain the skeletal graph of the desired binary mask: the vessel length can be evaluated with the Euclidean distance, or counting the number of pixels of the dark line between junction-junction and junction-end points.

Obviously the number of pixels in the vessel of a network is what I need for a possible evaluation on the classifiable power of the features set in the dorsum of the hand.
The Euclidian distance is only an approximation of the distance between the main bifurcations and end points.
The vessel length can be a feature quite discriminative, the singular histograms for 16 images are shown in Figure 6.21 and Figure 6.22 , the other histograms can be found in Appendix.

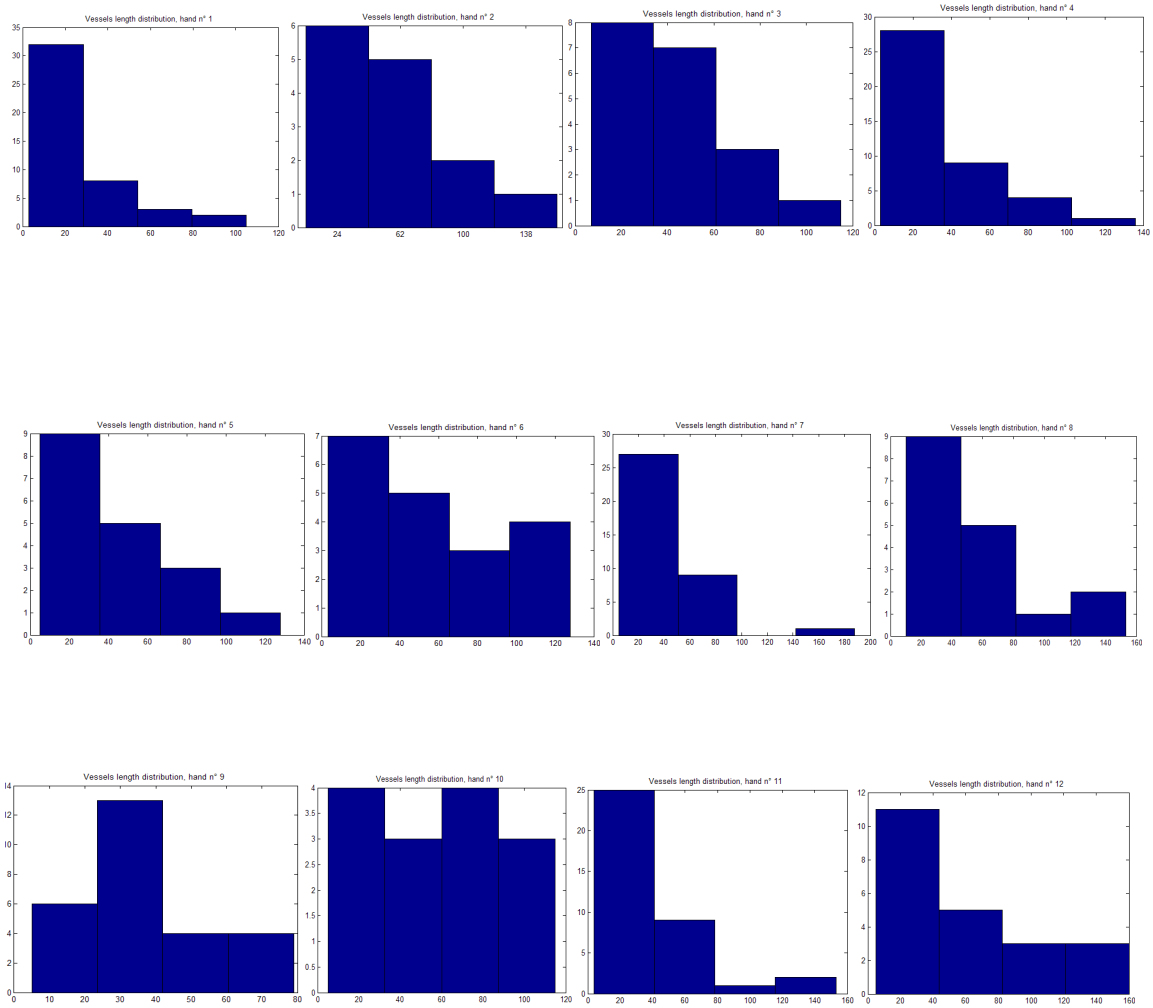

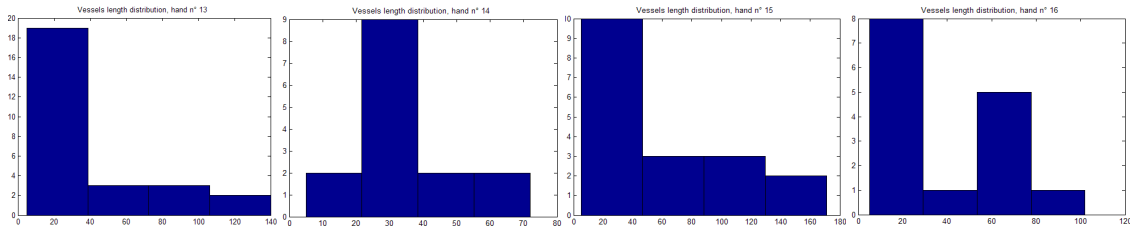

Figure 6.21: Histograms of the lengths for the left hands.

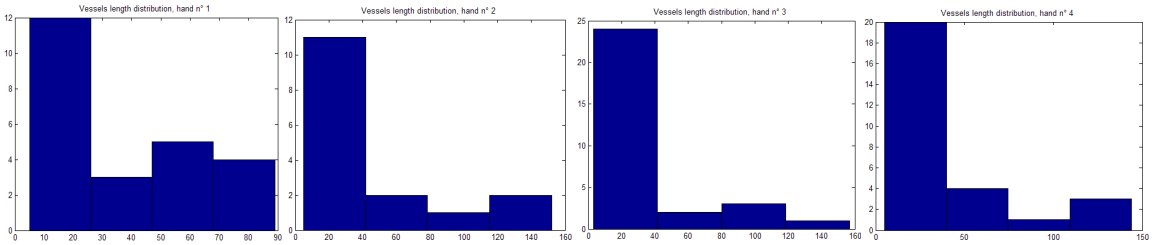

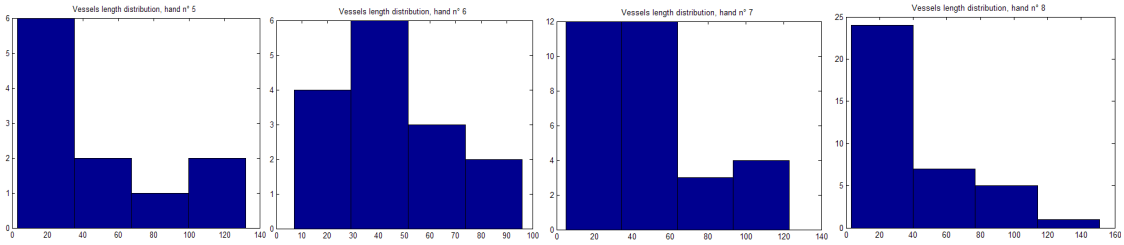

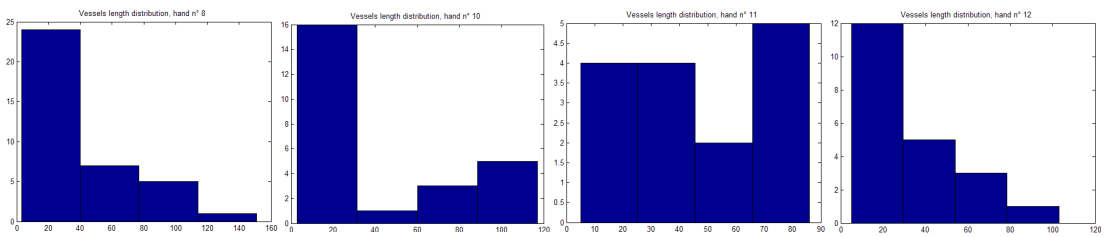

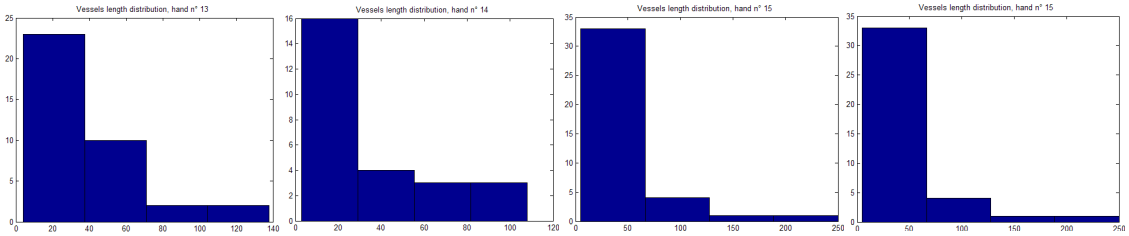

Figure 6.22: Histograms of the lengths for the right hands.

6.3.3.1 Discussion

Similar comments as for the histograms of the branching angles could be done also for the histograms of the vessel length.

Different values of the length fall in the same range for each images, as Figure 6.21 and 6.22 show.

The variability can be large, depending as usual from other variables, such as the acquisition of the images and the next segmentation step to detect the network.

The singular feature is not enough to perform a comment on the distinctive power of the length of the vessels.

In conclusion, singularly the histograms of angles and vessels lengths are poor of information and a lot of previous variables can assume a big role in the final result.

As said before, looking at the shape of the histograms, the result is different from the branching angles, because there is not a great variability in the distribution. There is a peak at the beginning of the histograms, small values, and the distribution decreases after, around bigger values.

6.3.4 Sum of Squares Distances within the Features Detected

6.3.4.1 SSD for the Branching Angles and the Vessels Lengths

The loss of information obtained with only one feature considered, addresses the evaluation of the quantifiability of the feature from a different point of view.

A whole histogram that plots a comparison of all the images, is required and performed, because the interest is in comparing the images.

Sum of squares distances (SSD) is used to examine the probability distributions of each image, for each feature considered respectively.

The goal is to obtain a superior triangular matrix, size 36x36, with the differences between all the images taken in couples.

After that, the histogram of the entire matrix is plotted, one for the angles and one for the vessels length.

The result is displayed in Figure 6.23, 6.24, 6.25 and 6.26.

The SSD is evaluated as follows:

$$SSD = \sum_{k=1}^{n} [v_{1k} - v_{2k}]^2$$

Where $\underline{v}_1$, $\underline{v}_2 \in \Re^n$ are two vectors representing the two distributions of the feature.

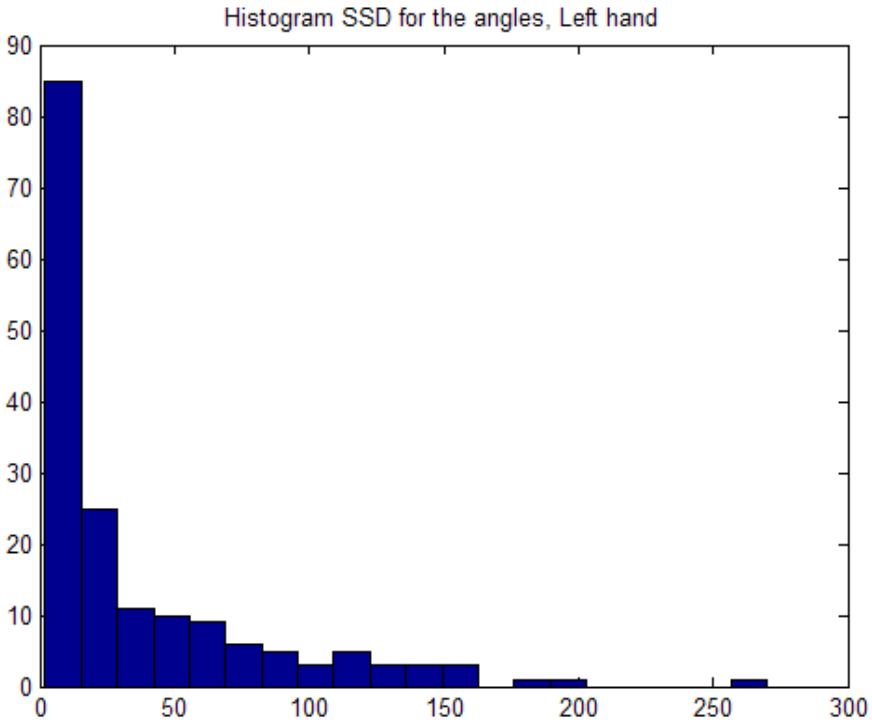

Figure 6.23: Histogram of the SSD for the branching angles, left hands.

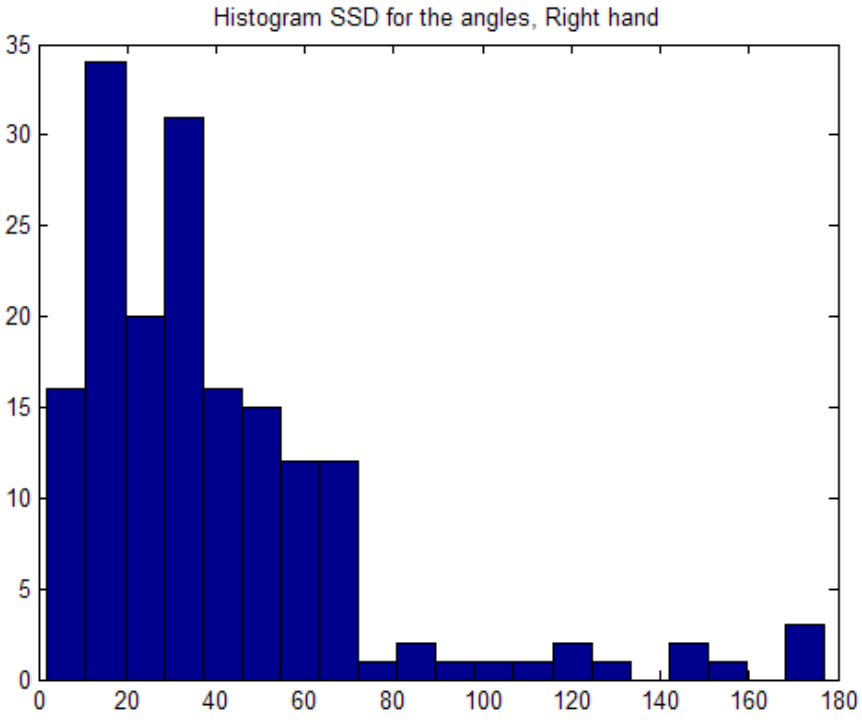

Figure 6.24: Histogram of the SSD for the branching angles, right hands.

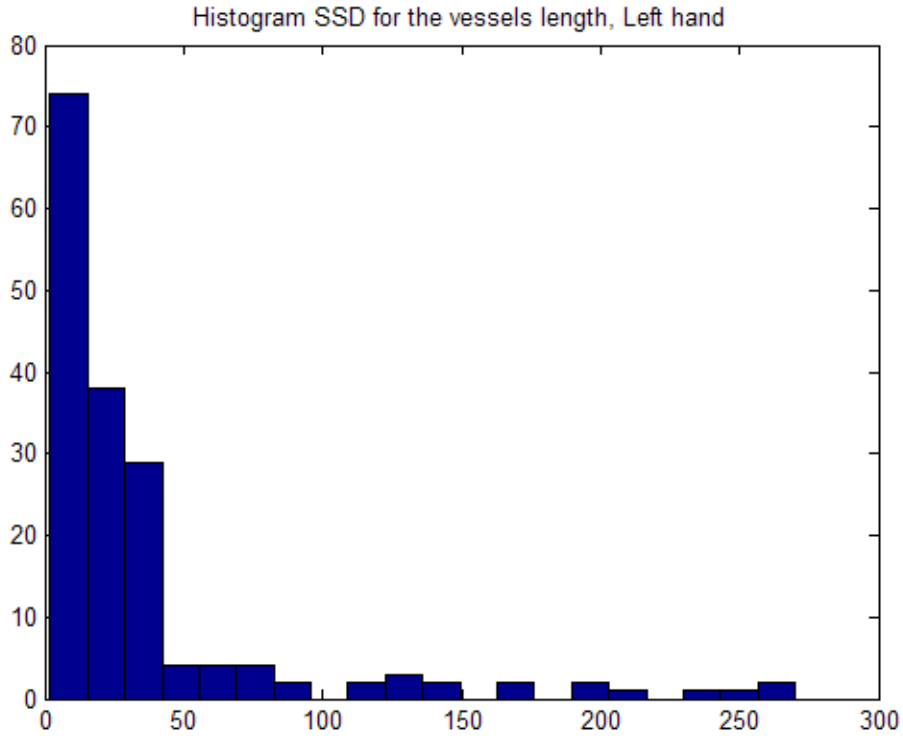

Figure 6.25: Histogram of the SSD for the vessels length, left hands.

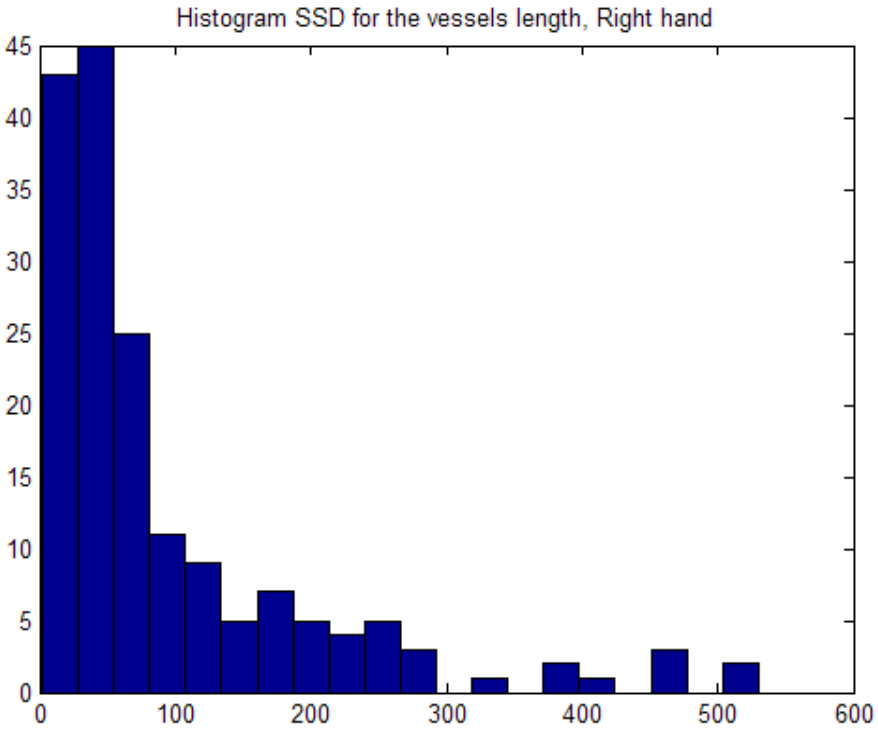

Figure 6.26: Histogram of the SSD for the vessels length, right hands.

6.3.4.2 Discussion

The evaluation of the results is done considering, also in this case, the range of variability in the x axis of the histogram.
Looking at the graph, the distribution is grouped near the smallest values as Figure 6.23, 6.24, 6.25 and 6.26 show; this is noticeable for the four histograms.
Considering that the matrix is made of differences, if the value that fills a position of the matrix is quite small, it means that the difference between the images is minimal, as consequence, the two images could be similar.
If the differences is quite big, it means that the distributions of the feature are quite far from each other, and the images could be considered different.
It is only a suggestion, conceiving that the matrix is formed of difference values.

Applying these considerations to the histograms obtained, I can observe that all the graphs are quite similar, and they display a group of values near the smallest values, the first bin.
Only few values are big and randomly distributed on the histograms.
The hands seem quite similar, taking in consideration only these plots.

Anyway, I cannot give specific conclusions, because a lot of variables influence the result, as the initial binary mask, whence I originate the skeleton of the vessel network, is obtained from different steps, such as the acquisition of the images, detection of the network with segmentation methods.
Other suggestions can be done, basing on different way to compare the binary mask.

6.3.5 Joint Histogram of the Features

Relative frequency of the couples of features can be generated, to see if the group of features can be more discriminative than the singular ones.
The joint histogram of the couples, angle and length of the vessel, is generated.

Each image is characterized by two numbers, a weighted mean of the angles and the weighted mean of the vessels lengths of an image.

The two numbers representing the image are considered as the x and y coordinates of a Cartesian plane.

The x and y axis are divided into bins; the number of bins is difficult to choose. I used the Scott's rule [56], where for each variable, the width of each bin is evaluated by equation:

$$w = 3.49 * \theta * n^{-1/3}$$

where θ is the standard deviation of the data, and n is the number of data.

The number of bins is calculates as equation:

$$numBin = \frac{range}{w}$$

For each image the calculus of the two feature data is done.

The plane is divided by the bins, it appears as a sort of grid.

The couple (x_k, y_k) of the k image is analyzed as a possible point of the plane and it's collocated inside the correspondent bin situated in the grid.

The bin is increased by one, at the end a grid with bins of different heights is obtained.

The result is shown in Figure 6.27 and 6.28.

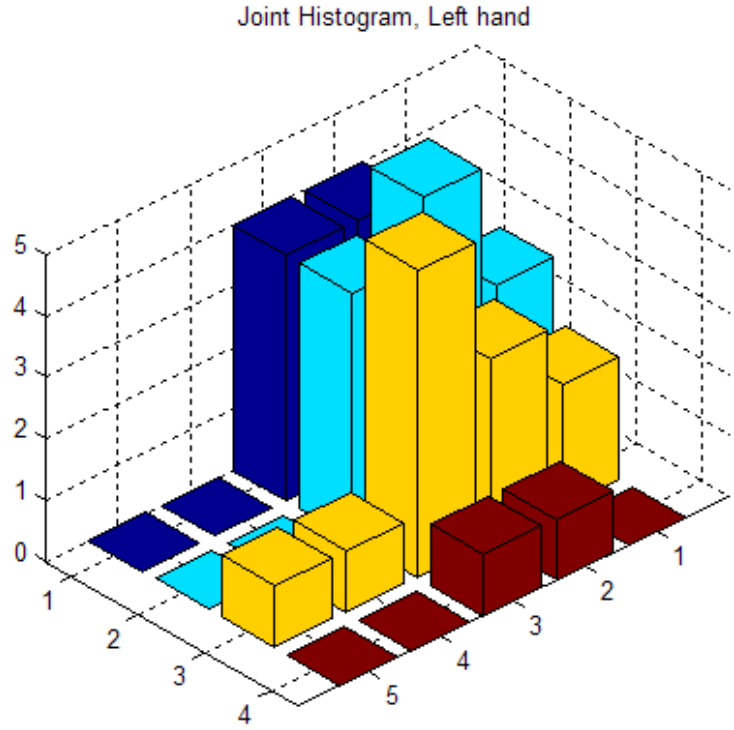

Figure 6.27: Joint histogram for the left hands.

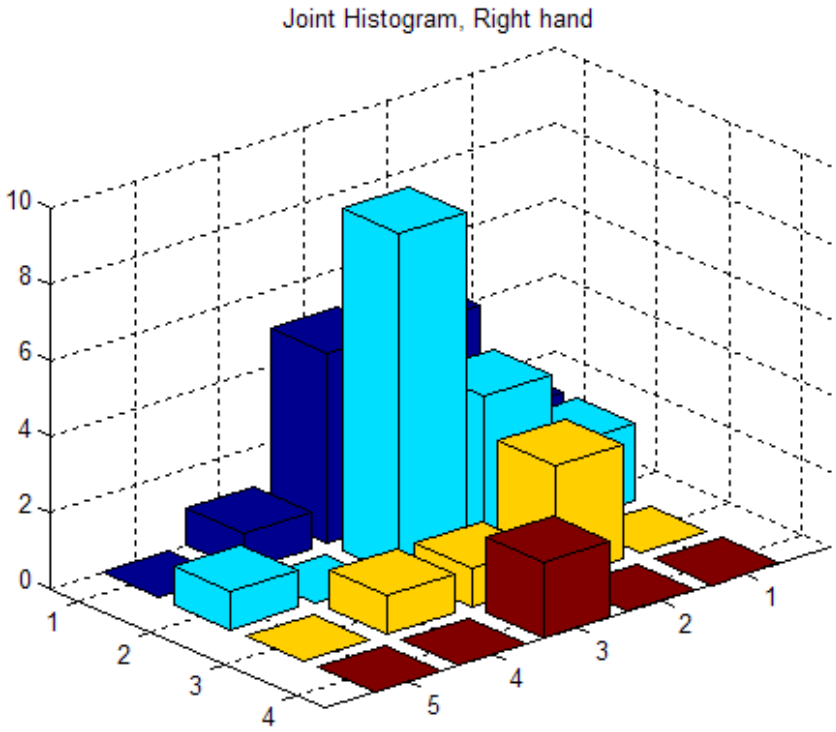

Figure 6.28: Joint histogram for the right hands.

6.3.5.1 Discussion

The results seem better than the histograms obtained considering only the single features, with the information gained through the joint histogram, comments can be drawn.

Adding other elements, obtaining a vector of features, with more than two elements, i.e. branching angles and vessel's length, we could gain a bigger discrimination and better results.

The images analysed are only thirty-six, and the joint histogram cannot be informative with only few images, but the result shown in Figure 6.27 and 6.28 , is better than Figure 6.23, 6.24, 6.25, 6.26.

Robust conclusions cannot be done because the final result is a summary of all the previous steps.

The precision of the binary masks is not enough to perform precise comments; the venous pattern is derived from the application of a vessel tracking algorithm, and first of all, it depends from the original IR images.

These images were not well contrasted, and the size of the database of images can't give us the possibility of draw specific comments.

This is a preliminary initial pilot study, choices have to be done, analysing the initial images and deciding the best way to work firstly with them.

6.4 Pattern Matching

The next step was addressed to the pattern matching techniques, as it is one of the main interest of the group of Professor Black. Looking at the shape of the binary masks, they are all different and the result of the matching could be interesting for any kind of conclusion.

The pattern matching could be done with the application of an optimizer algorithm to find the best set of parameters to match the images, determining relative positions and orientations of the images. In this case two binary masks containing the vessel network are the images to align geometrically, with translations on x and y, rotations and scale operations.

6.4.1 Results of the PSO

Particle Swarm Optimization technique is used to achieve the optimal value of the parameters to match the images of the database, taking one of them as the reference image.
The third binary mask of the database was kept fixed, searching for the best result, changing step by step the specific parameters of the optimizer algorithm.
Examples of the resulting images are shown in Figure 6.29 , and in the Appendix there is the patter matching result done for each image of the dataset.

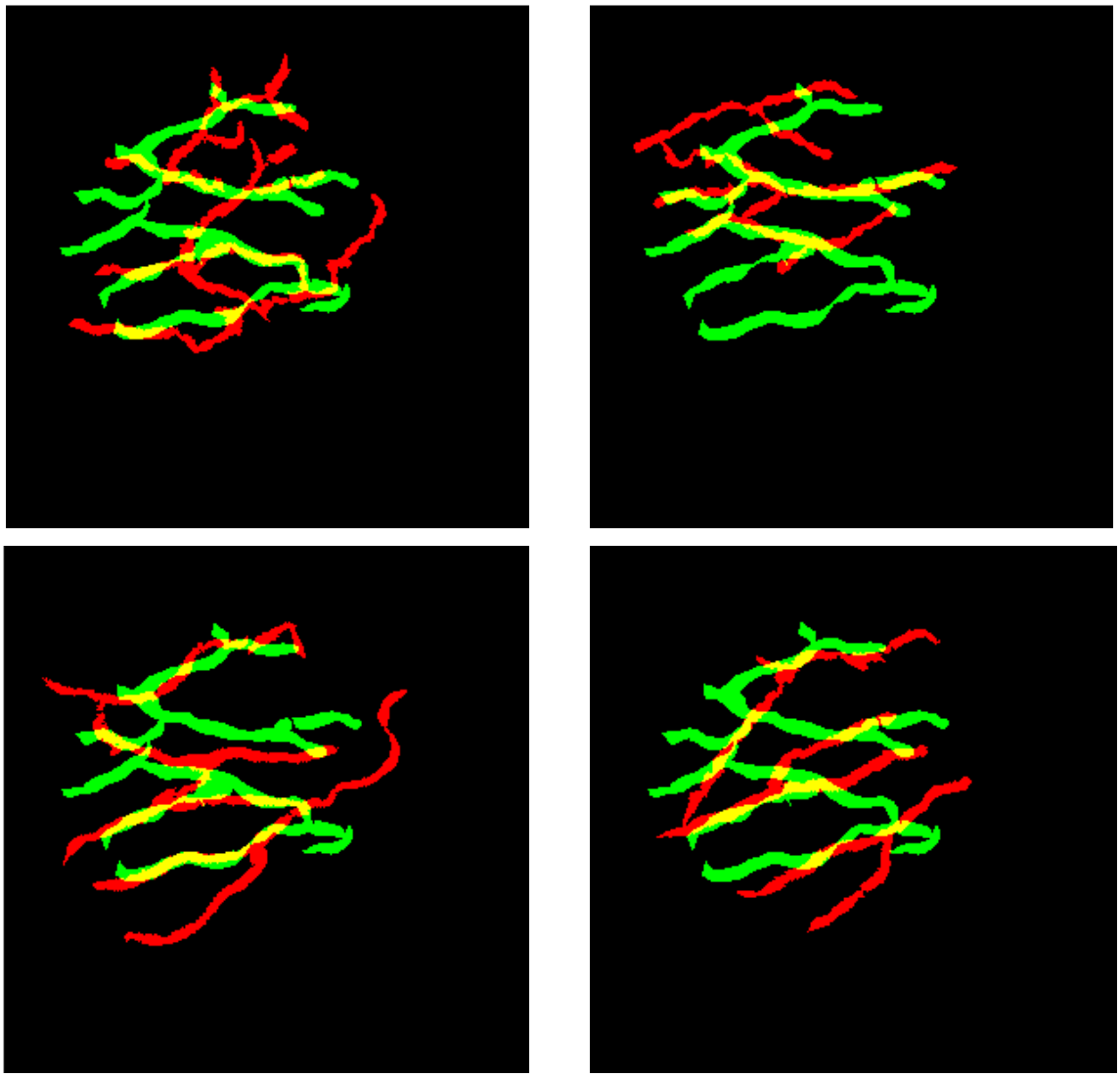

Figure 6.29: Examples of results of the pattern matching with PSO.

The design of the penalty function and the function to modify the sensed image and obtain a possible registered image to compare with the reference one, required a lot of time and experiments.

A lot of parameters are used in the PSO, that aid to obtain the best result.
The parameters, that I am talking about, are the number of particles (possible solutions), depending on the number of the variables to find through the optimizer; the number of iterations, the algorithm requires computational time to solve the problem if the number of iterations is high.

The range of the values of the variables, on which the algorithm has to explore to find a combination of possible solutions, is another parameter to change.
The specific values of the two main equations, basis of PSO, i.e. the acceleration parameters, are changed, depending from the final result. The rapidity of the algorithm to search and explore the range of the possible solutions depends from those values.
The equations are the updating of the velocity and position of the particles at each iteration, looking for the best global and local state at that point.
The inertia weight is another parameter, kept fixed, and developed to better control exploration and exploitation.

The final set of parameter is done by:

$$\theta = \left[-\frac{\pi}{6}, \frac{\pi}{6}\right] \qquad Xtrasl = [-40,\ 40] \qquad Ytasl = [-40, 40] \qquad scale = [0.8, 1.4]$$

The choice of the range for the parameters was the hardest evaluation, done looking at the final match of the two binary masks, seeking for the best alignment and overlap of them.
I tried to compare, first, the same mask with itself, but one geometrically modified, looking for the overlay of the two images.

6.4.2 Discussion

There are not enough information to draw any sort of conclusions on the discriminative power of the features in the venous pattern of the back hand images, observing the pattern matching results.
The matching between the two images is giving us correct results, because it is noticeable an improved match iteration after iteration, and the registered image is overlapping the reference one.
Therefore, the chosen set of parameters and variables of the PSO is suitable.
The reason why I cannot base and obtain conclusions on the uniqueness of the network, is because the binary masks are gained from various steps.
Firstly, it involves the acquisition method and the quality of the IR images that I used as basis to obtain the masks.

Secondly, the way to track the veins is compromised by the quality of the images, e.g. the contrast of the veins from the background.
Other improved algorithm for segmentation could be utilized, and first of all, other algorithm to enhance the images could work better.
A difference selection and acquisition of the IR images could help the actuation of the next steps.
This is a preliminary initial pilot study, so a choice of the functions to apply was required.

The simple acquisition of the single image could be modified, e.g. observing immediately the results and trying to improve the contrast of the images during the session.
In other words, lots of variables play a big role in the final result. The pattern matching as a method to evaluate the eventual uniqueness of the vascular network of the back hand, could be the right way to achieve conclusions, observing the amount of overlap between the two images compared.

Chapter 7

Conclusions

The shape of vascular patterns in the same part of the body is distinct for each person, and it is stable over a long period of time, as a person's pattern of blood vessels is believed to be handwritten into the body at birth, and remains relatively unaffected by ageing, except for predictable growth, as with fingerprints.

In addition, as the blood vessels are hidden underneath the skin and are invisible to the human eye, vein patterns are much harder for intruders to copy as compared to other biometric features.

It is intricate enough to allow sufficient criteria for positively detecting various subjects even identical twins.

However, as the vein pattern formed by superficial blood vessels lies underneath the skin surface, the invisibility of veins to any traditional visual inspection system manages successful image acquisition of vein patterns as technical challenge.

Veins can be identified in the living using near infrared light, whereby reflected or transmitted images of blood vessels can be detected via the reaction between light and the deoxygenated blood in the subcutaneous vessels.

Near-IR rays generated from a bank of light emitting diodes (LEDs) penetrate the region of interest and are absorbed by the deoxygenated haemoglobin. Due to the difference in absorbance between veins and other tissues, the reflected near-IR rays produce an image

in which regions of high absorbency (veins) appear as dark lines in an image captured by a charge-coupled device (CCD).

The image can be processed and manipulated to construct the venous pattern from the captured image and, as future works, subjected to mathematical algorithms and modelling profiles for forensic/biometric identification purposes.
Additional processes and digitalisation of the infrared images are used to extract a venous vascular pattern with the object of identifying and analysing various features, such as vessels branching points and angles, vessel widths, vessel lengths, and converting these into a multidimensional image map.
The analysis of the shape through pattern matching could be a way to obtain other information on the uniqueness of the vessels network.

Algorithm to enhance the veins and divide the background from these dark lines are required.
The contrast has to be improved, to permit the application of algorithm for the detection of the venous pattern.
A combination of two functions, working on the intensities of the infrared image, is applied.
Firstly, a change, based on the histogram of the image, is performed locally through the Contrast Limited Adaptive Histogram Equalization (CLAHE).
Secondly, a function that works checking the value of the intensity of each pixel, is applied, changing the intensity of the pixels, depending if they belong to a vein or to the background.

After these methods, a contrasted image is obtained, ready to be processed, detecting the venous pattern.
A vessel tracking algorithm is applied to draw the vascular network.
The tracking operation starts manually providing an initial point and checking the valley that characterize a vein in general.
The depth of the valley has to be clear enough to be found and detected by the algorithm.
This is the reason because, first of all, the veins have to be well contrasted, and emphasized beside the background.

The algorithm gives back a binary mask of the detected venous pattern.

Morphological operations are applied to improve the aspect of the mask.
After all, other operations, as skeletonization, a thinning morphological operation, are performed with the object of identifying and after analysing various features.

The feature chosen to be analysed and evaluated as distinctive characteristic of the venous pattern, are the branching angles and the vessels length.
They are studied separately, without important and interesting results.
Another statistical approach is applied considering the two features together, as a couple of values, one is the average of angles and one is the average of the lengths of the vessels, for each image, to see if the result is informative.

In conclusion the main points achieved by this preliminary initial pilot study are the enhancement of infrared images in the spatial domain, the vein pattern segmentation, the vessel tracking, skeletonization, pattern matching, PSO and feature detection.

7.1 Analysis of the Limits

Infrared images are not enough precise, as consequence, from all the successive steps, could arise different artifacts, that influenced the final result.
A bigger number of images in the database is required for a better vision of the results.
Errors in the detection of the venous pattern could appear, such as false vessels, tendons detected as vessels, false or missed junction points.
The vessel tracker could be improved, because a lot of starting points are use-provided, and sometimes the tracker is not able to detect the vein, and it stops immediately after the seed point.
The last observation derives from the contrast of the infrared images.
A vessel tracking algorithm that requires only one starting point, finding automatically all the vessels network, could be better.
Talking about the feature detection, a vector of two elements, branching angles and vessels length, is not enough for statistical purposes.

This is a preliminary initial pilot study, that wants only to address the next studies and give suggestions to achieve the objective of the project.

7.2 Possible Improvements and Future Works

The acquisition of the infrared images needs improvements, because it is the starting point of the pattern recognition process. From the quality of the IR images depends all the successive steps.
Vein pattern is better defined when the hand is closed in a fist and the skin on the back of the hand is taut.
Another improvement could be the way to enhance the network of the veins, but if the image is well contrasted, a significant enhancement is not required.
The vessel tracking algorithm could be improved, seeking for a fully automatic method to track the venous pattern, with only one seed point, user-provided [36].

Important aspects to better design the tracking algorithm need to be explored, such as the tolerance to the broken edges and still keep tracking a vessel, to the noise, as artifacts of the image.
It should not be stopped by bifurcations, keep tracking along the branches and extract most of the vascular network, while minimizing user intervention.

Future works could be design the basis of feature and model prediction data contained within the superficial venous pattern of the limbs and whether the image information has a viable forensic application with regards to stability of the data.
The application to other parts of the human body, as upper and lower limbs, is one of the main point to achieve for forensic/biometric purposes.

Appendix

Histograms of the Branching Angles for the Left Hands

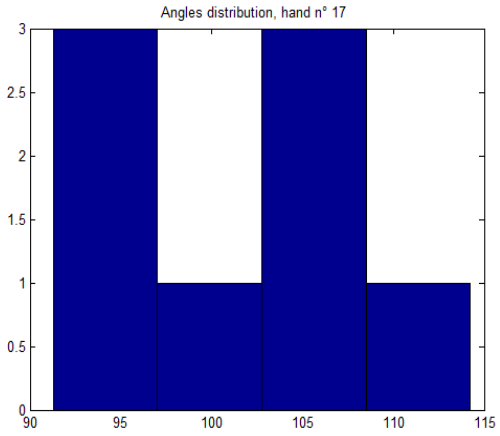

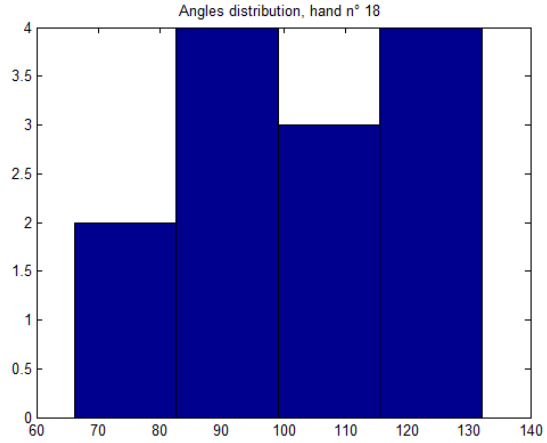

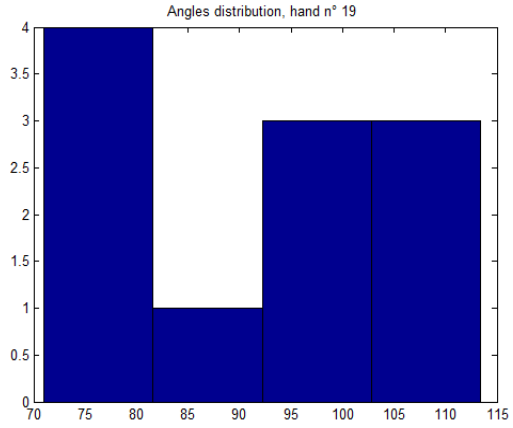

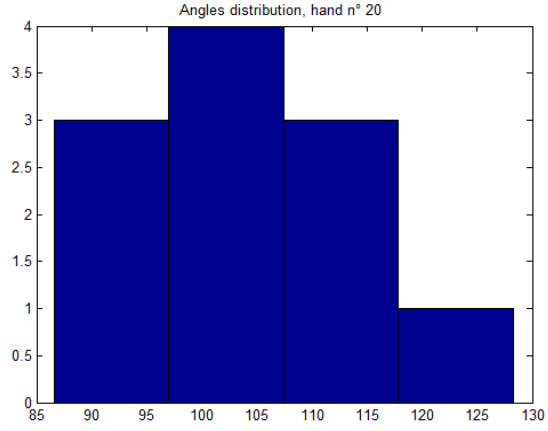

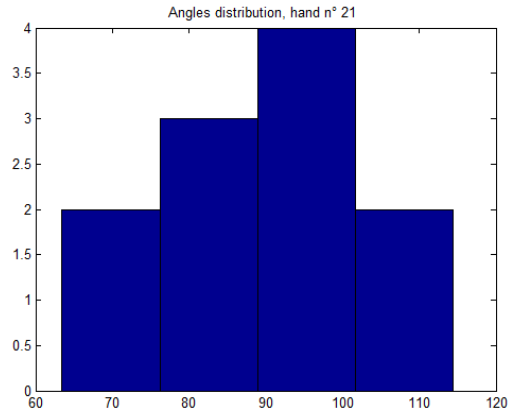

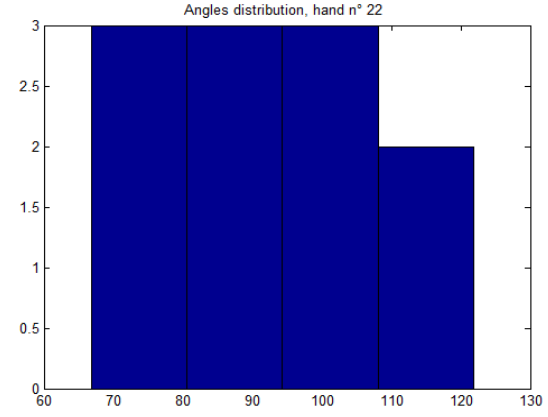

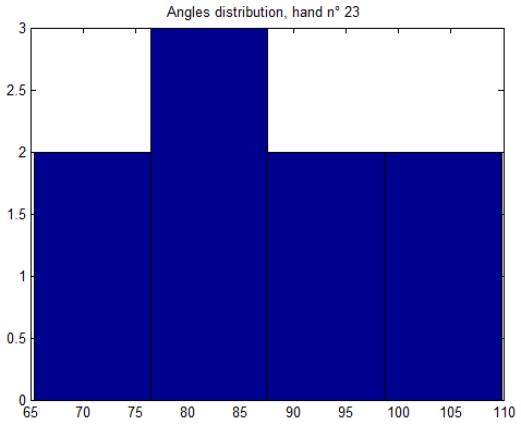
Angles distribution, hand n° 23

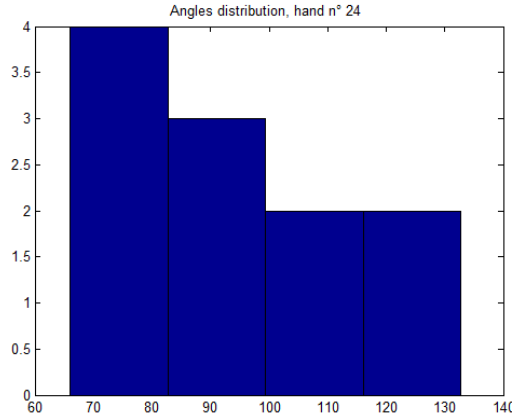
Angles distribution, hand n° 24

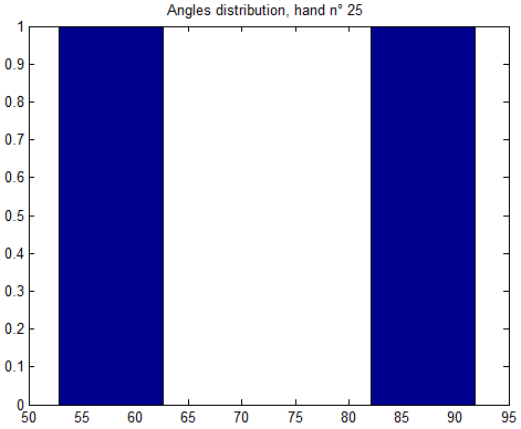
Angles distribution, hand n° 25

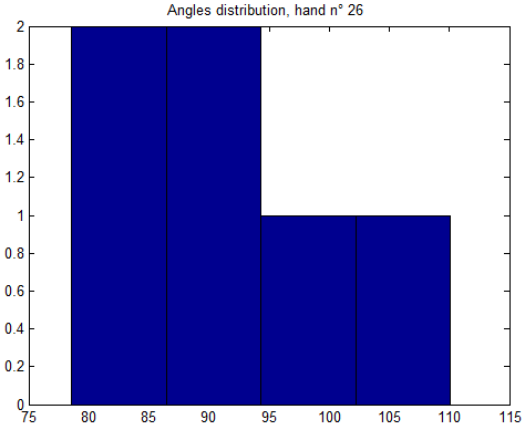
Angles distribution, hand n° 26

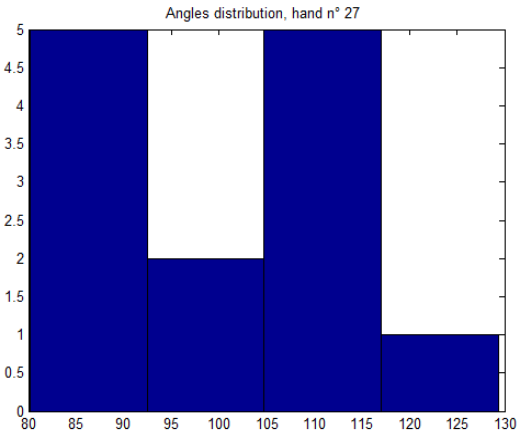
Angles distribution, hand n° 27

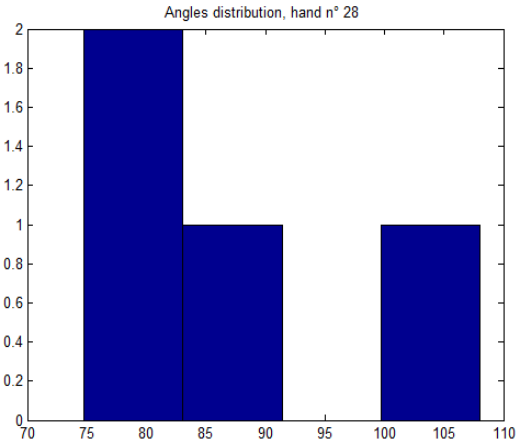
Angles distribution, hand n° 28

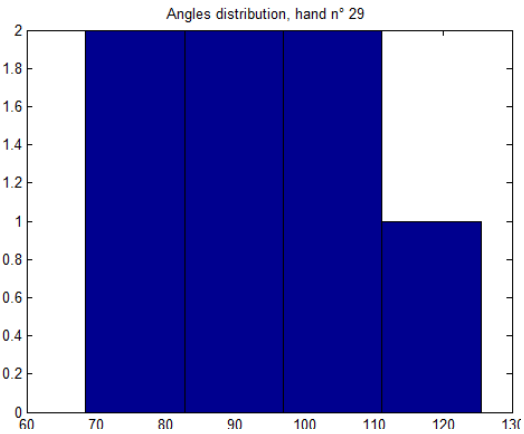
Angles distribution, hand n° 29

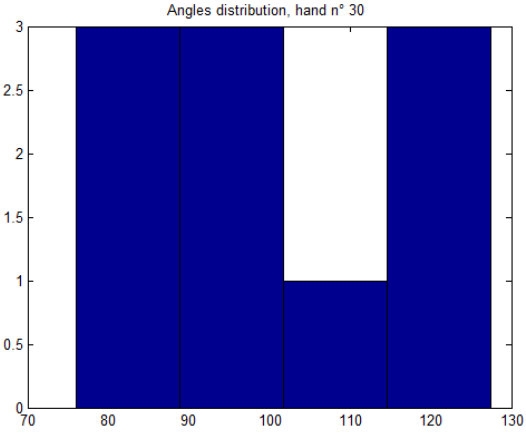
Angles distribution, hand n° 30

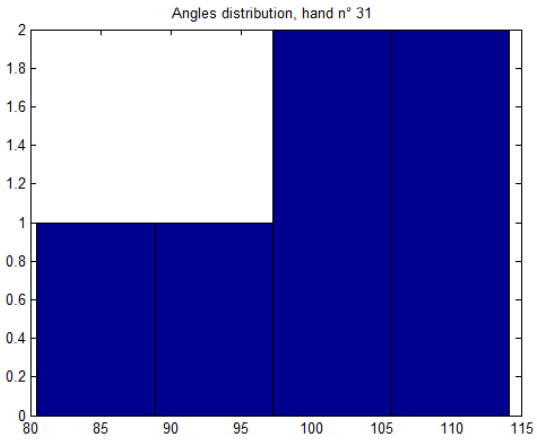
Angles distribution, hand n° 31
2
1.8
1.6
1.4
1.2
1
0.8
0.6
0.4
0.2
0
80
85
90
95
100
105
110
115

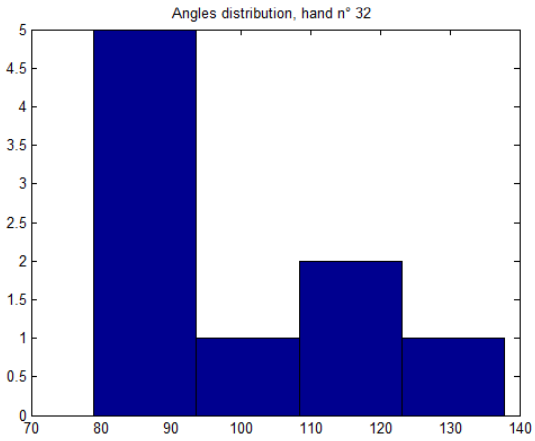
Angles distribution, hand n° 32
5
4.5
4
3.5
3
2.5
2
1.5
1
0.5
0
70
80
90
100
110
120
130
140

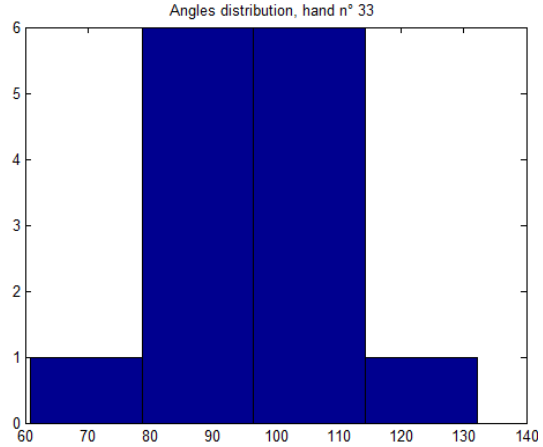
Angles distribution, hand n° 33
6
5
4
3
2
1
0
60
70
80
90
100
110
120
130
140

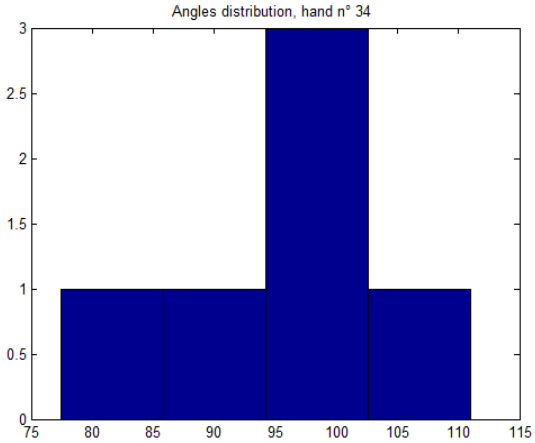
Angles distribution, hand n° 34
3
2.5
2
1.5
1
0.5
0
75
80
85
90
95
100
105
110
115

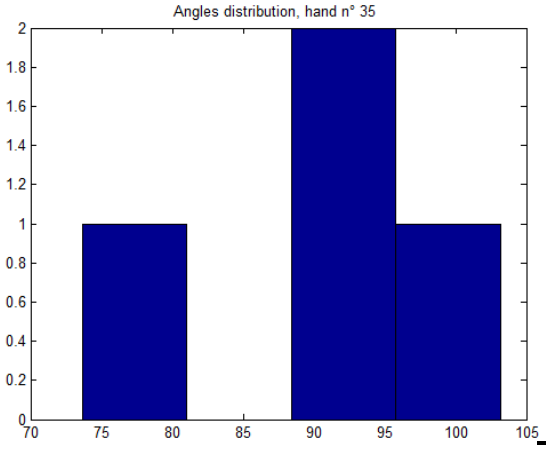
Angles distribution, hand n° 35
2
1.8
1.6
1.4
1.2
1
0.8
0.6
0.4
0.2
0
70
75
80
85
90
95
100
105

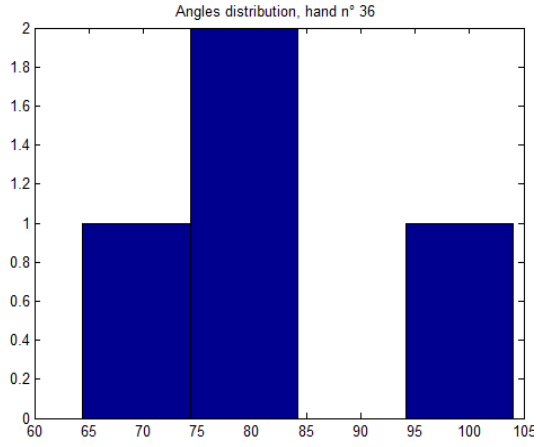
Angles distribution, hand n° 36
2
1.8
1.6
1.4
1.2
1
0.8
0.6
0.4
0.2
0
60
65
70
75
80
85
90
95
100
105

Histograms of the Branching Angles for the Right Hands

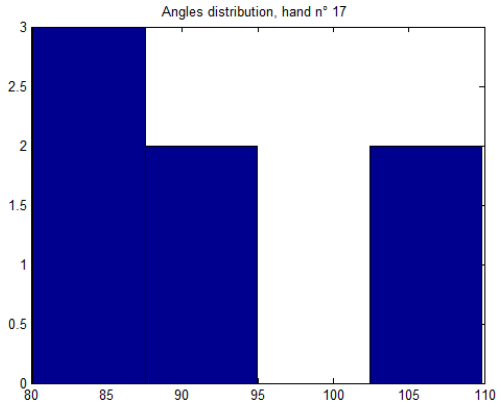

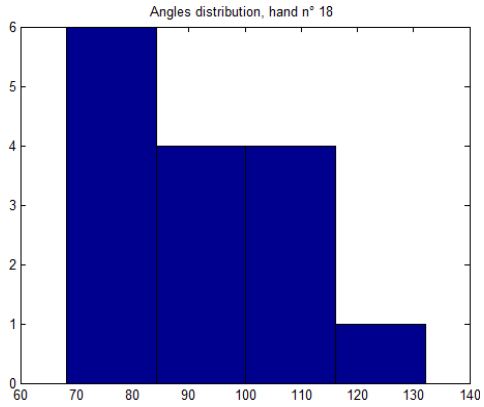

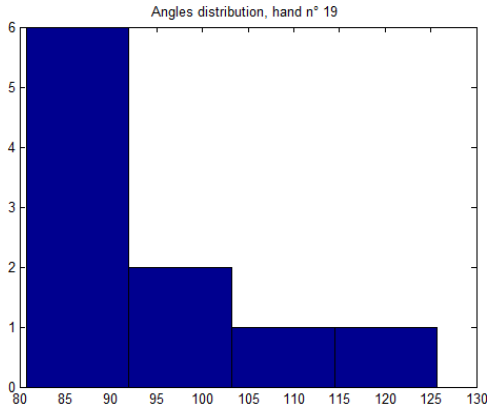

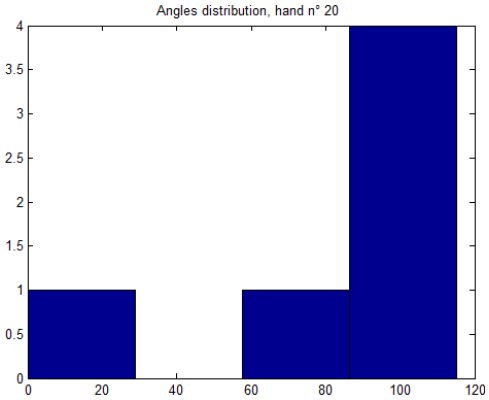

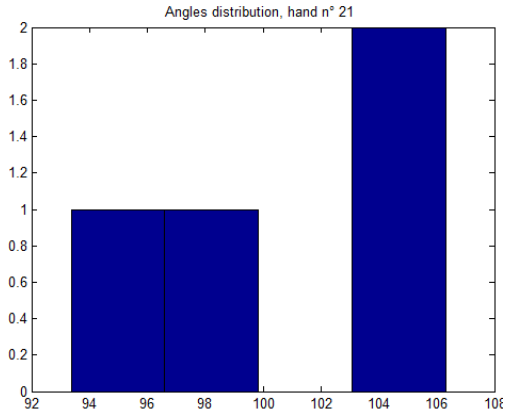

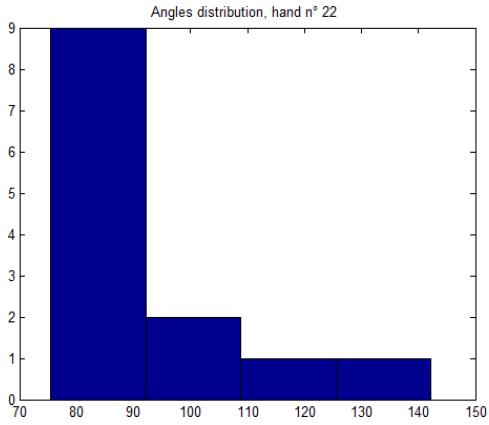

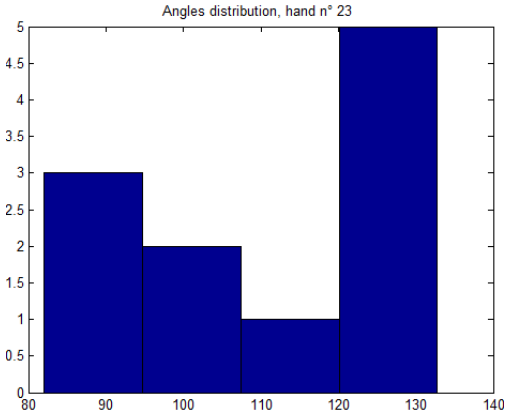
Angles distribution, hand n° 23

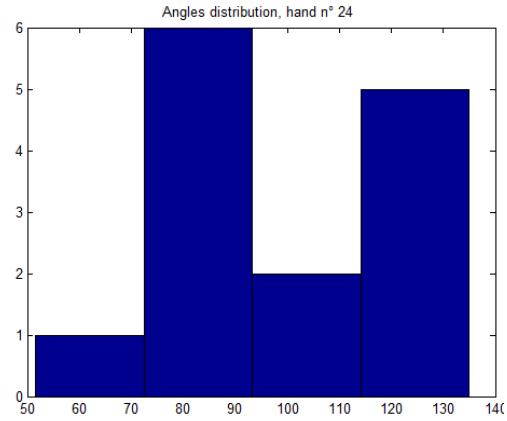
Angles distribution, hand n° 24

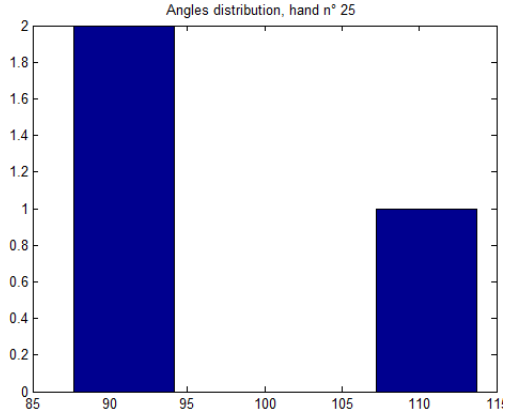
Angles distribution, hand n° 25

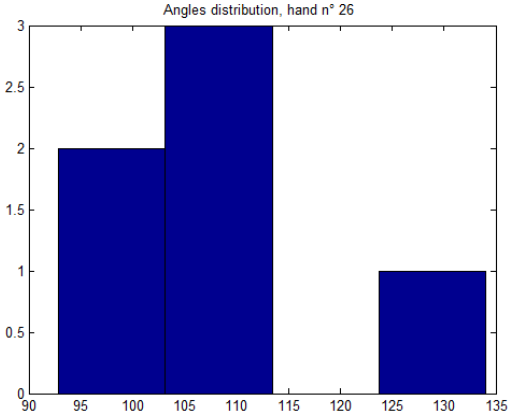
Angles distribution, hand n° 26

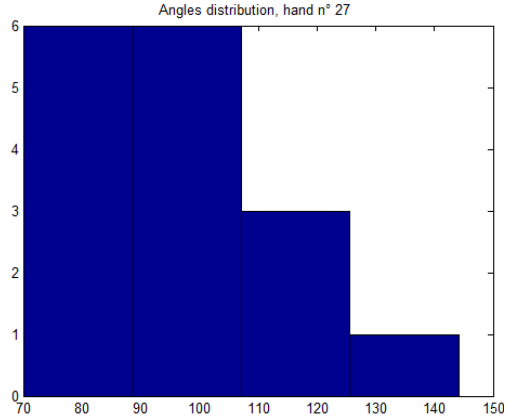
Angles distribution, hand n° 27

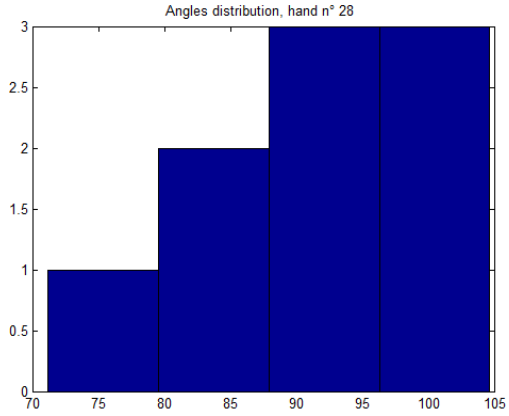
Angles distribution, hand n° 28

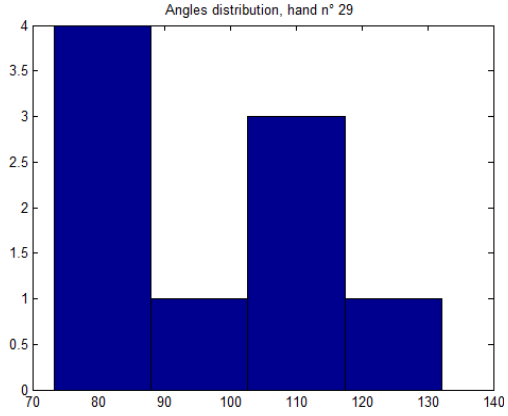
Angles distribution, hand n° 29

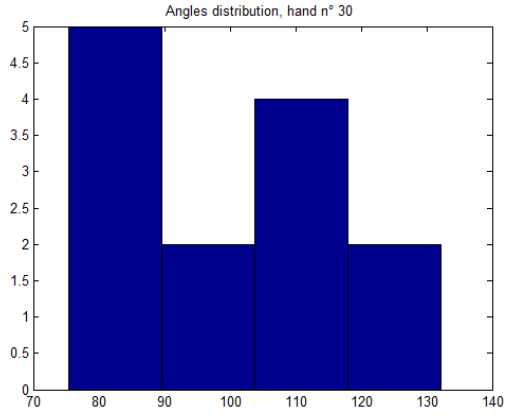
Angles distribution, hand n° 30

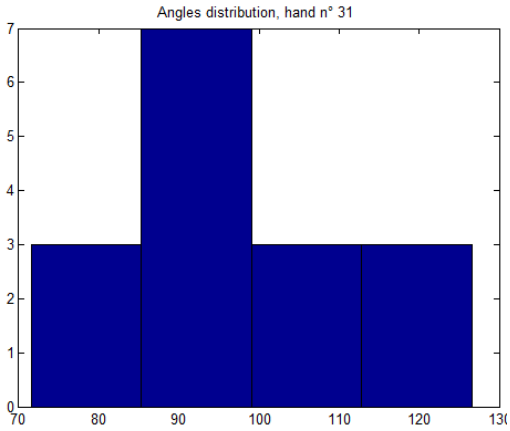
Angles distribution, hand n° 31
0 1 2 3 4 5 6 7
70 80 90 100 110 120 130

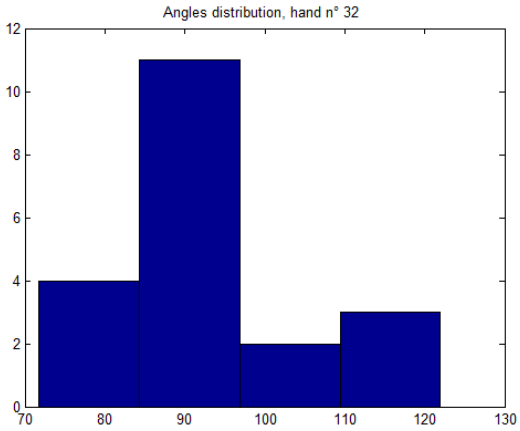
Angles distribution, hand n° 32
0 2 4 6 8 10 12
70 80 90 100 110 120 130

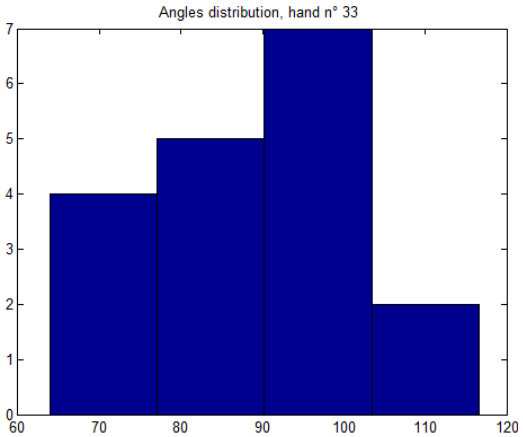
Angles distribution, hand n° 33
0 1 2 3 4 5 6 7
60 70 80 90 100 110 120

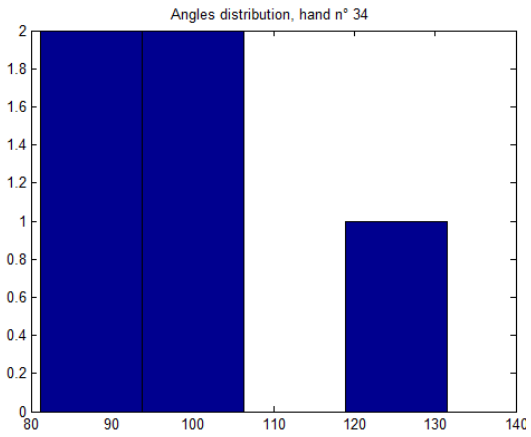
Angles distribution, hand n° 34
0 0.2 0.4 0.6 0.8 1 1.2 1.4 1.6 1.8 2
80 90 100 110 120 130 140

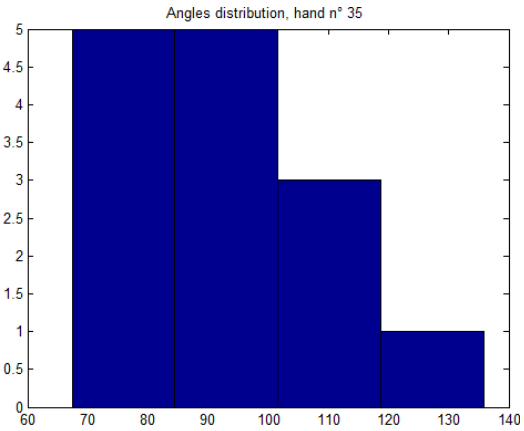
Angles distribution, hand n° 35
0 0.5 1 1.5 2 2.5 3 3.5 4 4.5 5
60 70 80 90 100 110 120 130 140

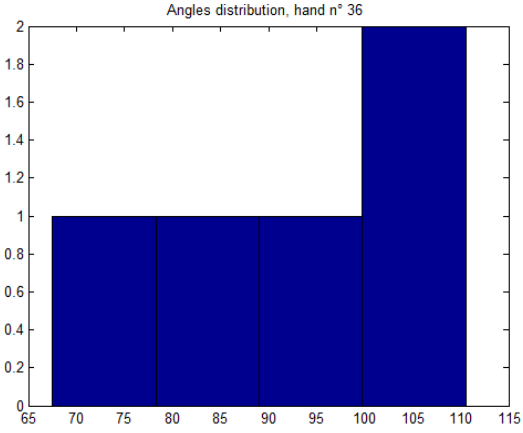
Angles distribution, hand n° 36
0 0.2 0.4 0.6 0.8 1 1.2 1.4 1.6 1.8 2
65 70 75 80 85 90 95 100 105 110 115

Histograms of the Vessels Length for the Left Hands

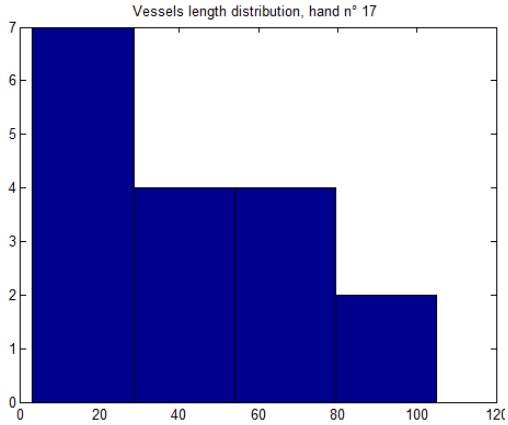

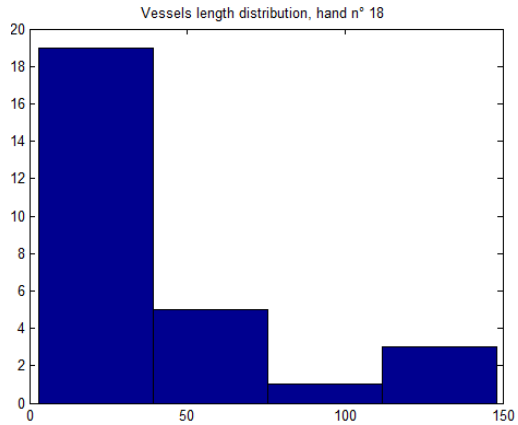

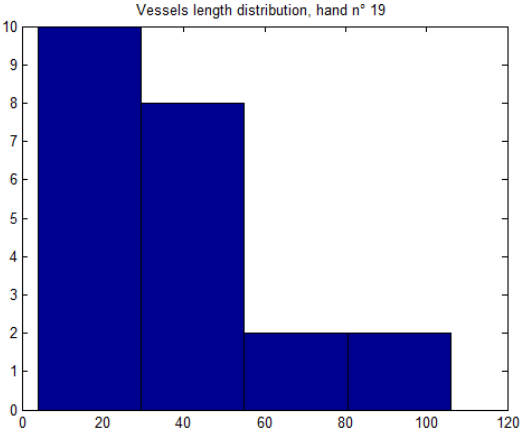

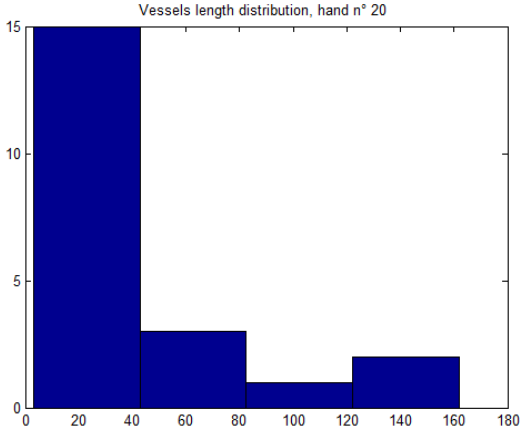

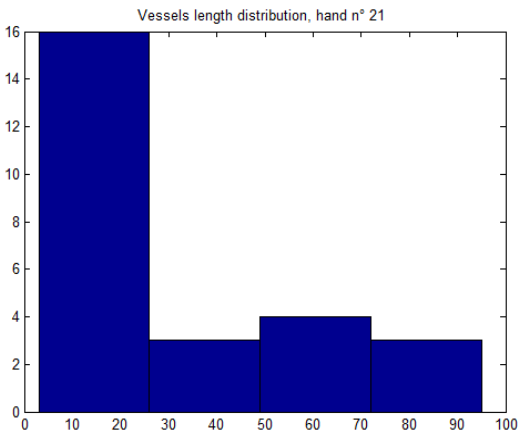

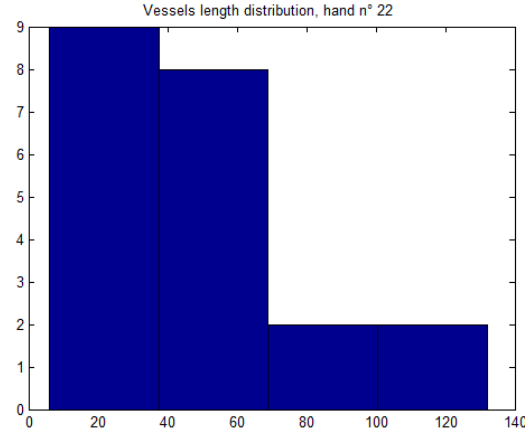

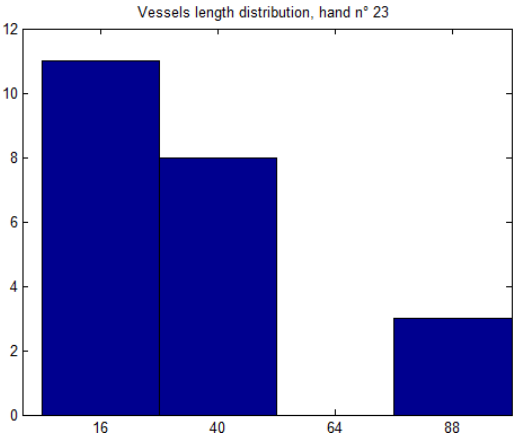

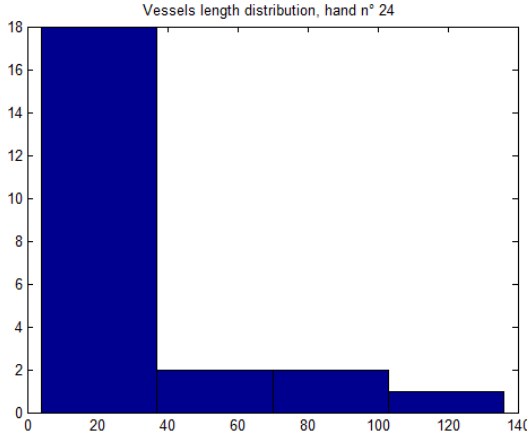

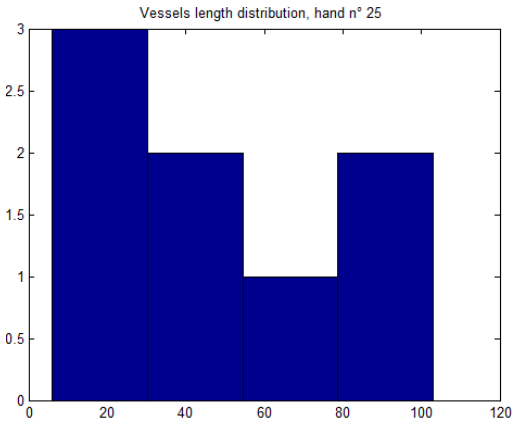
Vessels length distribution, hand n° 25
0 0.5 1 1.5 2 2.5 3
0 20 40 60 80 100 120

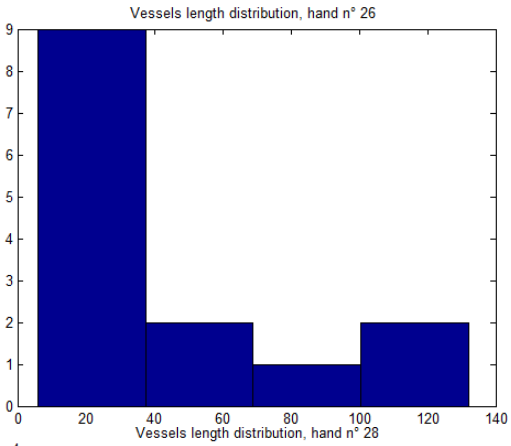
Vessels length distribution, hand n° 26
0 1 2 3 4 5 6 7 8 9
0 20 40 60 80 100 120 140

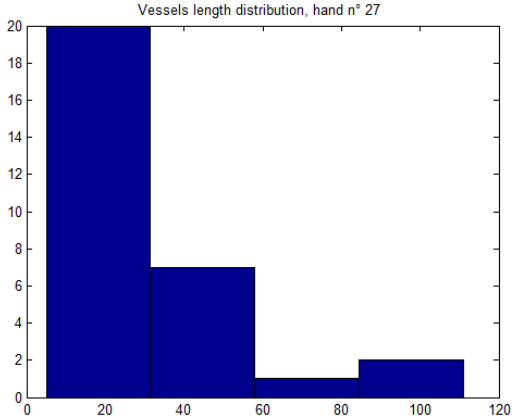
Vessels length distribution, hand n° 27
0 2 4 6 8 10 12 14 16 18 20
0 20 40 60 80 100 120

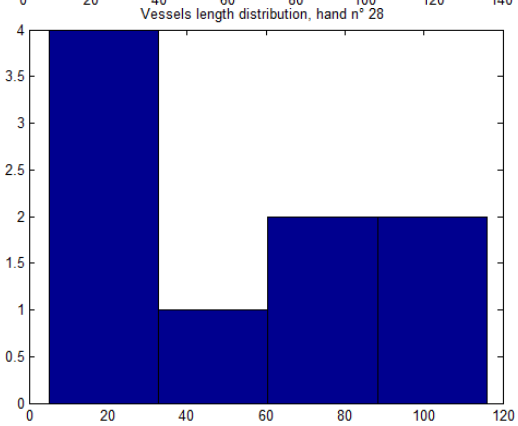
Vessels length distribution, hand n° 28
0 0.5 1 1.5 2 2.5 3 3.5 4
0 20 40 60 80 100 120

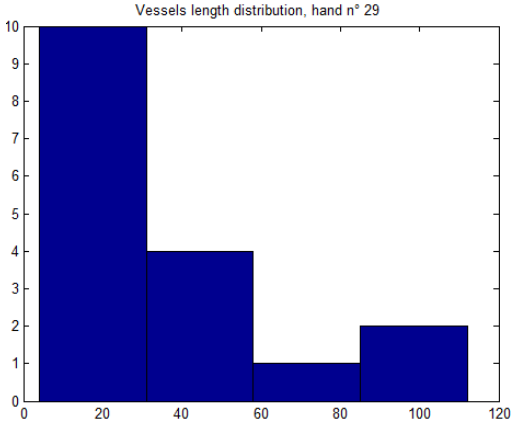
Vessels length distribution, hand n° 29
0 1 2 3 4 5 6 7 8 9 10
0 20 40 60 80 100 120

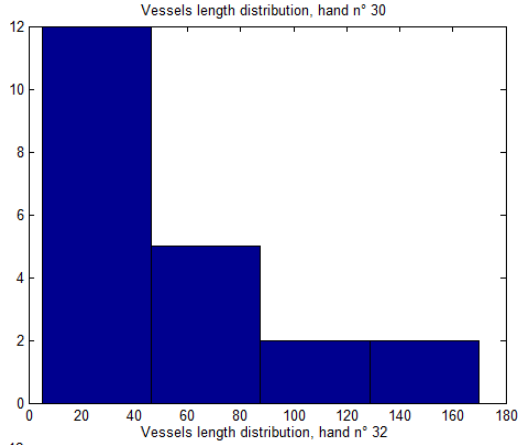
Vessels length distribution, hand n° 30
0 2 4 6 8 10 12
0 20 40 60 80 100 120 140 160 180

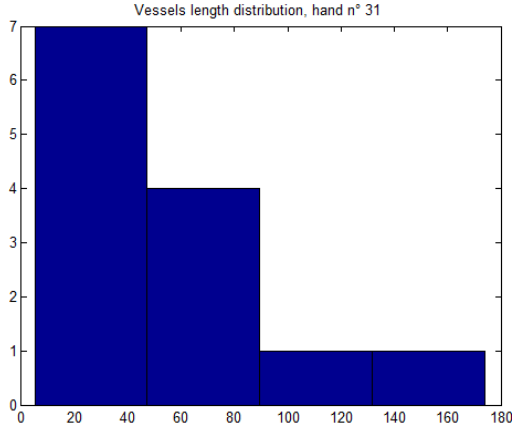
Vessels length distribution, hand n° 31
0 1 2 3 4 5 6 7
0 20 40 60 80 100 120 140 160 180

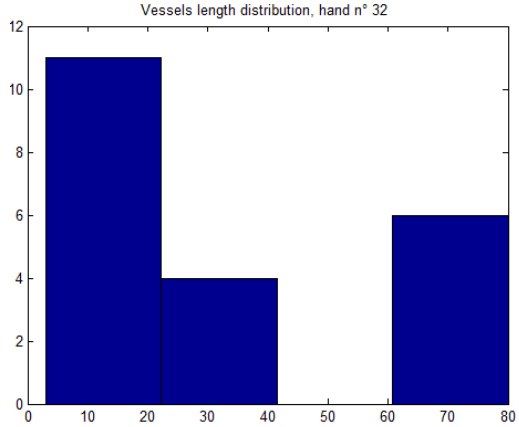
Vessels length distribution, hand n° 32
0 2 4 6 8 10 12
0 10 20 30 40 50 60 70 80

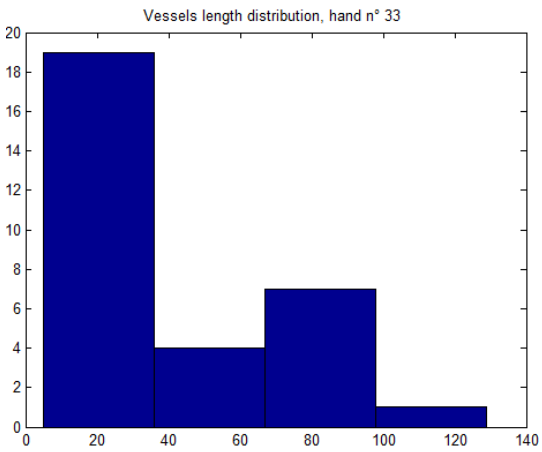

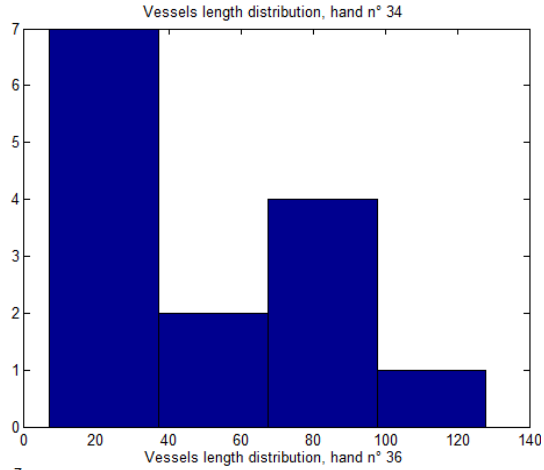

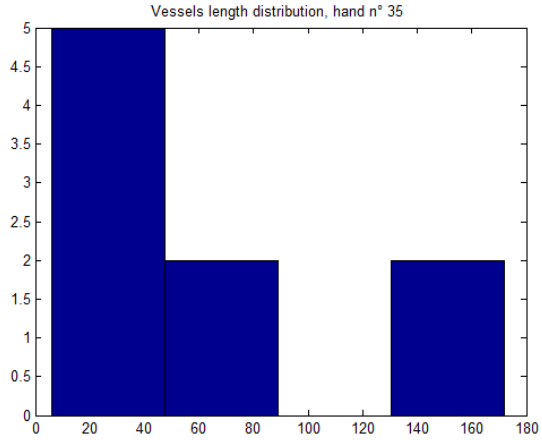

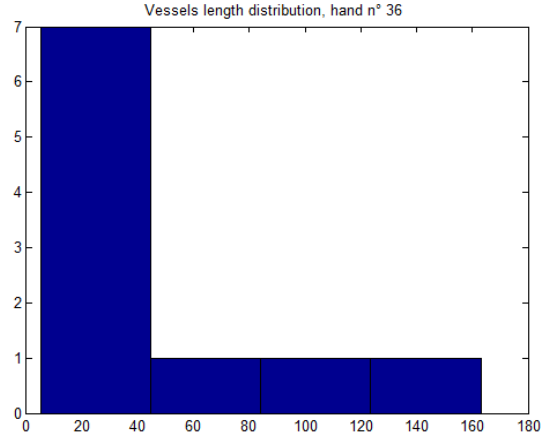

Histograms of the Vessels Length for the Right Hands

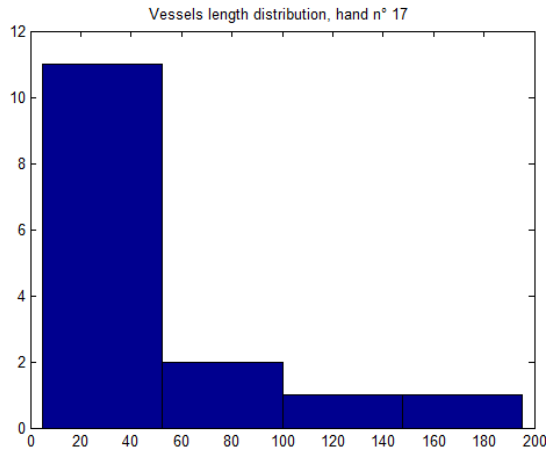

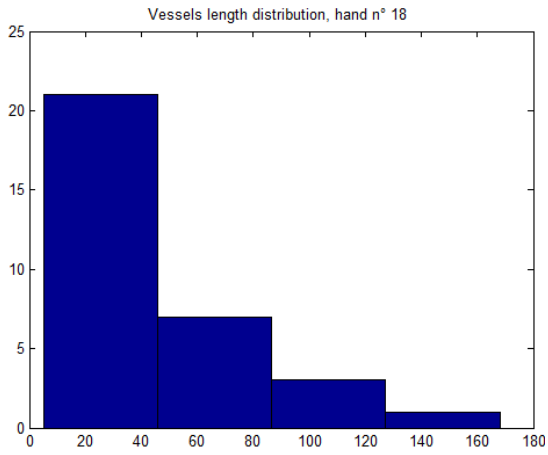

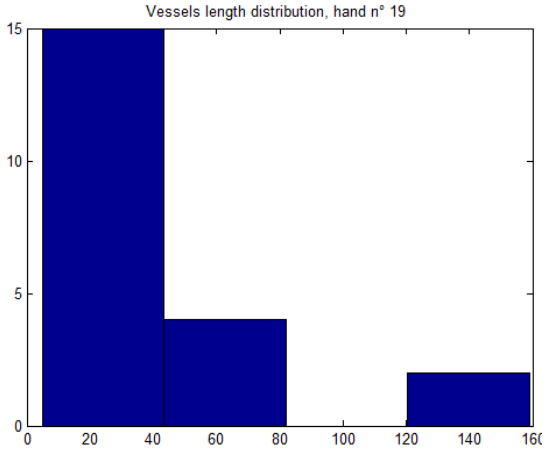
Vessels length distribution, hand n° 19
0 5 10 15
0 20 40 60 80 100 120 140 160

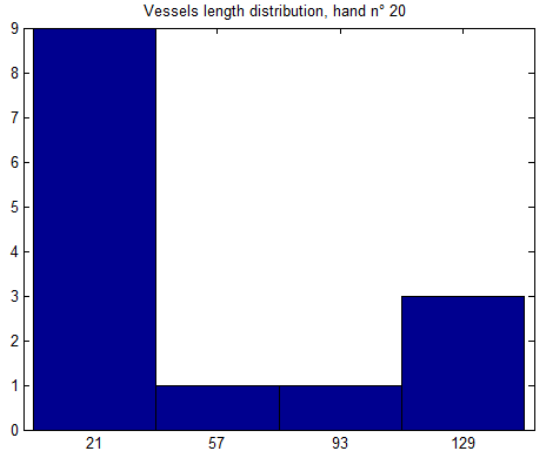
Vessels length distribution, hand n° 20
0 1 2 3 4 5 6 7 8 9
21 57 93 129

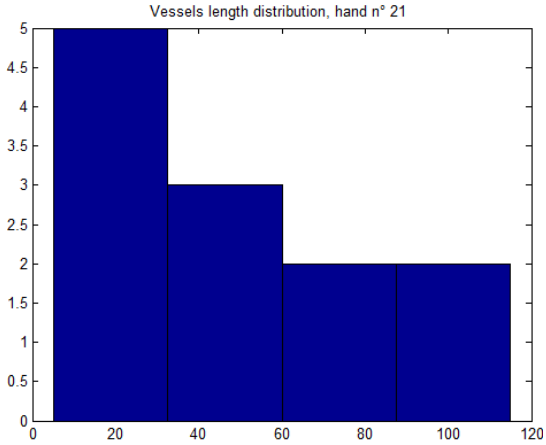
Vessels length distribution, hand n° 21
0 0.5 1 1.5 2 2.5 3 3.5 4 4.5 5
0 20 40 60 80 100 120

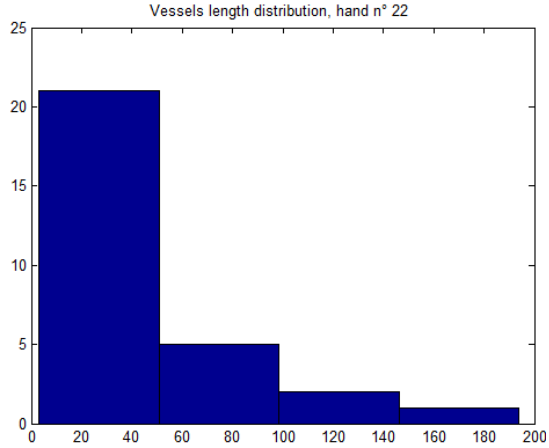
Vessels length distribution, hand n° 22
0 5 10 15 20 25
0 20 40 60 80 100 120 140 160 180 200

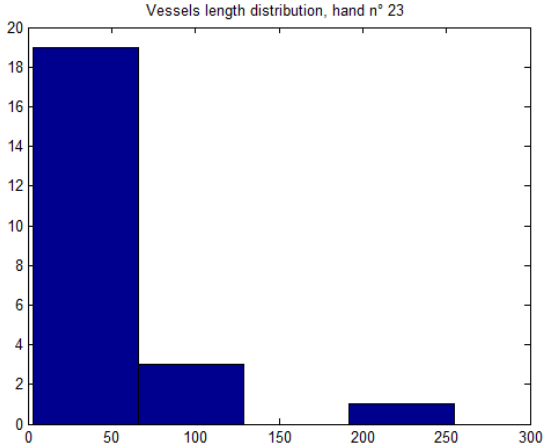
Vessels length distribution, hand n° 23
0 2 4 6 8 10 12 14 16 18 20
0 50 100 150 200 250 300

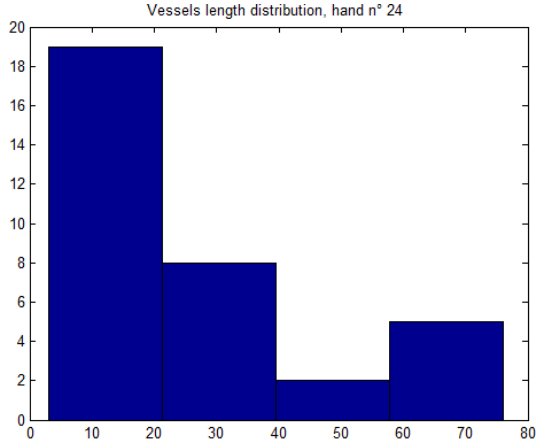
Vessels length distribution, hand n° 24
0 2 4 6 8 10 12 14 16 18 20
0 10 20 30 40 50 60 70 80

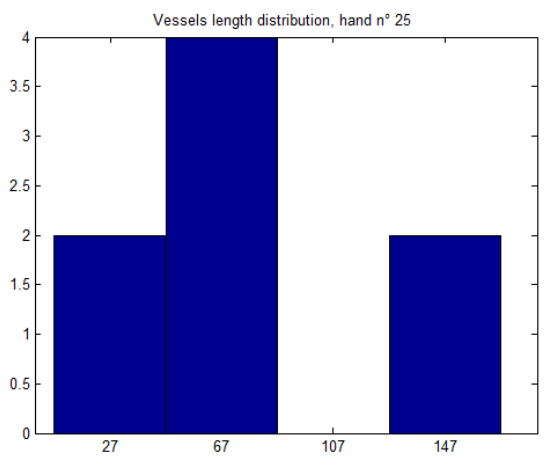
Vessels length distribution, hand n° 25
0 0.5 1 1.5 2 2.5 3 3.5 4
27 67 107 147

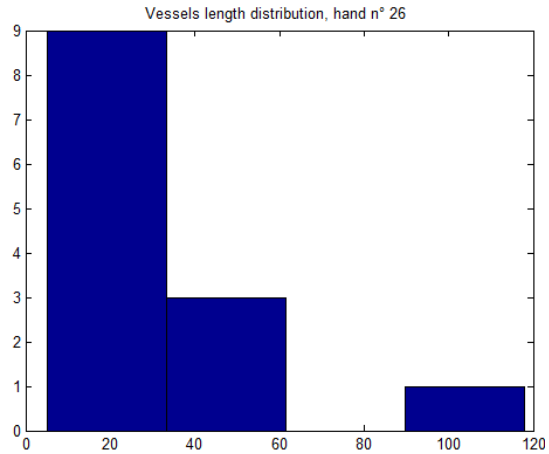
Vessels length distribution, hand n° 26
0 1 2 3 4 5 6 7 8 9
0 20 40 60 80 100 120

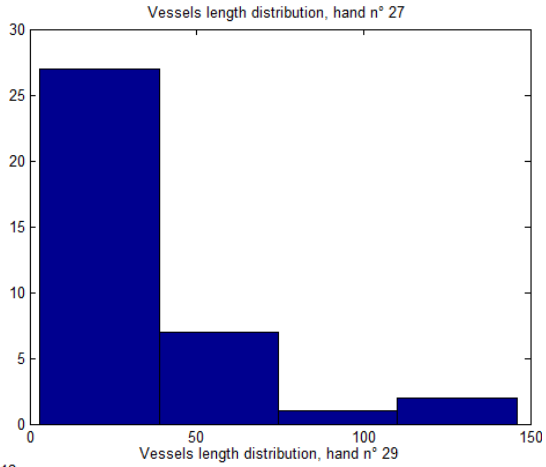
Vessels length distribution, hand n° 27
30
25
20
15
10
5
0
0
50
100
150

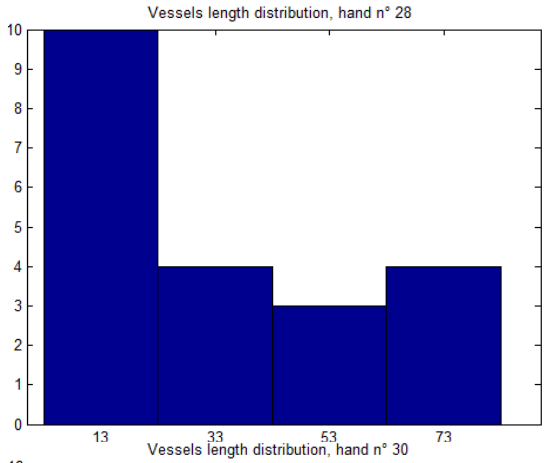
Vessels length distribution, hand n° 28
10
9
8
7
6
5
4
3
2
1
0
13
33
53
73

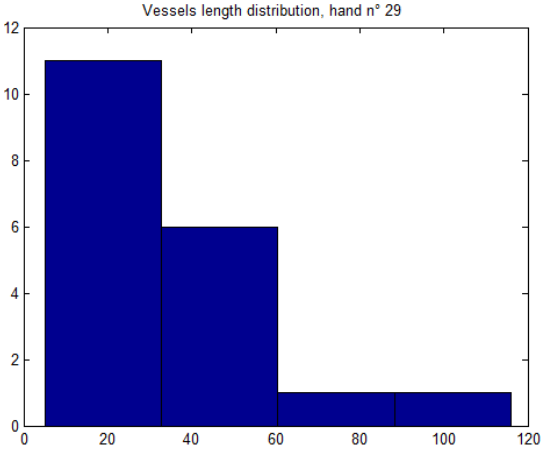
Vessels length distribution, hand n° 29
12
10
8
6
4
2
0
0
20
40
60
80
100
120

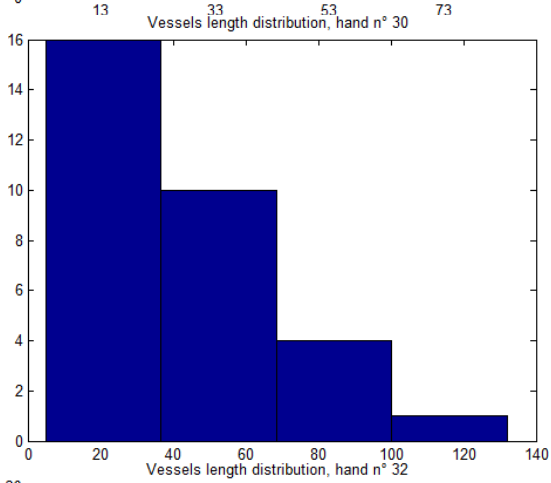
Vessels length distribution, hand n° 30
16
14
12
10
8
6
4
2
0
0
20
40
60
80
100
120
140

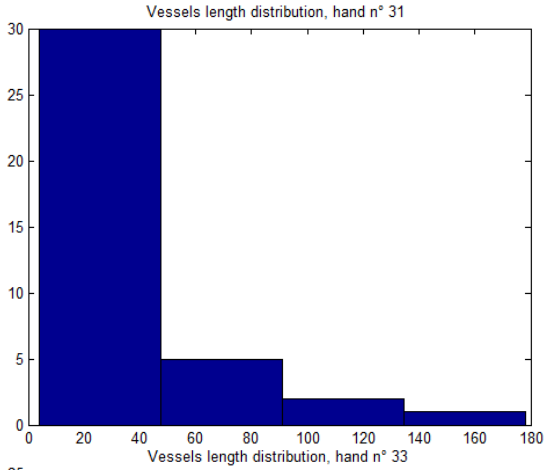
Vessels length distribution, hand n° 31
30
25
20
15
10
5
0
0
20
40
60
80
100
120
140
160
180

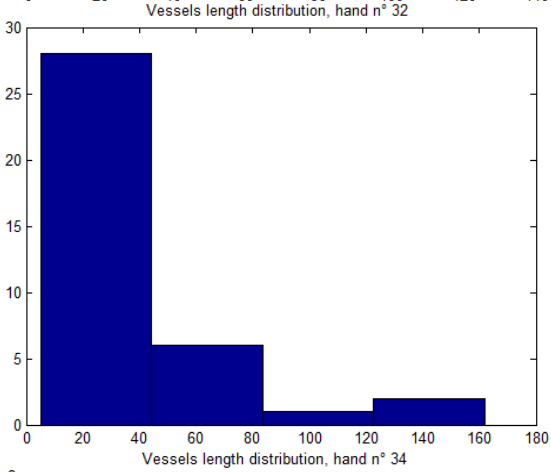
Vessels length distribution, hand n° 32
30
25
20
15
10
5
0
0
20
40
60
80
100
120
140
160
180

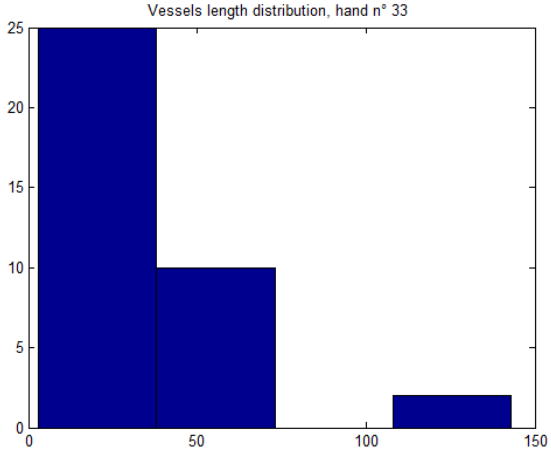
Vessels length distribution, hand n° 33
25
20
15
10
5
0
0
50
100
150

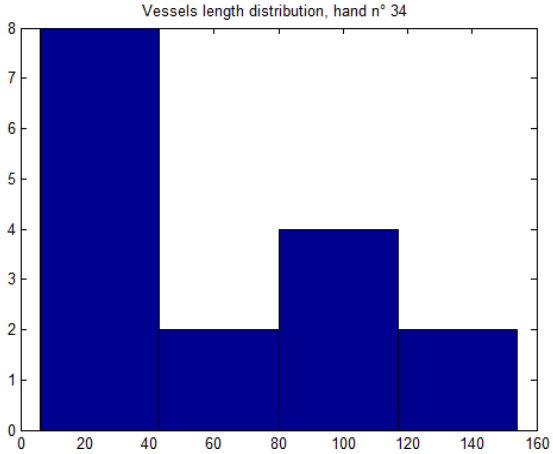
Vessels length distribution, hand n° 34
8
7
6
5
4
3
2
1
0
0
20
40
60
80
100
120
140
160

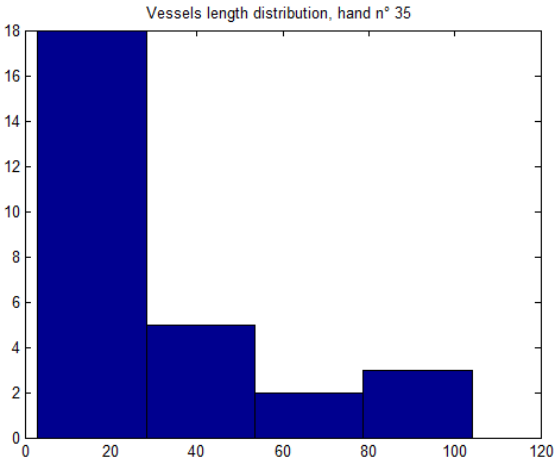

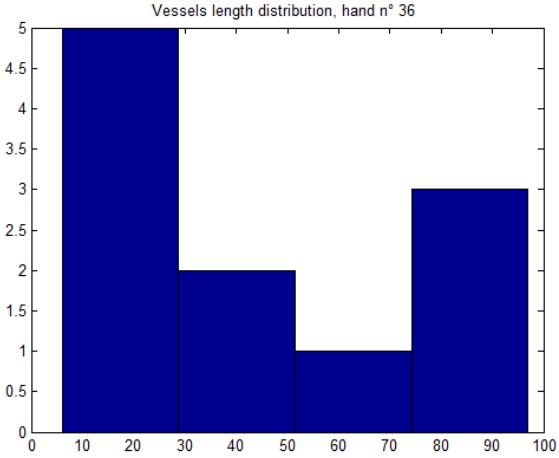

Results of the Pattern Matching with PSO

Left Hand

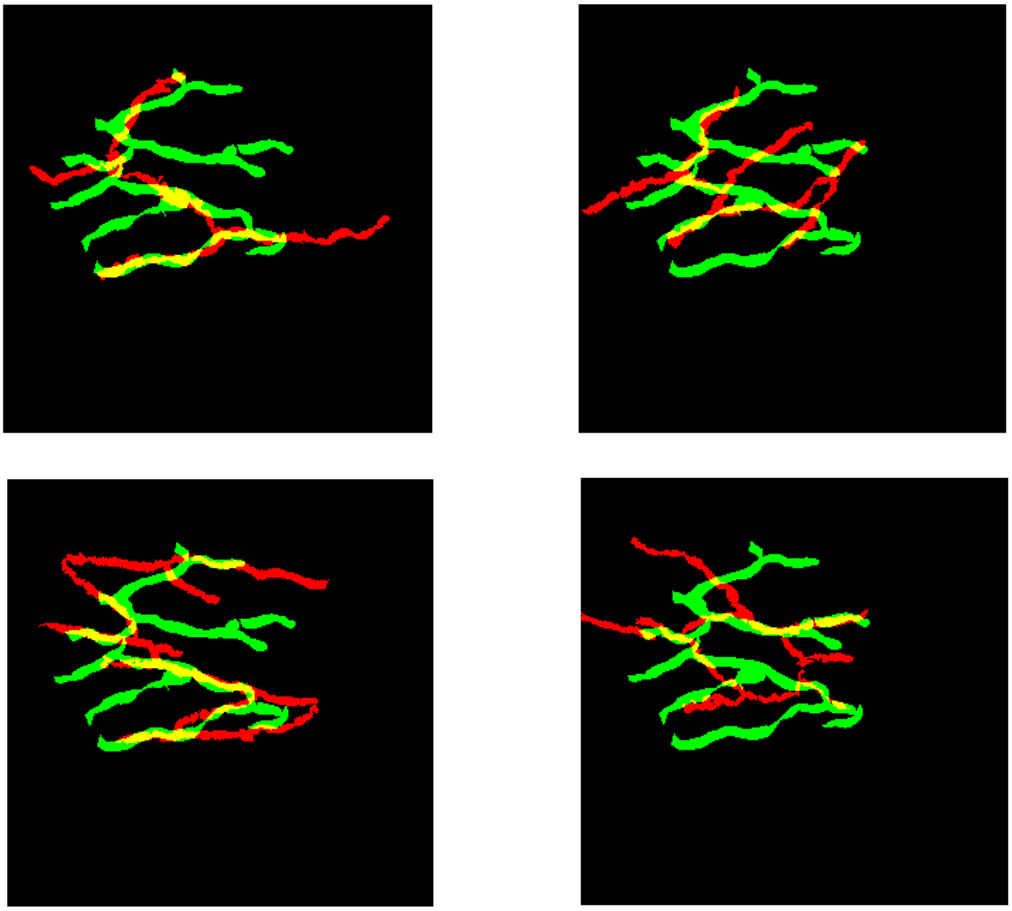

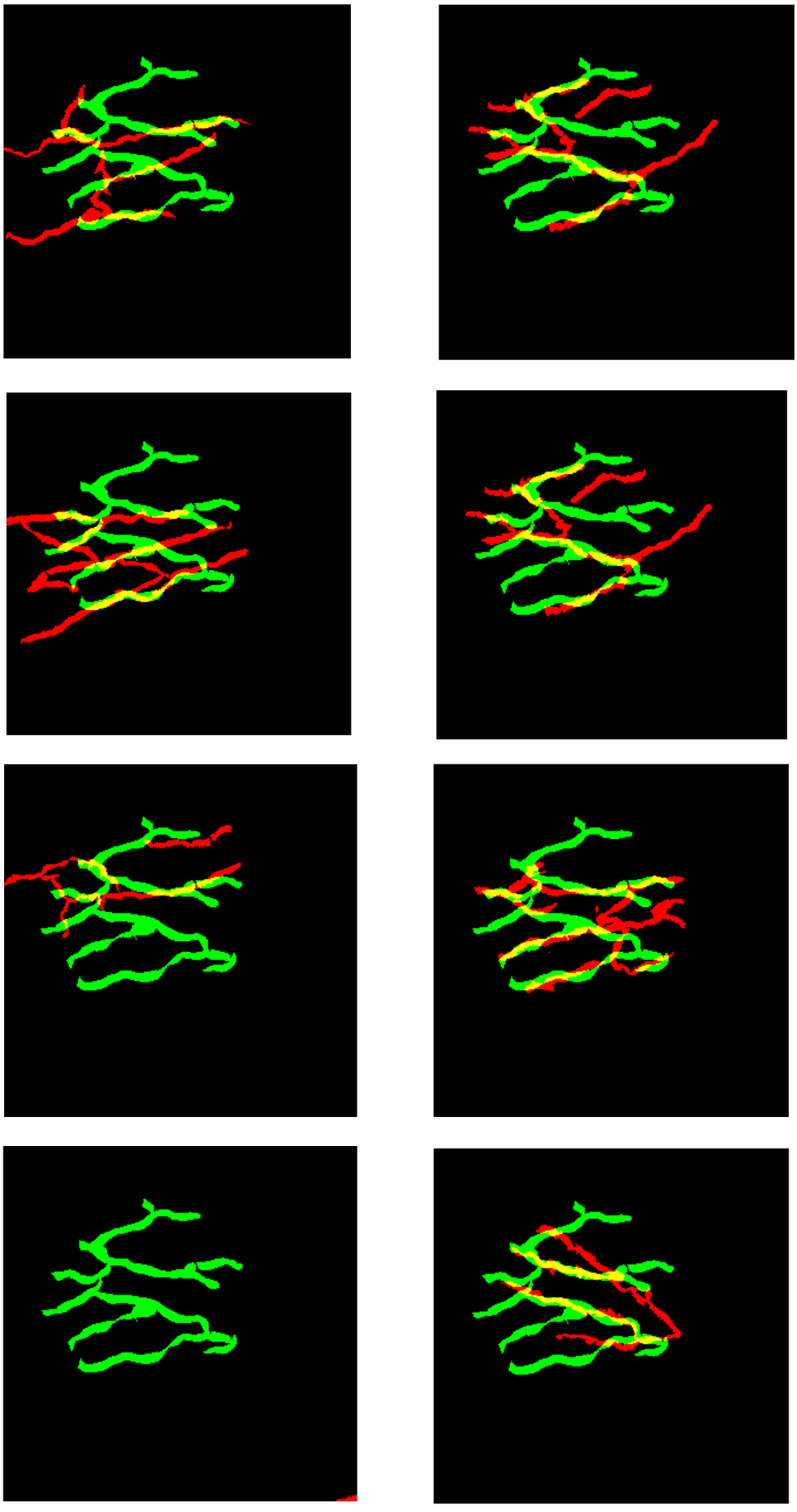

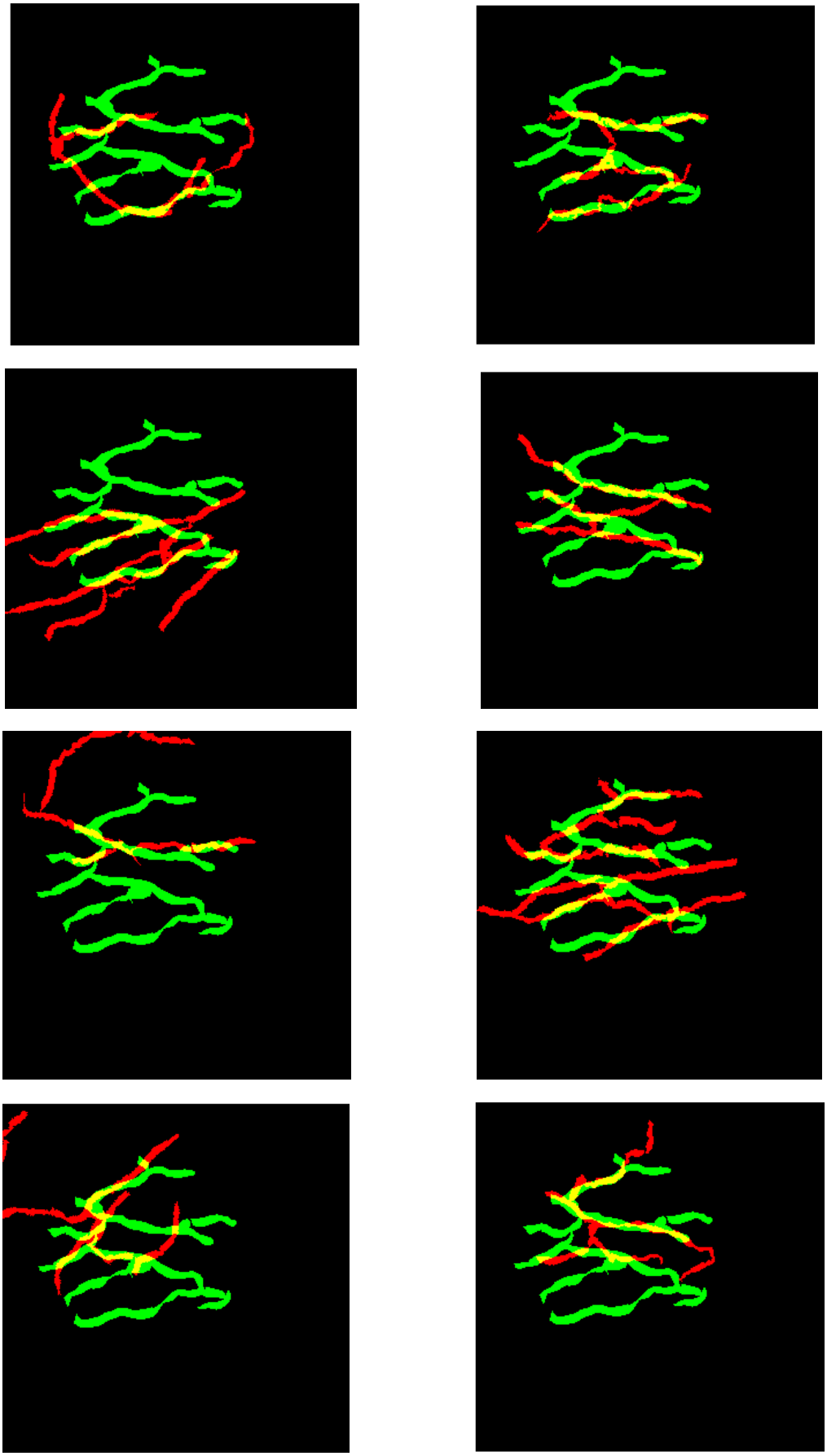

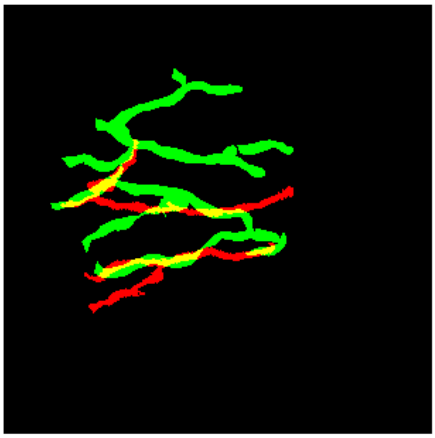

Right Hand

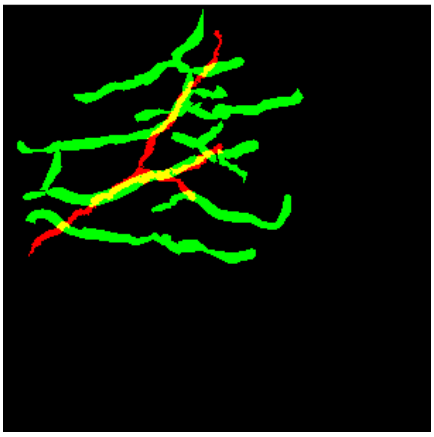

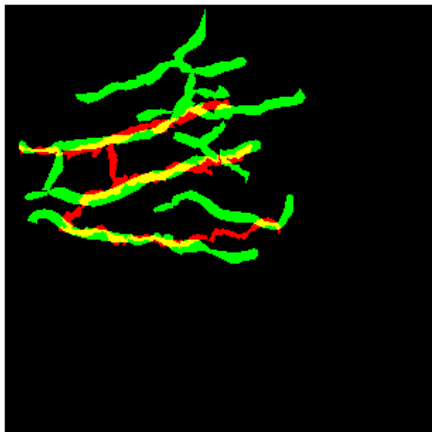

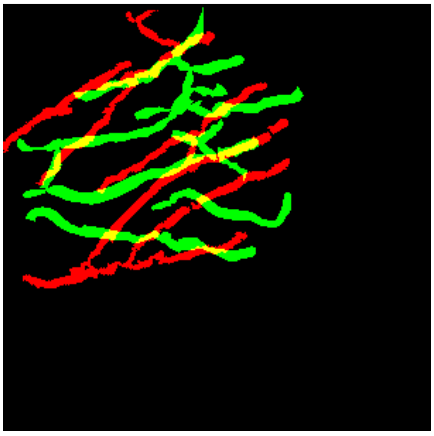

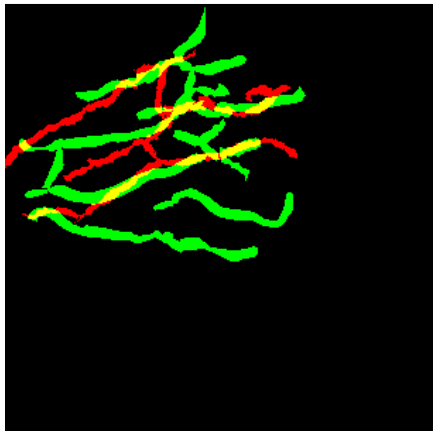

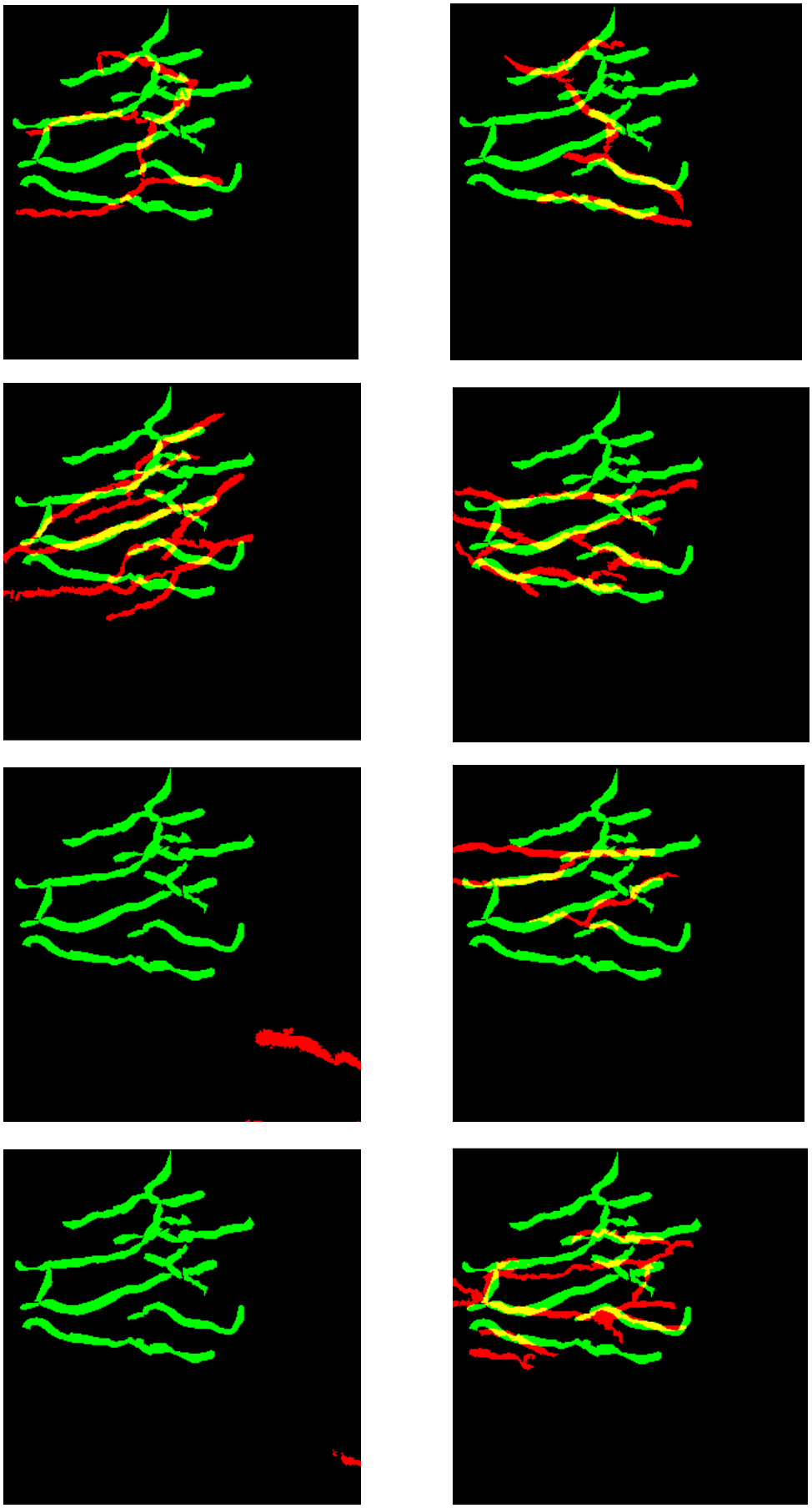

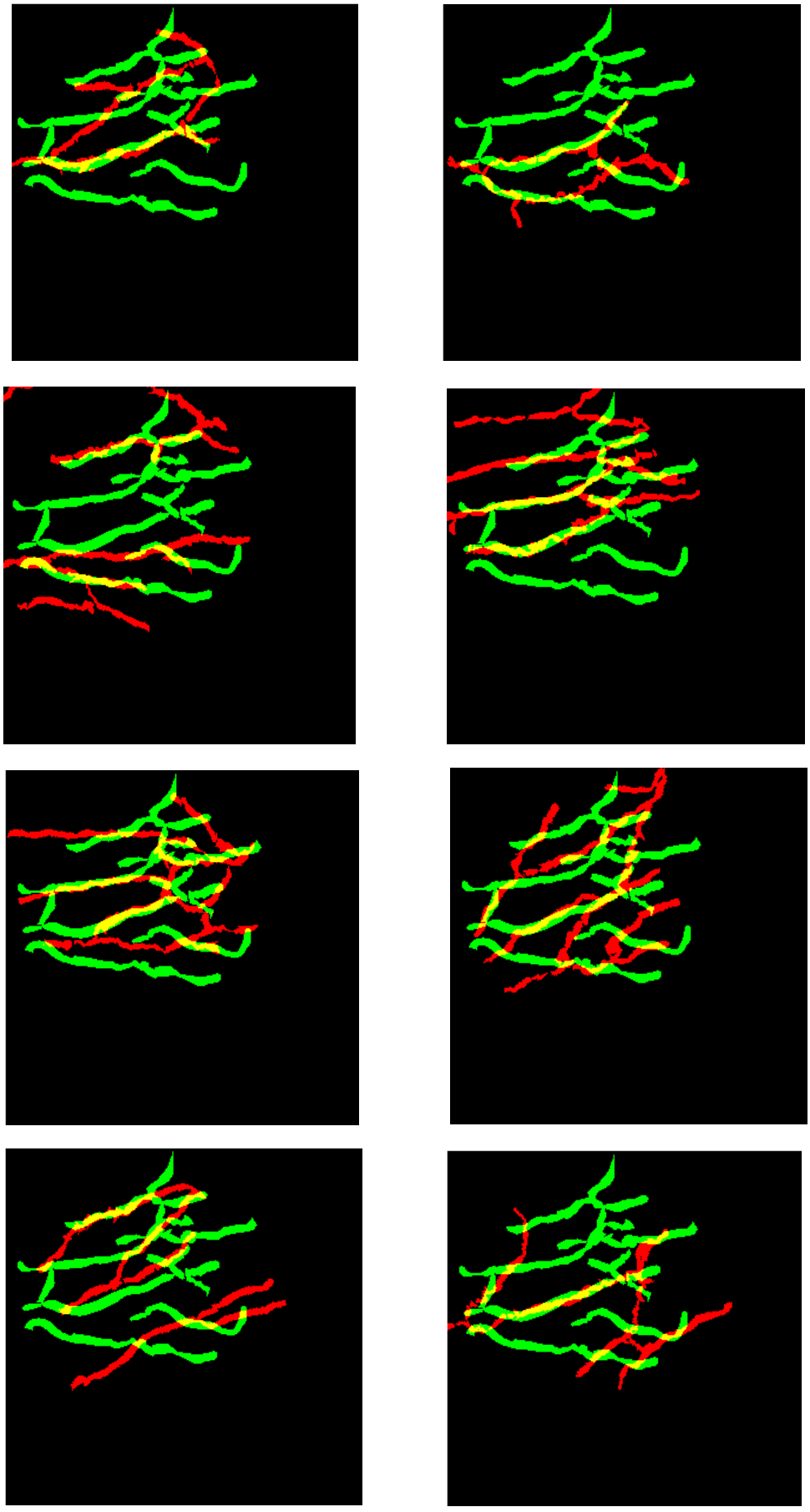

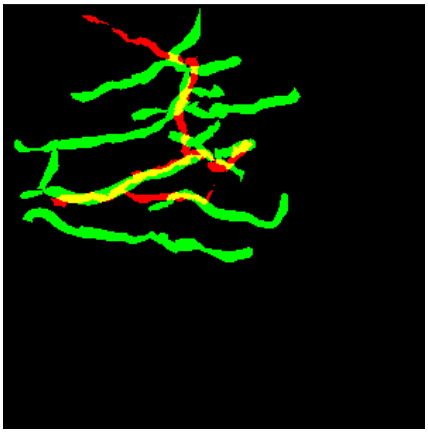

Bibliography

[1] Jain, Ross, Prabhakar, *An introduction to Biometric Recognition*, IEEE Transactions Circuits and Systems for Video Technology, vol. 14, n° 1, January 2004

[2] R. Heyer, *Biometric Technology Review 2008*, Land operations division, Defence science and technology organisation, 2008

[3] Jain, Hong, Bolle, *On-line Fingerprint Verification*, IEEE Transactions on Pattern Analysis and Machine Intelligence, vol. 19, n°4, April 1997

[4] Shanin, Badawi, Kamel, *Biometric Authentication using Fast Correlation of Near-infrared Hand Vein Petterns*, International Journal of Biological and Life Sciences 2:3, 2006

[5] Pankanti, Orabhakar, Jain, *On the Individuality of Fingerprints*

[6] Wang, Leedham, *A thermal hand vein pattern verification system*, Pattern Recognition and Image Analysis, Springer Berlin, vol. 3887/2005, 2005, pp 58-65

[7] Zhanov, Ferguson, Eidt, Howard, Fink, Waner, *Infrared Imaging of subcutaneous veins*, Lasers in Surgery and Medicine 34:56-61 (2004)

[8] A. Badawi, *Hand vein biometric verification prototype: A testing performance and patterns similarity*, International Journal of Biomedical Sciences, 2007

[9] J. D. Woodward, N. M. Orlans, P. T. Higgins, *Biometrics: identity assurance in the information age*, Osborne McGrawHill 2003

[10] A. K. Jain, R. Bolle, S. Pankanti, *Personal identification in networked society*, Kluwer Academic Publishers 1999

[11] H. Meadows, *Limb Vein Pattern Analysis for Forensic Human Identification*, PhD Thesis, University of Dundee

[12] T. Tanaka, N. Kubo, *Biometric authentication by hand vein patterns*, SICE 2004 Annual Conference, 2004

[13] Choi, Tran, *Hand vascular pattern technology*, Handbook of Biometrics (Jain, Flynn, Ross), Springer, chap. 13, pp 253-270, 2008

[14] Wang, Leedham, S. Y. Cho, *Infrared imaging of hand vein patterns for biometric purposes*, IET Computational Vision, 2007, 1, (3-4) pp 113-122

[15] Nyström, Fridén, Lister, *Superficial venous anatomy of the human palm,* Scand J Plast Reconstr Hand Surg, 24: 121-127, 1990

[16] Mehra, Kaul, Das, *Unusual Venous drainage pattern of face: a case report,* J. A nat. Soc India 52(1) 64-65, 2005

[17] Doyle, *Venous patterns in the cubital fossa,* I. J. Med. Sc., Seventh series, vol. I, n° 3, March 1968

[18] Craven, *The cubital fossa,* Anaesthesia and Intensive Care Medicine, pp 248-249, 2004

[19] Caggiati, Rosi, Heyn, Franceschini, Acconda, *Age-related variations of varicose veins anatomy,* Journal of Vascular Surgery, December 2006

[20] Coultras, Chawengsakophak, Rossant, *Endothelial cells and VEGF in vascular development,* Nature, vol. 438, December 2005

[21] Bryson, *Guide to IR and ultraviolet photography,* 2005

[22] Im, Park, Y. W. Kim, S. W. Kim, Han, Chung, *A biometric identification system by extracting hand vein patterns,* Journal of the Korean Physical Society, vol. 38, n° 3, pp 268-272, March 2001

[23] Im, Choi, S. W. Kim, *A direction-based vascular pattern extraction algorithm for hand vascular pattern verification,* ETRI Journal, vol. 25, n° 2, April 2003

[24] Chaudhuri, Chatterjee, Katz, Nelson, Goldbaurn, *Direction of blood vessels in retinal images using 2-dimensional matched filters,* IEEE Transactions on Medical Imaging, vol. 8, n° 3, September 1989

[25] S. Crisan, Tarnovan, T. E. Crisan, *Vein pattern recognition. Image enhancement and feature extraction algorithms,* 15th Symposium on Novelties in Electrical Measurements and Instrumentation, Romania, 2007

[26] J. Zhao, H. Tian, W. Xu, X. Li, *A new approach to hand vein image enhancement,* Proceedings of the 2009 Second International Conference on Intelligent Computation, Technology and Automation, vol. 1, pp 499-501, 2009

[27] Perona, Malik, *Scale-space and edge detection using anisotropic diffusion,* IEEE Transactions on Pattern Analysis and Machine Intelligence, vol. 12, n° 7, July 1990

[28] Wang, Leedham, Cho, *Minutiae feature analysis for infrared hand vein pattern biometrics,* Pattern Recognition 41, pp 920-949, 2008

[29] Sepasian, Mares, Balachandran, *Image enhancement for fingerprint minutiae-based algorithms using CLAHE, standard deviation analysis and sliding neighborhood,* Proceedings of the World Congress on Engineering and Computer Science, 2008

[30] Bhagavatula, Savvides, *Correlation pattern recognition for biometrics,* the International Society for Optical Engineering, 2006

[31] Villaseñor-Mora, Sanchez-Marin, Goray-Sevilla, *Contrast enhancement of mid and far infrared images of subcutaneous veins,* Infrared Physics and Technology 51, pp 221-228 (2001)

[32] Wang, Liu, Li, Zhou, *A real-time contrast enhancement algorithm for infrared images based on plateau histogram,* Infrared Physics and Technology 48, pp 77-82, 2006

[33] Can, Shen, Turnet, Tanenbaum, Roysam, *Rapid automated tracing and feature extraction from retinal fundus images using direct exploratory algorithms,* IEEE Transactions on Information Technology in Biomedicine, vol. 3, n° 2, June 1999

[34] Gonzalez, Woods, *Digital Image Processing,* II edition, Prentice Hall, New Jersey, 2002

[35] Lalonde, Gagnon, Boucher, *Non-recursive paired tracking for vessel extraction from retinal images,* Conference Vision Interface, Montréal, May 2000

[36] Miura, Nagasaka, Miyatane, *Feature extraction of finger vein patterns based on repeated line tracking and its application to personal identification,* Machine Vision and Applications (2004) 15: 194-203

[37] E. Grisan, *Automatic analysis of retinal images: retinopathy detection and grading,* PhD thesis, University of Padua, February 2005

[38] Tolias, Panas, *A fuzzy vessel tracking algorithm for retinal images based on fuzzy clustering,* IEEE Transactions on Medical Imaging, vol. 17, n° 2, April 1998

[39] Chutatape, Zheng, Krishman, *Retinal blood vessel detection and tracking by matched Gaussian and kalman filters,* Proceedings of the 20th Annual International Conference of the IEEE Engineering in Medicine and Biology Society, vol. 20, n° 6, 1998

[40] E. Grisan, Pesce, Giani, Foracchia, A. Ruggeri, *A new tracking system for robust extraction of retinal vessel structure,* Proceedings of the 26th Annual International Conference of the IEEE EMBS San Francisco, USA, September 1-5, 2004

[41] Najim, *Digital filters design for signal and image processing,* France 2004, Hermes Science

[42] Foracchia, E. Grisan, A. Ruggeri, *Luminosity and contrast normalization in retinal images,* Medical Image Analysis 9 (2005), pp 179-190

[43] Zana, Klein, *Segmentation of vessel-like patterns using mathematical morphology and curvature evaluation,* IEEE Transactions on Image Processing, vol. 10, n° 7, July 2001

[44] B. Zitovà, J. Flusser, *Image registration methods: a survey*, Image and Vision Computing, vol. 21, issue 11, pp 977-1000, October 2003

[45] Kembhaul, *Image registration, medical imaging and image analysis*, December 2005

[46] Kirbas, Quek, *A review of vessel extraction techniques and algorithms,* ACM Computer Surveys, vol. 36, 2, June 2004, pp 81-121

[47] Ortega, Penedo, Rouco, Barreira, Carreira, *Personal verified based extraction and characterisation of retinal feature points,* Journal of Visual Languages and Computing 20 (2009), pp 80-90

[48] Jain, Duin, Mao, *Statistical pattern recognition; a review*, IEEE Transactions on Pattern Analysis and Machine Intelligence, vol. 22, n° 1, January 2000

[49] Zaldi, *Medical image segmentation: quo vadis,* Computer Methods and Programs in Biomedicine 84(2006) 63-65

[50] R. Eberhart, J. Kennedy, *Particle Swarm Optimization,* IEEE International Conference on Neural Networks, 1995

[51] Li, Sato, *Multimodality image registration by particle swarm optimization of mutual information,* Advanced Intelligence Computing Theories and Applications with aspects of Artificial Intelligence (2007), pp 1120-1130

[52] Talbi, Batouche, *Particle swarm optimization for image registration,* Proceedings 2004 International Conference on Information and Communication Technologies: from Theory to Applications, 19-23 April 2004, pp 397-398

[53] R. C. Eberhart, Y. Shi, *Particle swarm optimization: developments, applications and resources,* IEEE Proceedings of the Congress on Evolutionary Computation, 2001

[54] Y. Del Valle, G. K. Venayagamoorthy et al., *Particle swarm optimization: basic concepts, variants and applications in power systems,* IEEE Transactions on Evolutionary Computation, vol. 12, n° 2, April 2008

[55] C. Di Ruberto, *Recognition of shapes by attributed skeletal graphs,* Pattern Recognition 37 (2004), 21-31

[56] Birgè, Rosenholc, *How many bins should be put in a regular histogram,* 2002